

https://dspace.org/

Kinetic aspects of the adsorption of Copper onto bio-waste adsorbents

Mabusela, Kagiso Baatseba

2021

https://hdl.handle.net/10539/31894

Downloaded from a DSpace repository. https://dspace.org/

UNIVERSITY OF THE WITWATERSRAND, JOHANNESBURG

Kinetic Aspects of the Adsorption of Copper onto Bio-waste Adsorbents

Kagiso Baatseba Mabusela

A dissertation submitted to the Faculty of Engineering and the Built Environment, University of the Witwatersrand, Johannesburg, in fulfilment of the requirements for the degree of Master of Science in Engineering.

Johannesburg, 2021

Declaration

I declare that this dissertation is my own unaided work. It is being submitted to the degree of Master of Science in Engineering to the University of the Witwatersrand, Johannesburg. It has not been submitted before for any other degree or examination in any other University.

Kagiso Baatseba Mabusela

Student Number: 550653

Date: 22/02/2021

Signature:



ABSTRACT

Adsorption kinetics is one of the main factors that must be understood before the applicability of any adsorbent. However, a large majority of the work done in adsorption studies just describe the macroscopic trend of adsorption uptake by using common models, often without careful appraisal of the adsorbent characteristics and validity of the model. Furthermore, adsorption is dependent on factors such as adsorbent and adsorbate type, their properties and operating conditions. Therefore, the aim of this work was to compare and thus, understand the mechanisms and kinetic aspects of copper adsorption using banana and orange peels as adsorbents for future modeling purposes. Furthermore, in order to have insight into and evaluate the kinetics, initial metal concentration, adsorbent dosage, temperature, adsorption type and shaking speed were examined.

The banana and orange peels were characterized by various techniques such as Brunauer-Emmett-Teller (BET), scanning electron microscope (SEM), X-ray diffraction, Fourier transform infrared spectroscopy (FTIR), and titration methods. The results showed that both peels have heterogeneous structures, mesoporous pores and contain different functional groups, with orange peels being acidic and amorphous, whereas banana peels were crystalline and basic. After characterization analysis, the design of experiments (DOE) methodology using two-level five-factor full factorial (2^5) was used in order to determine the relationship between factors affecting the process and the amount of copper adsorbed. In this study, the temperature, initial metal concentration, bio-adsorbent dosage, type of adsorbent and agitation rate were investigated. Furthermore, the significance of each factor and associated interactive effects were evaluated using DOE and percent copper removed was used as the measured response. From the results, initial copper concentration, adsorbent dosage and shaking speed were found to be statistically significant.

These parameters were further optimized using response surface methodology (RSM). Experiments were designed and carried out at various conditions according to the central composite rotatable design (CCRD). The results of the response surface methodology showed that the theoretical optimum conditions for the maximum copper recovery of 84.3% within the range of conditions studied were found to be at an initial metal concentration of 51.3 mg/L, shaking speed at of 146 rpm and adsorbent dosage of 3.5g/L.

The data from RSM was fitted to the Freundlich and Langmuir isotherms. The data of both the orange and banana peels fitted the Langmuir isotherm well with correlation coefficient factors (R^2) greater than 90%. Furthermore, to confirm and support the best fitting model as indicated by R^2, the error statistics were calculated. The highest R^2 values and the lowest values for Chai-square test, sum of squares of the errors and Marquardt's percentage standard deviation were found when modeling the equilibrium data using the Langmuir isotherm. The kinetics of Copper (Cu) ions onto

banana and orange peels were evaluated using reaction-based models namely, pseudo-first- and pseudo-second-order models, and diffusion-based models such as the Weber-Morris, Banghan's pore diffusion model, Boyd model, and Film diffusion model. The results obtained revealed that banana peels showed stronger conformity to both reaction models. The data were further evaluated using diffusion models. The models confirmed the existence of both pore and film diffusion. Lastly, possible governing mechanisms were evaluated. The fitting of the models revealed that there is more than one mechanism responsible for the uptake of copper. Ion-exchange was identified as the dominant mechanism in the copper uptake by both banana and orange peels. Some other types of interactions, like complexation and electrostatic interactions, were also proven to be involved in the adsorption process.

PUBLICATIONS AND PRESENTATIONS

K.B Mabusela, G.S Simate, P Musonge (2018). Kinetic aspects of metal ion adsorption onto biowaste Adsorbents, In Proceedings of the 3rd International Conference on Composites, Biocomposites and Nanocomposites, Port Elizabeth, South Africa.

DEDICATION

This thesis is dedicated to me - Kagiso Baatseba Mabusela

You were never guaranteed an easy road, but you have kept going. You are a born fighter.

A conqueror!

You are worthy and deserving.

And always remember that you are capable of creating and having it all.

So rise and stand in your authentic brilliance!!!

ACKNOWLEDGMENTS

There are a number of individuals without whom this work may not have been written and to whom I am greatly indebted.

To my parents – Joshua and Onicca Mabusela, who throughout my life have been a source of encouragement and inspiration to me, a very special thank you for providing a loving environment and nurturing me through the years of my formal education. I would also like to say a heartfelt thank you to my siblings especially my baby sister, Tshireletso B Mabusela for always believing in me and encouraging me to follow my dreams.

To my husband, IJ Oyasor, thank you for being my strength and standing beside me with love and unconditional support. I greatly appreciate your support, wisdom and believe in me.

Marike Khuyts, your warm welcoming spirit, great energy and mentoring have been truly exceptional and encouraging. Thank you for inspiring a new sense of confidence in my abilities and work.

My deepest thanks go to the supervisor who shepherded me through the bulk of the work, Professor GS Simate. Your sage advice, insightful criticisms, and encouragement that aided the writing of this dissertation in innumerable ways. I would also like to thank Professor P Musonge, whose steadfast of this dissertation constantly gave me the motivation to perform to my maximum ability. I was very fortunate to have been able to work with both of you since undertaking my Master's degree.

A warm thank you to my friends / learning partners- Thabelo, Reuben, Noeleen, Penny, Varshan, Mati, Tumelo, Gabriella, Lindi and Prince who played such important roles along the journey, as we mutually engaged in making sense of the various challenges we faced and in providing encouragement to each other at those times when it seemed impossible to continue.

I greatly appreciate the support received through the collaborative work undertaken with Durban University of Technology (DUT) under the National Research Foundation (NRF): Collaborative Postgraduate Research Training Programme and the University of the Witwatersrand for the Postgraduate Merit Award (PMA). I am also very grateful and thankful to all the staff in Richard Ward in the school of chemical and metallurgical engineering who were always so helpful and provided me with their assistance throughout my dissertation.

TABLE OF CONTENTS

ABSTRACT iii

PUBLICATIONS AND PRESENTATIONS v

DEDICATION vi

ACKNOWLEDGMENTS i

TABLE OF CONTENTS i

LIST OF FIGURES iv

LIST OF TABLES vii

1. Introduction 1

1.1 Introduction 1

1.2 Problem statement 2

1.3 Goals and objectives 2

1.4 Research Methodology 3

1.5 Dissertation layout 3

1.6 Summary 4

2 Literature Review 5

2.1 General introduction 5

2.2 Heavy metals and conventional metal-removal technologies 5

2.3 Adsorbents and adsorbent classification 6

2.3.1 Agricultural waste peels 7

2.4 Analysis of data from the literature 7

2.4.1 Equilibrium isotherms 7

2.4.2 Batch Kinetic Modeling 9

2.5 Theoretical Aspects 11

2.5.1 Mechanisms of biosorption 11

2.5.2 Equilibrium isotherms 13

2.5.3 Batch kinetic models 15

2.5.4 Error Functions 21

2.6 Conclusion 22

3 Method and Materials 23

3.1 Introduction 23

3.2 Materials 24

3.2.1 Sample preparation 24

3.2.2 Preparation of heavy metal solution 24

3.3 Experimental methods 24

3.3.1 Batch Experiments 24

3.3.2 Design of experiments and process optimization 26

3.3.3 Methodology for data analysis 26

3.3.4 Calculations and Model Fitting 29

3.4 Analytical techniques 31
3.4.1 Agitation and solution analysis equipment 31
3.4.2 The emission scanning electron microscope 33
3.4.3 Energy Dispersive X-Ray Spectroscopy 33
3.4.4 Brunauer-Emmett-Teller surface area 33
3.4.5 X-ray diffraction 34
3.4.6 Fourier transform infrared spectroscopy 34
3.4.7 Determination of surface charges and pH 34
3.4.8 The point of zero charge 35
3.5 Summary 35
4 Characterization of Banana and Orange Peels 36
4.1 Scanning Electron Microscopy 36
4.2 Energy dispersive X-ray spectroscopy 38
4.3 BET characterization 40
4.3.1 BET surface area and porosity 40
4.3.2 Particle size 42
4.3.3 Pore size, shape and distribution 42
4.4 X-Ray Diffraction Spectroscopy 44
4.5 Fourier transform infrared spectroscopy 46
4.5.1 Identifying the peaks on the peels 46
4.5.2 Results after adsorption 48
4.6 Point of zero Charge and Surface Charges 50
4.7 Summary 52
5 Preliminary studies of the adsorption of metal ions onto banana and orange peels 54
5.1 The controlled operating conditions 54
5.1.1 Operative pH 54
5.1.2 Equilibrium time 55
5.2 Particle size 56
5.3 The efficiency of untreated peels for removal of metal ions 58
6 Identification of Significant Factors 61
6.1 Introduction 61
6.2 Materials and methods 61
6.2.1 Bio-adsorbent samples and solution preparation 61
6.2.2 Experimental Plan for Statistical Design of Experiments (DOE) 61
6.3 Results and discussion 62
6.3.1 Influence of factors 62
6.3.2 Significant factors 66
6.4 Summary 69
7 Optimization of influential factors 71
7.1 Methods and materials 71
7.1.1 Adsorbent and adsorbate preparation 71
7.1.2 The experimental design for central composite design and response surface methodology 71
7.2 Results and discussion 73
7.2.1 Development of the fitted model and validation 73
7.2.2 Derivation of the model 74

7.2.3 Checking for adequacy for the developed model 74
7.2.4 Response Surfaces 75
7.2.5 Determination of optimum conditions 77
7.2.6 Confirmatory Experiments 77
7.3 Summary 78
8 Adsorption isotherms and statistical validity 79
8.1 Analysis of Adsorption isotherms 79
8.1.1 The effect of isotherm shape 79
8.1.2 Langmuir isotherm 80
8.1.3 Freundlich isotherm model 83
8.1.4 Experimental vs Predicted 84
8.2 Statistical validity 86
8.3 Summary 88
9 Adsorption Batch kinetics and mechanisms 89
9.1 Kinetic reaction models 90
9.1.1 Pseudo first-order model 90
9.1.2 Pseudo second-order model 91
9.2 Diffusion models 95
9.2.1 Weber-Morris 95
9.2.2 Pore diffusion model – Banghan's model 99
9.2.3 Boyd model 100
9.2.4 Film diffusion 103
9.3 Mechanisms of Copper adsorption 107
9.3.1 Physical adsorption 107
9.3.2 Electrostatic interactions 108
9.3.3 Ion exchange 109
9.3.4 Surface Complexation 109
9.4 Final remarks and conclusions 110
9.5 Summary ..... Error! Bookmark not defined.
10 Conclusion and Recommendations 113
10.1 Introduction 113
10.1.1 Characterization 113
10.1.2 Isotherms and statistical validity 115
10.1.3 Batch kinetic models 115
10.2 Industrial application. 116
10.3 Final remarks and recommendations 116
11 References 120
12 Appendices 131

LIST OF FIGURES

Figure 2.1: Possible classification of low-cost adsorbents 7
Figure 2.2: Biosorption mechanisms. 12
Figure 2.3: Types of adsorption equilibrium isotherm relations 14
Figure 2.4: Modeling of adsorption kinetics: constituents and input data 16
Figure 3.1: The outline of the experimental procedure. 23
Figure 3.2: An adsorption model selection for system design. 30
Figure 3.3: Algorithm for linear isotherm model regression using error functions 31
Figure 3.4: Adsorption shaking test equipment (Labcon shaking incubator) 32
Figure 3.5: Atomic Absorption Spectrophotometer (AAS) equipment for metal ion concentration analysis 32
Figure 4.1: SEM of banana peels. The micrographs (A and B) depicts banana peels before adsorption at x 2.00 and x 100 magnification while the banana peel micrographs (C and D) were observed at x 2.00 and x 100 magnification after adsorption. 37
Figure 4.2: SEM of orange peels. The micrographs (A and B) depicts orange peels before adsorption at x 2.00 and x 500 magnification while the orange peel micrographs (C and D) were observed at x 2.00 and x 500 magnification after adsorption. 38
Figure 4.3: EDX image of banana peels before (A) and after (B) adsorption. 39
Figure 4.4: EDX image of orange peels before (A) and after (B) adsorption. 39
Figure 4.5: A diffractogram of an XRD analysis of orange peels before adsorption showing the intensity as a function of the diffraction angles. 44
Figure 4.6: A diffractogram of an XRD analysis of banana peels before adsorption showing the intensity as a function of the diffraction angles. 45
Figure 4.7: FTIR spectrum of dried banana and orange peels before adsorption. 47
Figure 4.8: FTIR spectrum for the banana peel after and before adsorption 48
Figure 4.9: FTIR spectra of the orange peel before and after adsorption. 49
Figure 4.10: Point of zero charge of fruit peels in 0.1M KNO_3. 50
Figure 5.1: Adsorption of metal ions onto banana peels. 56
Figure 5.2: Adsorption of metal ions onto orange peels. 56
Figure 5.3 Effect of particle size on % heavy metals removed using banana peels. 57
Figure 5.4 Effect of particle size on % heavy metals removed using orange peels. 57
Figure 5.5: Percentage removed of metal ions using orange peels. 58
Figure 5.6: Percentage removed of metal ions using banana peels. 59
Figure 6.1: Effect of adsorbent type on the recovery of Cu ions. 62
Figure 6.2: Effect of temperature on the percentage of Cu ions removed. 63
Figure 6.3 Effect of temperature on the percentage of Cu ions removed. 64
Figure 6.4: Effect of initial concentration on the recovery of Cu ions. 65
Figure 6.5: Effect of shaking speed on the removal of Cu ions. 66
Figure 6.6: The normal plot of main factors and factor interactions from the 2^5 full factorial design. 67
Figure 6.7: Pareto chart 68
Figure 6.8: Normal plot of residuals. 69
Figure 6.9: Plot of residuals- Externally Standardized Residuals vs Predicted. 69
Figure 7.1: Relationship between experimental and predicted copper recovery. 75
Figure 7.2. Response surface and contour plots at a constant shaking speed. 76
Figure 7.3: Response surface and contour plots at constant adsorbent dosage. 76
Figure 7.4: Response surface and contour plots at a constant initial metal concentration. 77

Figure 8.1: Arithmetic plot of metal ion concentration C_0 (mg/L) vs adsorbent loading q_e (g adsorbed/g solid) of orange peels at an initial concentration range of 5 – 50 mg/L at a constant mass dosage of 3.5g/L.....80
Figure 8.2: Arithmetic plot of metal ion concentration C_0 (mg/L) vs adsorbent loading q_e (g adsorbed/g solid) of banana peels at an initial concentration range of 5 – 50 mg/L at a constant mass dosage of 3.5g/L.....80
Figure 8.3: Langmuir adsorption isotherm for copper adsorption on orange peels at an initial concentration range of 5 – 50 mg/L at a constant mass dosage of 3.5g/L. 81
Figure 8.4: Langmuir adsorption isotherm for copper adsorption on banana peels at an initial concentration range of 5 – 50 mg/L at a constant mass dosage of 3.5g/L. 82
Figure 8.5: Freundlich adsorption isotherm for copper adsorption on orange peels at an initial concentration range of 5 – 50 mg/L at a constant mass dosage of 3.5g/L. 83
Figure 8.6: Freundlich adsorption isotherm for copper adsorption on banana peels at an initial concentration range of 5 – 50 mg/L at a constant mass dosage of 3.5g/L. 83
Figure 8.7: Experimental and predicted equilibrium isotherm data by both Langmuir and Freundlich models for the adsorption of Cu ions on orange peels. 84
Figure 8.8: Experimental and predicted equilibrium isotherm data by both Langmuir and Freundlich models for the adsorption of Cu ions on banana peels.....85
Figure 9.1: Experimental data fitted into the pseudo-first order kinetic model for the adsorption of Cu ions onto orange peels as an adsorbent at an initial concentration of 50mg/L.....90
Figure 9.2: Experimental data fitted into the pseudo first-order kinetic model for the adsorption of Cu ions onto banana peels as an adsorbent at an initial concentration of 50mg/L. 91
Figure 9.3: Experimental data fitted into the pseudo second-order kinetic model for the adsorption of Cu ions onto orange peels as an adsorbent at an initial concentration of 50mg/L. 92
Figure 9.4: Experimental data fitted into the pseudo second-order kinetic model for the adsorption of Cu ions onto banana peels as an adsorbent at an initial concentration of 50mg/L.....92
Figure 9.5: Intraparticle diffusion plots of the adsorption of Cu ions onto orange peels at an initial concentration of 50g/mL. 96
Figure 9.6: Intraparticle diffusion plots of the adsorption of Cu ions onto banana peels at an initial concentration of 50g/mL. 96
Figure 9.7: Intraparticle diffusion plots showing the dual nature of the kinetics of adsorption of Cu ions onto orange peels at an initial concentration of 50g/mL. 97
Figure 9.8: Intraparticle diffusion plots showing the dual nature of the kinetics of adsorption of Cu ions onto orange peels at an initial concentration of 50g/mL. 97
Figure 9.9: Experimental data of the adsorption of Cu ions onto orange peels fitted to the linear form of the Bangham's pore diffusion model at an initial concentration of 50mg/L with an adsorbent mass of 3.5g/L in a 0.1L solution. 100
Figure 9.10: Experimental data of the adsorption of Cu ions onto banana peels fitted to the linear form of the Bangham's pore diffusion model at an initial concentration of 50mg/L with an adsorbent mass of 3.5g/L in a 0.1L solution.....100
Figure 9.11: Adsorption of copper using orange peel by equation 2.12 of the Boyd and Reichenburg kinetic model at an initial concentration of 50mg/L. 101
Figure 9.12: Adsorption of copper using banana peel by equation 2.12 of the Boyd and Reichenburg kinetic model at an initial concentration of 50mg/L. 101
Figure 9.13: Adsorption of copper using orange peel by equation 2.13 of the Boyd and Reichenburg kinetic model at an initial concentration of 50mg/L. 102
Figure 9.14: Adsorption of copper using banana peel by equation 2.13 of the Boyd and Reichenburg kinetic model at an initial concentration of 50mg/L. 102

Figure 9.15: Liquid film diffusion model for the adsorption of Cu using orange peels at an initial solution concentration of 50mg/L. 104
Figure 9.16: Liquid film diffusion model for the adsorption of Cu using banana peels at an initial solution concentration of 50mg/L. 104

LIST OF TABLES

Table 2.1: Conventional metal removal technologies 6
Table 2.2 Frequently used adsorption isotherm models 8
Table 3.1: Metal sample conditions to determine concentration using the Atomic Absorption Spectrophotometer 32
Table 4.1: Physiochemical properties of unmodified banana peels in their size ranges (106, 300 and 500 microns) 40
Table 4.2: Physiochemical properties of unmodified orange peels in three size ranges (106, 300 and 500 microns) 40
Table 4.3: Representative internal surface area ranges for different adsorbents**.** 42
Table 4.4: IUPAC classification of pores 43
Table 4.5: Surface Charge of fruit peels. 51
Table 4.6: A summary of the physical and chemical properties of the adsorbents**.** 52
Table 6.1: Experimental factors and levels for controlled factors. 66
Table 6.2: Experimental factors and levels for held factors. 66
Table 7.1: Relationship between coded and actual values of the variable**.** 72
Table 7.2: Experimental layout and runs for the central composite rotatable design. 72
Table 7.3: Observed values for Cu recovery**.** 73
Table 7.4: ANOVA for the quadratic model**.** 74
Table 7.5: Model fit of statistics. 75
Table 7.6: Copper recovery at optimal conditions 78
Table 8.1: The linear modeling isotherm equations that were used. 79
Table 8.2: Adsorption isotherm model parameters for the adsorption of Cu ions on banana and orange peels as adsorbents. 81
Table 8.3: The effect of the separation factor on the adsorption of Cu on banana and orange peels. 82
Table 8.4: Parametric conditions of the Freundlich constant, n. 84
Table 8.5: Error functions used to statistically determine the best adsorption isotherm for the experimental data studied. 87
Table 8.6: The calculated values of the respective error functions. 87
Table 9.1*:* Reaction and diffusion kinetic models that were used to evaluate the experimental data of the adsorption of Cu ions onto banana and orange peels. 89
Table 9.2: Model parameters for the adsorption of copper from using banana and orange peels 90
Table 9.3: Model parameters for the adsorption of copper from using banana and orange peels 92
Table 9.4 Diffusion model parameters for the adsorption of copper using banana and orange peels as adsorbents. 95
Table 9.5: Diffusion coefficients for the adsorption of Cu ions by orange and banana peels. 105

1. Introduction

1.1 Introduction

While water covers 70% of the world's surface, the availability of freshwater for human consumption is becoming scarce. This is due to the increasing use of toxins such as pesticides, heavy metals, anions, pharmaceuticals, and hydrocarbons (Sud et al., 2008). At present, different methods such as biological, precipitation, membrane technology, electrochemical, and adsorption have been developed to remove these substances from wastewater (Worch, 2012). Amongst these methods, the adsorption technique has received considerable attention because it is cost- and energy-effective, easy to design and operate. The adsorption processes uses various adsorbents such as activated carbon, molecular sieves, polymeric adsorbents, and some other low-cost materials that have been developed to remove solute from wastewater (Volesky, 1990). However, the recent worldwide trend aimed at achieving higher environmental standards encourages the usage of low-cost adsorption systems. Thus, adsorption (also referred to as biosorption) using various low-cost adsorbents derived from agricultural waste or natural products has been extensively investigated for heavy metal removal from contaminated wastewater.

A number of parameters and/or aspects are used to ascertain the performance of an adsorption system. For example, kinetics aspects of an adsorption process are usually considered in order to obtain the details about its performance and mechanisms (Dada et al., 2017). Ideally, kinetic information of a given adsorbent is of great significance in any study and/or application. The solute uptake rate, for instance, can be determined from the kinetic analysis which can subsequently be used to determine the residence time required to complete the adsorption reaction. In addition, based on the kinetic information, one can calculate the size of an adsorption system (Plazinski et al., 2009a). Adsorption kinetics is, therefore, the basis for determining the capacity and efficiency of fixed-bed or other flow-through systems.

On the other hand, though there is an increase in biosorption research, it is uncertain if such a high number of research activities have significantly improved knowledge in the field or aided any industrial exploitation (Gadd, 2009). In fact, despite some proprietary biosorption processes that have been developed for commercial use in the past decade, such as AlgaSORBTM and AMT_BioclaimTM (Kratochvil and Volesky, 1998), they have been unsuccessful. Therefore, it is important to analyse and investigate the reasons underlying the lack of commercial use. One reason is generally the low technology readiness including poor understanding of mechanisms and kinetics of the process (Vijayaraghavan and Balasubramanian, 2015). For example, most studies

conducted have concentrated mainly on the uptake capacities of different bioadsorbents with little, to no evidence given of possible mechanisms, interactions and kinetics. Therefore, there is a need to concentrate on research that will help better understand the mechanisms and kinetics which drive the biosorption process.

In this regard, literature has repeatedly pointed out that reliable, simple and effective models need to be developed. However, despite a large number of models proposed, tested and critically reviewed (Rangabhashiyam et al., 2014b; Vijayaraghavan and Yun, 2008; Xu et al., 2013), there is still no significant shift in understanding kinetics. On this account, there seems to be little evidence to suggest that the development of a new model would bring about any significant changes. Thus, there is a need to study the well-tested and reported kinetic models when analysing the phenomenon of biosorption. Therefore, the purpose of this research is to provide a pragmatic understanding of the mechanisms and kinetic aspects of the adsorption of Cu onto orange and banana peels to establish an understanding of adsorption mechanisms and kinetics for modeling purposes. The study entails adsorbent characterization and mathematical model selection to describe data obtained from experiments.

1.2 Problem statement

At present, heavy metals are of prime concern in source and treated water due to their severe health and environmental effects. Conventional methods for the removal of these metals are not economical and generate huge quantities of toxic chemical sludge (Salman H. Abbas et al., 2014). Thus, the need to develop sustainable, eco-friendly technologies to replace conventional technologies to minimize anthropogenic environmental impacts is pivotal. A number of research studies have indicated that biosorption is a potential alternative for the removal of metal ions from aqueous solutions. The present study will concentrate on biosorption using agricultural bio-waste for the treatment of metal ions that are generated from Acid Mine Drainage (AMD). However, it must be noted that most studies that have been conducted have concentrated mainly on the uptake capacities of different bioadsorbents with little to no evidence given of possible mechanisms and kinetic interactions. Therefore, there is definitely a need to pursue research that can enable a better understanding of the mechanisms and kinetics which drive the biosorption process. Hence, in this work kinetic models will be evaluated to better understand adsorption performance and mechanisms.

1.3 Goals and objectives

The main aim of this research is to provide a pragmatic understanding of the mechanisms and kinetic aspects of the adsorption of Cu onto orange and banana peels.

The specific objectives are as follows:

- To characterize adsorbents in order to understand their surface morphology
- To evaluate factors that affect the adsorption capacity of the bio-material using DOE
- To optimize the process using RSM.
- To critically evaluate suitable equilibrium isotherms and kinetic models so as to analyse the adsorbate-sorbent interaction.

1.4 Research Methodology

This section involves the following major tasks: literature review, experimental design, laboratory testing, laboratory test data analysis, conclusions, recommendations, and documentation.

1.5 Dissertation layout

This dissertation consists of ten chapters including this chapter (Chapter 1) that provides the motivation for the research, the problem statement, and the overall objectives of this study. The layout of the dissertation is schematically summarized in a flowchart in Figure 1.1.

Chapter 2 is the literature review, which includes the general knowledge of the adsorption process and governing processes; general principles of equilibrium isotherms and kinetic models that were used. Chapter 3 (experimental design) describes the materials and methods used in the study. The subsequent chapters (Chapter 4 through to 9) describe and discuss the laboratory tests and results. The dissertation concludes in Chapter 10 with a summary of the findings and recommendations. Appendices of laboratory test results and other important data are also included.

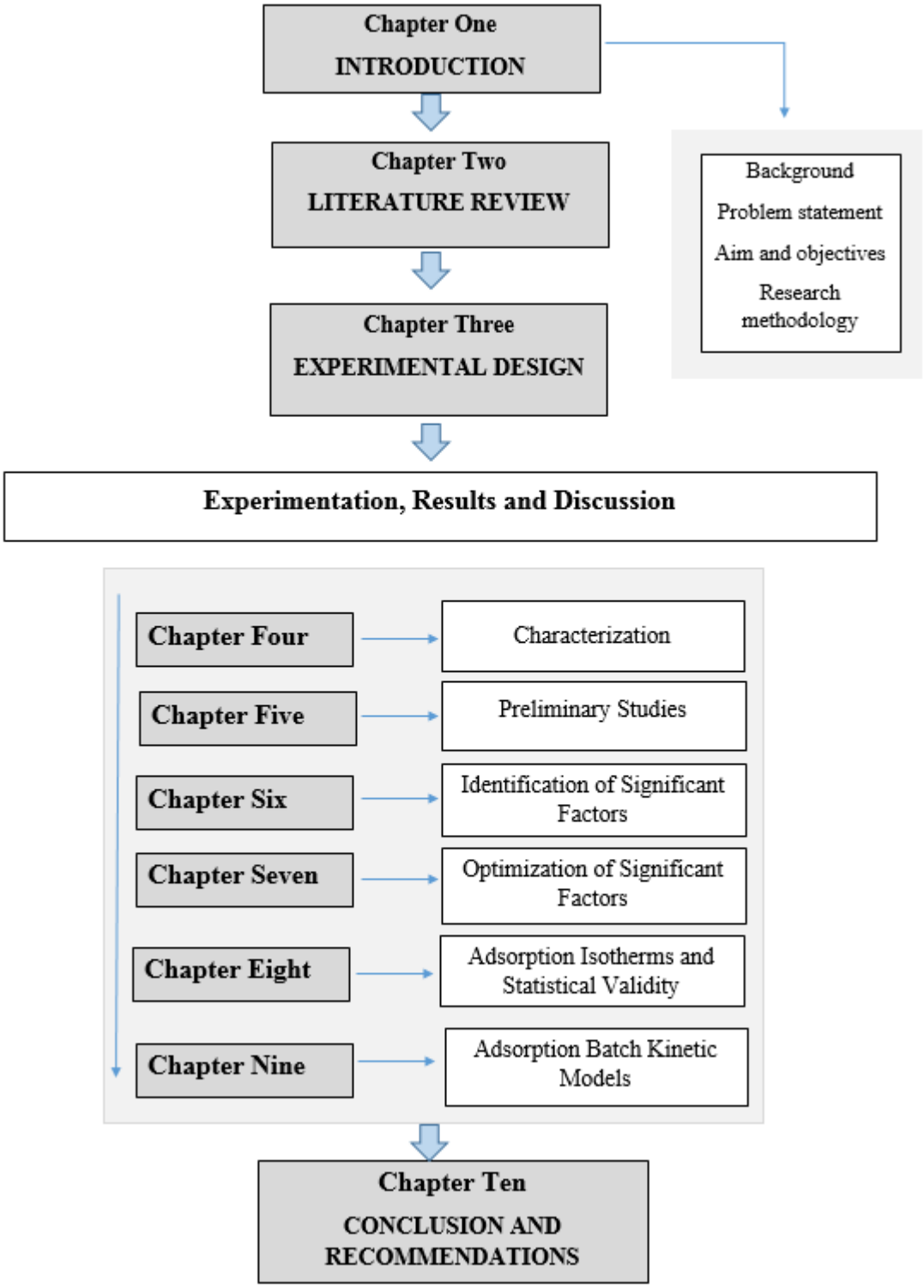

Figure 1.1: Dissertation Layout.

1.6 Summary

The background, problem statement, and research objectives were addressed in this introductory chapter. The methodology of research was then briefly described, followed by the structure of the dissertation.

2 Literature Review

2.1 General introduction

Heavy metal pollution in aquatic systems has become a serious threat to the environment. These metals are non-biodegradable and accumulate in the food chain. They are also toxic even at low concertations (Srivastava and Goyal, 2010). Unfortunately, the conventional treatment methods that exist are not effective and economical for treating large volumes of effluent containing low metal concentrations (Gupta et al., 2000). Thus, bioadsorption has emerged as an alternative technology for treating these waste streams in an eco-friendly and cost-effective way.

For the past decades, biosorption has been used for the removal and/or recovery of organic and inorganic substances from aqueous solutions by biological materials. These include living or dead microorganisms and their components: seaweed, plant materials, industrial and cultural waste, and natural residues (Bhatnagar et al., 2015). This concept is multidimensional and has been evolving over the past decades. The challenges with defining biosorption can be attributed to the existence of many mechanisms, the adsorbent used, environmental factors and metabolic processes in the case of living organisms (Fomina and Gadd, 2014). Biosorption has been proposed as a cost-effective treatment technology for the past decade and there has been increasing research. However, despite the significant progress that has been made in understanding this complex phenomenon, the commercialization of this process has been limited thus far (Gadd, 2009). This can be attributed to the low technology readiness including poor understanding of mechanisms and kinetics of the processes (Vijayaraghavan and Balasubramanian, 2015). Kinetic models have been developed to investigate and identify mechanisms of adsorption. Thus, the literature reviewed below demonstrates some of the available models that have been used, their limitations and how the following research intends on addressing some of them.

2.2 Heavy metals and conventional metal-removal technologies

Heavy metal pollution is one of the major environmental problems the world is facing today. Most heavy metals are harmful to the environment, living organisms and human wellbeing (Tripathi and Ranjan, 2015). Industrial effluents are major contributors to heavy metal pollution and the metal ions accumulate in the environment causing long term damage (Salman H. Abbas et al., 2014). Therefore, their elimination and reduction from water is very important to protect the environment and public health. The conventional treatment technologies that have been used extensively to treat metal ion bearing streams are listed in table 2.1. However, they are expensive (due to non-degradable materials used), generate a lot of secondary toxic waste streams and inefficient at treating low metal concentration streams. Furthermore, as environmental regulations tighten up,

they become progressively inadequate (Volesky, 2001). Thus, biosorption has emerged as an alternative technology because it has the potential to be effective, economical and eco-friendly. Various adsorbents have been used to treat waste contaminated by metal ions. The next section will elaborate more on this subject.

Table 2.1: Conventional metal removal technologies

Method	Disadvantages	Advantages
Chemical precipitation	- Suitable for higher concentrations - Difficult separation - Not effective - Sludge production	- Simple and cheap
Chemical oxidation or reduction	- Chemicals requires (not universal) - Biological systems (very slow process) - Climate sensitive	- Mineralization
Electrochemical treatment	- Suitable for high concentrations - Expensive	- Metal recovery
Reverse osmosis	- High pressure - Membrane scaling - Expensive	- Pure effluent (for recycle)
Ion Exchange	- Sensitive to particles - Expensive resins - Not for metals	- Effective - Pure effluent metal recovery possible
Evaporation	- Energy intensive - Expensive - Resulting sledges	- Pure effluent (for recycle

2.3 Adsorbents and adsorbent classification

Adsorbents that are used for the treatment of wastewater are either of natural origin or as a result of an industrial production and/or activation process. Typical natural adsorbents are clay minerals, natural zeolites, oxides or biopolymers while engineered adsorbents can be classified as carbonaceous (activated carbon, polymeric, oxidative adsorbents and zeolite molecular sieves (Worch, 2012). However, a new class of absorbents often referred to as low-cost adsorbents (LCAs) has received a lot of attention. They are usually derived from waste or by-products and are may be classified according to figure 2.1, but for the context of the project, only agricultural waste will be expanded on.

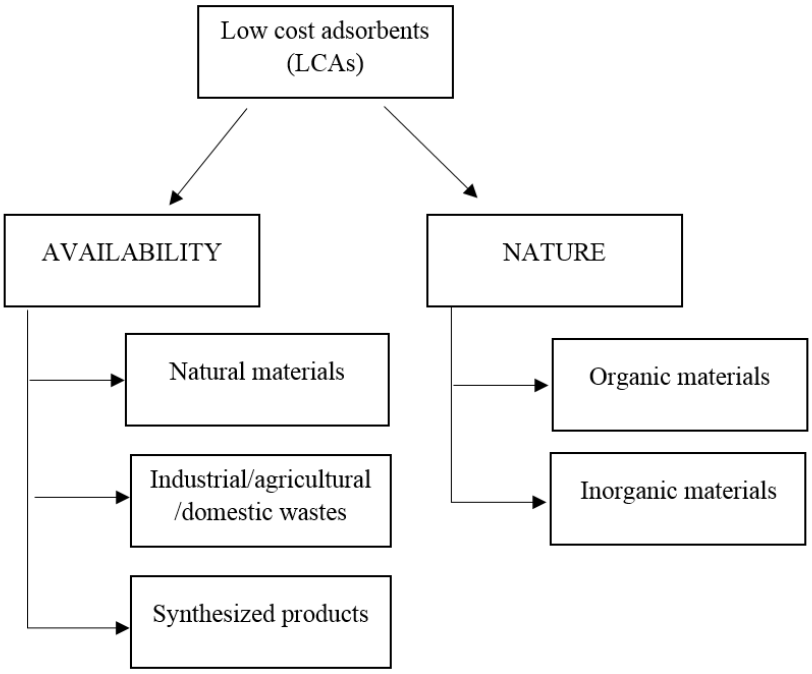

Figure 2.1: Possible classification of low-cost adsorbents

2.3.1 Agricultural waste peels

Agricultural waste peels pose an ecological burden for society because they are often discarded as waste and find little to no application anywhere which then poses serious disposal problems (Sud et al., 2008). However, waste peels have now stimulated new gateways for the production of renewable, low cost and sustainable adsorbents for water treatment (Tripathi and Ranjan, 2015). Among several agricultural wastes that have been investigated, fruit peels have been identified as potential adsorbent materials and some of the advantages are (Rangabhashiyam et al., 2014a):

- Materials are highly economical – normally one does not need to purchase, they are readily available as a waste product in most industries.
- There is no need for costly growth media like in living organisms
- The process is independent of physiological maintenance of aseptic conditions
- Reversible process: the process can be subjected for the cycle
- The formation of chemical and physical sludge is reduced

2.4 Analysis of data from the literature

2.4.1 Equilibrium isotherms

Batch equilibrium isotherms are expressions that are used to compare pollutant uptake capacities of different types of adsorbents and the affinities of different substances for the biosorbents (Liu and Liu, 2008). Numerous models have been used to describe biosorption - from single component models of which the Langmuir and Freundlich models are mostly used, to more complex multi-component models, some of which have been derived from Langmuir/Freundlich models (Volesky,

2003a). Even though, these models provide the basis for comparing and interpreting different adsorbent-sorbent systems, the base assumptions are often too simplistic and may not always apply for biological systems (Gadd, 2009). For example, the assumption that all binding sites have the same affinity despite the fact that biomass components usually have more than one binding site made up of different functional groups which in most cases have different affinities for adsorbate species, uptake capacity is also affected by changes in solution chemistry and pH. The simplicity used in the development of the models can be attributed to the fact that most of these models were originally developed form the adsorption of gases (Gadd, 2009). Table 1 summaries some of the widely used models.

Table 2.2 Frequently used adsorption isotherm models

Isotherm	Equation	Advantage	Disadvantage
Langmuir	$q = \frac{bq_m C_e}{1 + bC_e}$	Interpretable parameters	Not structured, monolayer sorption
Freundlich	$q = KC_e^{1/n}$	Simple expression	Not structured, no levelling off
Combination (Langmuir-Freundlich)	$q = \frac{bq_m {C_e}^{1/n}}{1 + b{C_e}^{1/n}}$	Combination of above	Unnecessarily complicated
Radke and Prausnitz	$\frac{1}{q} = \frac{1}{aC_e} + \frac{1}{bC_e^{\beta}}$	Simple expression	Empirical uses three parameters
Redlich-Peterson	$q = \frac{aC_e}{1 + bC_e^n}$	Approaches Freundlich at high concentrations	No special advantages
Brunauer (BET)	$q = \frac{BCQ^0}{(C_s - C)[1 + (B-1)C/C_s)]}$	Multilayer adsorption: inflection point	No "total capacity "equivalent
Dubinin-Radushkevich	$\frac{W}{W_0} = \exp\left[-k\left(\frac{\varepsilon}{\beta}\right)^2\right]$ (volume adsorbed)	Temperature independent: Polanyi potential theory	No limited behaviour in Henry's Law regime.

Note: Table was modified from work by (Volesky, 2003a)

There is a lot of development of new modified versions of isotherms and dynamic models. In spite of this, in most cases, no further work has been done or experiments performed to test the applicability of these models in other systems. For example, the modified BET model which is a one-dimensional model that was proposed to understand the behaviour of fixed bed with the assumption of straight run mode operation (Rangabhashiyam et al., 2014c) has only been used in one case with no further studies or evaluation done on other systems.

Although the information obtained is often useful, the following concerns have been reported by numerous researchers in the attempt to account for the inconsistencies and limitations that exist:

- The models that are used were initially developed for the adsorption of gases onto activated carbon and based on assumptions that are too simplistic for biological processes (Gadd, 2009).
- The equations cannot be applied to predict metal adsorption behaviour under changing pH, ionic strength and metal concentration in a solution (Schiewer and Volesky, 1995; Gadd, 2009)
- The application may also be limited when precipitation occurs. The Langmuir isotherm has been applied to some cases despite being theoretically invalid (Volesky, 2003a).
- The use of wrong units has led to the misapplication of the Langmuir equation in calculating thermodynamic parameters. Thus, the use of molar concentrations in comparative and mechanistic studies should be used in biosorption modeling (Tran et al., 2017).
- Other problems may include the use of unrealistically high sorbate concentrations compared with industrial or environmental context, and unattained equilibrium values (Fomina and Gadd, 2014; Tran et al., 2017).

2.4.2 Batch Kinetic Modeling

Equilibrium isotherms consist of different conditions for the biosorption process which are related to the time required for a system to reach thermodynamic stability (Ho, 2006). The extent of biosorption is dependent on the initial and final equilibrium states whereas the rate of biosorption is dependent on the process route from the initial to the final step (Ho, 2006). Sorption solid-liquid kinetics are controlled by several independent processes which take place concurrently and also involve transport phenomenon and chemical reactions (Vijayaraghavan and Yun, 2008). In porous media, these include four steps (Ho, 2006; Qiu et al., 2009): transport of the sorbate in the bulk solution, film diffusion from the bulk solution through the boundary layer of the fluid adjacent to the external surface of the biosorbent particle, diffusion through the particle, and the chemical binding reactions of the sorbate. Ideally, to properly understand the adsorption kinetics, an expression must be obtained for each step. However, this could generate a complex overall kinetic model equation that could be difficult to evaluate. Thus, most models only consider the rate-limiting steps. This facilitates the resolution of the model by reducing the number of equations. Normally, the transport process in the bulk solution and the film diffusion through the boundary layer of biosorbent are considered the rapid processes (Borba et al., 2006). Therefore, in most cases, intraparticle diffusion or chemical binding reactions are more likely to control the sorption kinetic mechanisms (Lodeiro et al., 2007).

Various kinetic based models have been developed to investigate and identify mechanisms of adsorption. In recent years, reported adsorption mechanisms involving kinetic based models have

described the reaction order of adsorption systems based on the solution concentration (Ho, 2006). These range from first-order and second-order to reversible and irreversible ones. Furthermore, reaction order based on the capacity of the adsorbent has been presented using the Lagergren's first-order, Zeldowitch's model and Ho's second-order expression (Plazinski et al., 2009). The application of second-order models has been reviewed with the earliest empirical second-order equation being applied in adsorption of gases onto a solid followed by a solid-liquid reaction system between soil and soil minerals (Ho and McKay, 1998). In recent years, pseudo-second-order rate expressions have been applied for the adsorption of pollutants from aqueous solutions onto adsorbents (Michalak et al., 2013). This equation has been used a lot due to its simplicity- there is no need to know the equilibrium capacity from the experiments as they can all be calculated from the equation (Michalak et al., 2013).

Furthermore, the pseudo-first- and second- order equations have been widely used to describe the kinetics under various conditions (Ho and McKay, 1998, 1999; Ho, 2006). However, Liu and Shen (2008) have argued that the kinetic order of the biosorption should be estimated from a general rate equation as opposed to pre-set kinetics because the reaction order cannot be theoretically determined. As such, they proposed a general rate law to justify their argument (Liu and Shen, 2008). It is often challenging to propose general models because most models are derived from different assumptions and only suitable for a specific system (Xu et al., 2013). For example, Ho et al., (2001) developed a model that describes the sorption mechanisms of lead ions onto peat. Even though the model was a success, it has limited application as it does not cater to a wide array of conditions and adsorbents. Despite certain challenges, different general models based on Ficks's law have been developed. These include the pore diffusion model (PDM), homogeneous surface model (HSDM) and, the pore and surface diffusion model (PSDM) (Xu et al., 2013).

It is evident that adsorption models have been widely developed to describe the kinetic process of adsorption however, there still exits some problems. Some of these problems have been reviewed and reported by Tien (2008) and Tran et al., (2017):

- Preparation conditions are often described as optimum however, no evidence is provided to support the claim.
- Metal ion adsorption is dependent on pH. However, the effects of pH have only been reported in terms of the initial pH of the solution with no regard given to the changes in pH during the course of the adsorption experiment.
- The equilibrium data that has been reported is empirically fitted with isotherm equations using the initial pH solution as a parameter without taking into account that equilibrium data depends on the equilibrium and not initial conditions.

It appears that the majority of adsorption studies reported in the literature are mostly theoretical as most models have not been used to test and correlate with the available data. Additionally, the available data that has been tested suggests that there is need for system variables (for example, agitation speed, solute concentration, sorbent mass, solute temperature, etc) to be tested more extensively and for other kinetic models to be used to test experimental adsorption data if a mechanism cannot be identified.

For trustworthy predictions, experiments will be carried out to determine parameters because so far, there seems to be no reliable method to theoretically predict some key parameters. The following will be incorporated into the work to make it better than the work that has already been done:

- Preparation conditions are often described as optimum however, no evidence is provided to support the claim. Thus, Design of experiments (DOE) will be used to carry out experiments that will yield reliable results, while Response Surface Methodology (RSM) will be carried out to establish the optimum operating conditions for the influential factors.
- Mechanisms will be proposed. The approach put forward by Robalds et al.,(2016) will be used as a guide to identifying the possible mechanisms during the adsorption experiments because their work highlights the errors and inconsistencies regarding metal adsorption. They further demonstrate the different approaches for grouping mechanisms. Lastly, the results obtained will also be used to interpret the kinetic data obtained.
- Kinetic data will be fitted using a proposed model established on a solid theoretical basis. The model equation and parameters will be analysed and their significance for calculations of design fixed bed operations will also be evaluated.

2.5 Theoretical Aspects

In this section, mechanisms will be explained followed by general aspects of the equilibrium isotherms and kinetic models. Furthermore, possible theoretical grounds of the most commonly applied isotherms and kinetic models, will be discussed.

2.5.1 Mechanisms of biosorption

Although biosorption using agricultural waste is promising, a major limitation is due to the lack of knowledge about the mechanisms. From literature, it has been reported that adsorption could take place through a combination of mechanisms (Figure 2.2) (Demirbas, 2008; Lü et al., 2010).

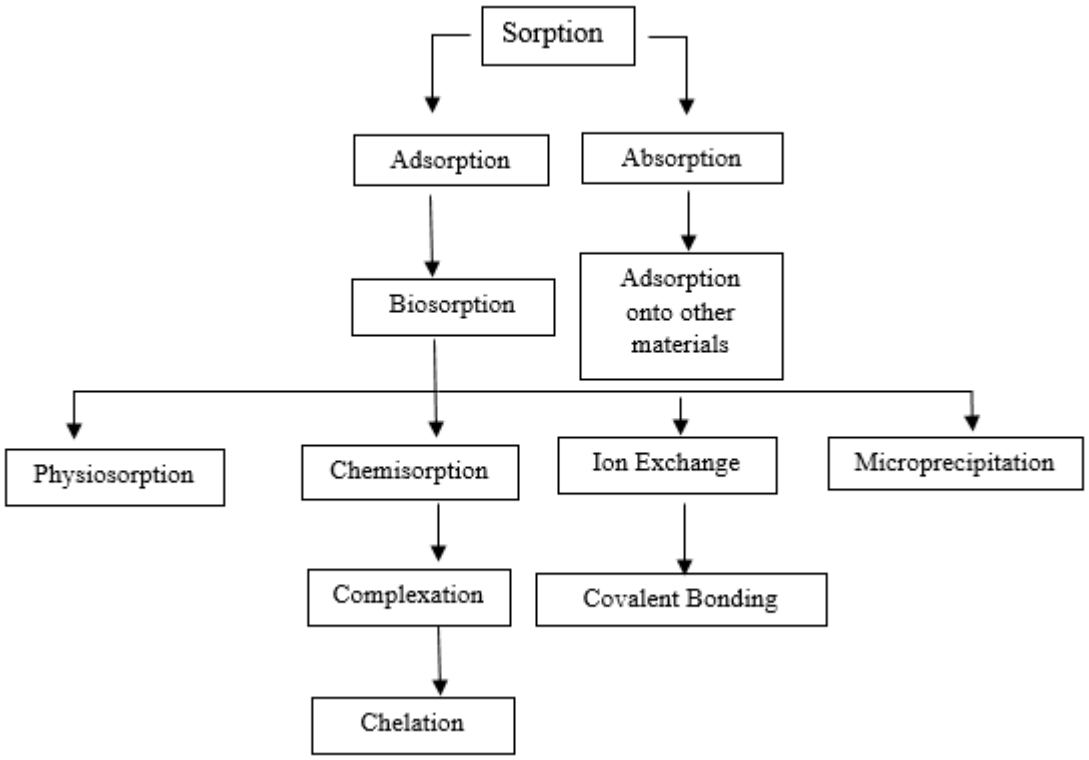

Figure 2.2: Biosorption mechanisms.

To date, it is still unclear to what degree adsorption is a chemical or physical process. Therefore, for the sake of the discussion of the results, in this section, two mechanisms of adsorption will be briefly explained. Physiosorption happens when the sorbate is bounded to the surface of the adsorbent mainly through Van der Waals forces while chemisorption involves electron exchange between the sorbent surface and sorbate molecule, resulting in a chemical reaction (Gutierrez et al., 2018). Identifying adsorbate-adsorbent interactions is the most challenging issue in the adsorption field because it depends on the type of adsorbent and adsorbate (Memon et al., 2008). Although speculations from literature give an idea, it is better to use instrumental techniques to identify the accurate mechanism. For example, an Fourier transform infrared spectroscopy (FTIR) can be used to obtain information about the functional groups on the surface of the adsorbent in order to understand how metal ions bind to adsorbents (explained in Chapter 4). However, even with this information, the mechanisms responsible for the adsorption of metal ions onto agricultural waste is still not easy to predict due to their diverse origins and chemical structures (Palma et al., 2011a). Hence, the results obtained will be compared to those in the literature to suggest possible mechanisms responsible for the adsorption of Cu ions onto banana and orange peels. However, when comparing the results to those in older studies, it must be noted that the preparation of the samples and process conditions were different.

2.5.2 Equilibrium isotherms

Within the scope of adsorption, adsorption equilibrium and the governing equations are importance because they provide the basic information required in assessing the feasibility of the adsorption process. Equilibrium data is necessary to characterize the adsorbent's ability to absorb pollutants, to select an appropriate adsorbent, and to design batch, flow-through or fixed bed adsorbers (Crittenden and Thomas, 1998).

In a solid-liquid adsorption system, the solute from the solution is removed and accumulates on the surface of the adsorbent while the solute remaining in the solution reaches dynamic equilibrium with the one adsorbed on the solid phase (Lasheen et al., 2012). Adsorption performance can be measured as the amount adsorbed (mg/g) at equilibrium or percentage removed expressed as equation 2.1 and 2.2 respectively.

$$q_{eq} = \left(\frac{C_0 - C_{eq}}{m}\right) V \tag{2.1}$$

Where c_0 and c_{eq} are the initial and equilibrium concentration, respectively. m is the adsorbent mass (mg) and V the volume of the adsorbate solution(L)

$$\%Removal = \left(\frac{C_0 - C_{eq}}{C_0}\right) \times 100 \tag{2.2}$$

Isotherm curves (Figure. 2.3) can be evaluated by varying the concentration/adsorbent dosage while keeping the other system parameters (such as pH and temperature) constant (Salman H. Abbas et al., 2014). Empirical models with adjustable parameters have been developed to describe the behaviour of experimental data over a specified range of operating conditions. Discussed below are some of the models that will be used in this project.

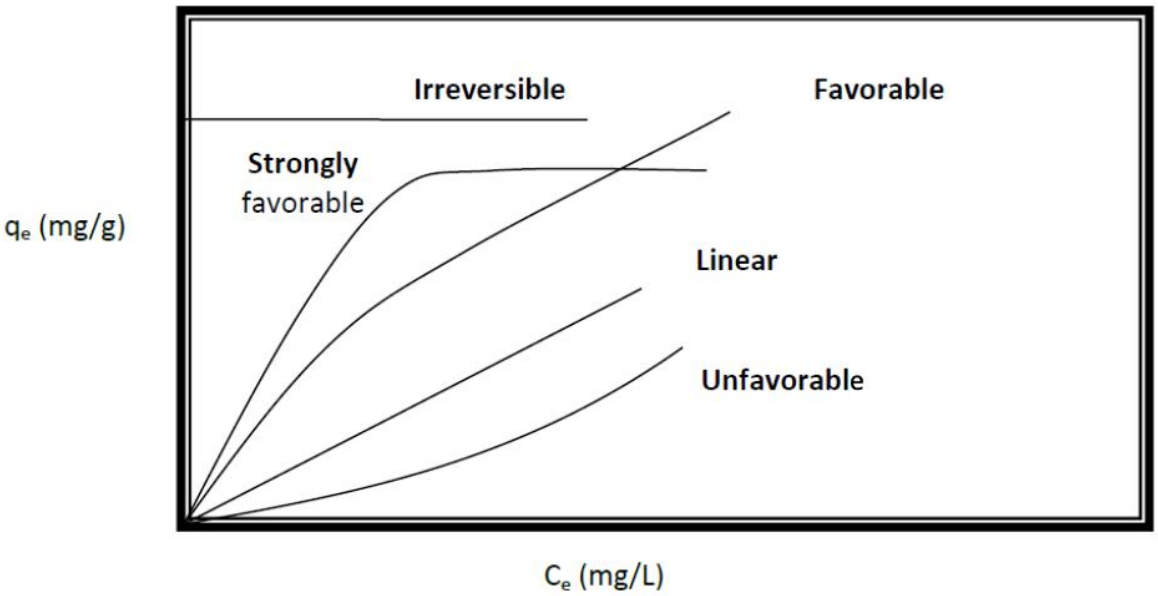

Figure 2.3: Types of adsorption equilibrium isotherm relations (Abbas et al., 2014)

The adsorption process can be complex and several isotherms have been proposed. However, for the scope of this project, attention will be given to (1) Langmuir and (2) Freundlich

Langmuir Isotherm

This is one of the most frequently applied isotherms and is governed by the following assumptions (Rangabhashiyam et al., 2014a): (1) monolayer adsorption, (2) adsorption takes place at specific homogenous sites on the adsorbent, (3) no further adsorption can take place once a pollutant occupies a site on the adsorbent, (4) all sites are identical and energetically equivalent and (5) there is no interaction between adsorbed molecules on neighbouring sites (Das et al., 2008; Rangabhashiyam et al., 2014a). Based on these assumptions, the Langmuir isotherm is represented by this expression:

$$q_e = \frac{Q_0 K_L C_e}{1 + K_L C_e} \tag{2.3}$$

Where C_e is the equilibrium concentration (mg/L), Q_0 represents the monolayer coverage capacity (mg/g) and K_L is the Langmuir isotherm constant (L/mg). This isotherm is characterized by different linear this linear form:

$$\frac{C_e}{q_e} = \frac{1}{bQ_0} + \frac{C_e}{Q_0} \tag{2.4}$$

Where the plot of $\frac{C_e}{q_e}$ vs $\frac{C_e}{Q_0}$ will yield a linear relationship. Furthermore, the key parameters can be represented by a dimensionless equilibrium parameter, R_L, referred to as a separation factor or equilibrium parameter (Foo and Hameed, 2010):

$$R_L = \frac{1}{1+ K_L C_0} \quad (2.5)$$

Where C_0 adsorbate initial concentration. R_L value indicates adsorption nature as unfavourable if $R_L>1$, linear if $R_L=1$, favourable if $0<R_L<1$ and irreversible if $R_L=0$.

Freundlich Isotherm

This isotherm was initially applied in non-ideal and reversible adsorption systems not restricted to monolayer formation. The empirical expression can be applied to multilayer adsorption with non-uniform distribution of adsorption heat and affinities over the heterogeneous surface (Rangabhashiyam et al., 2014a). The equation that describes the Freundlich isotherm is given by (Grassi et al., 2012):

$$q_e = K_f C_e^{1/n} \quad (2.6)$$

Where K_f id the Freundlich constant related to the maximum adsorption capacity (mg/g) and n Freundlich constant related to surface heterogeneity (dimensionless). It gives an indication of how favourable the adsorption process is. When n =1, the equation reduces to the linear form $q_e = k \times C_e$. Plotting q_e vs C_e yields a graph that allows for the determination (1/n) and K_f. Values of (1/n) range from 0 to 1, where the surface is said to be more heterogeneous of the value if closer to one. However, the linearized form can be expressed as (Grassi et al., 2012; Rangabhashiyam et al., 2014a):

$$ln\, q_e = ln\, K\, f + \frac{1}{n} ln\, C_e \quad (2.7)$$

Where plotting lnq_e vs lnC_e gives a slope equivalent to (1/n) and intercept of lnK_f

2.5.3 Batch kinetic models

In this section, a review of theoretical models describing the adsorption kinetics of pollutants onto adsorbents is presented. The adsorption models are made up of diffusion models and surface reaction models. In general, a kinetic model includes mass transfer equations, equilibrium relationships (Figure 2.4), and the material balance (Equation 2.1) for the reactor applied. Adsorption kinetics is dependent on adsorption equilibrium data. Therefore, kinetic models can be applied only if the required equilibrium parameters are known. If necessary, an isotherm has to be measured before the kinetic experiment (Worch, 2012).

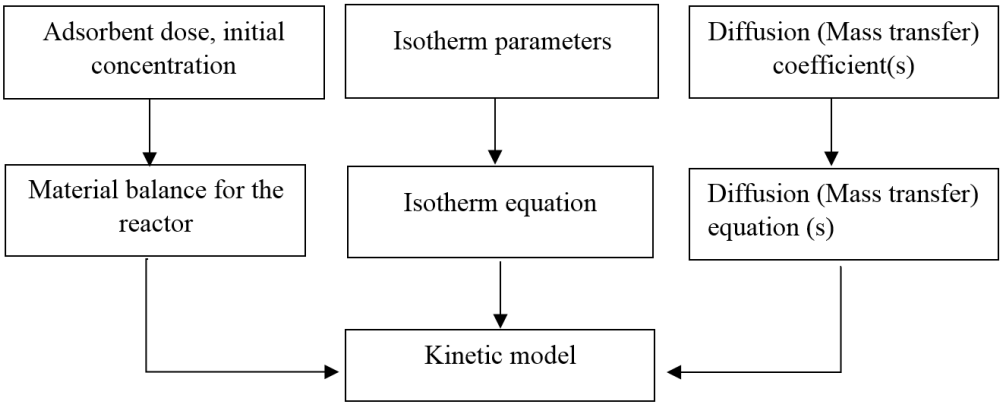

Figure 2.4: Modeling of adsorption kinetics: constituents and input data

The ability to predict the rate at which pollutants are removed from a solution is significant in the design of an effective sorption system. As a result, many attempts have been made to develop models that can adequately predict and describe the kinetics in an adsorption system (Plazinski et al., 2009b)

According to literature, adsorption can be described by the following conservative steps (Plazinski et al., 2009b; Sen Gupta and Bhattacharyya, 2011; Worch, 2012): (1) Transport to the solute in the bulk of the solution; (2) Diffusion of the solute across the liquid film surrounding the sorbent particles; (3) Diffusion of solute in the liquid contained in the pores of the sorbate particles and along the pore walls (intraparticle diffusion) and (4) Adsorption and desorption of solute molecules from the sorbent surface (Plazinski et al., 2009b). The overall process can be controlled by any or combined effect of any of these steps. Thus, in order to predict the contribution of the remaining steps, numerous models have been developed and compared to predict the behaviour of experimental data.

In an attempt to understand the mechanism of copper adsorption onto the surface and pores of the peels, the following kinetic model equations are used to analyse the adsorption experimental data for determination of the related kinetic parameters.

2.5.3.1 Diffusion models

The diffusion models assume that diffusion is the rate-limiting step. This part is divided into two parts, external mass transfer models and internal diffusional models.

Film diffusion

The film diffusion (also referred to as external diffusion) is concerned with the transport of the adsorbate from the bulk liquid to the external surface of the adsorbent particle (Worch, 2012).

The film diffusion mass transfer rate equation can be represented by (Boyd et al., 1947):

$$ln\left(1-\frac{q_t}{q_e}\right)=ln\left(\frac{6}{\pi}\right)-\left(\frac{D_i}{r^2}\right)\pi t \quad (2.8)$$

Where D_i (cm^2/s) is the film diffusion coefficient, q_e and q_t (mg/g) the values of the amounts adsorbed per unit mass at equilibrium, r_0 the radius of the adsorbent particles assumed to be spherical and time t. The values of the film diffusion coefficient, D_i, can be determined from the slope (S_i) of the linear plot of $\ln\left(1-\frac{q_t}{q_e}\right)$ vs t using the following equation (Nibou et al., 2010):

$$D_i=\frac{S_i r_0^2}{\pi^2} \quad (2.9)$$

Moreover, if film diffusion is the rate-limiting step, then the plot should be a straight line.

Internal diffusion models

In surface diffusion approach, it is assumed that the mass transfer occurs in the adsorbed state along the internal surface of the adsorbent particle.

Weber-Morris

Weber-Morris Model) is a well-known approximate equation for intraparticle diffusion and this model can be expressed as follows:

$$q_t = k't^{0.5}+C \quad (2.10)$$

where k' (mg/g $min^{1/2}$) is the intraparticle diffusion rate constant and C is the intercept, gives an idea about the boundary layer thickness, i.e., the larger the intercept, the greater the boundary layer effect. The significant part about this model is that the plot of q_t vs $t^{0.5}$ has to pass through the origin. Thus, the intra-particle model can easily be tested provided they pass through the origin which indicates a controlling influence of the diffusion process. The rate coefficient. k' could be obtained from the slope of the plots. However, it should be noted that equation approximates the pore diffusion kinetics without taking into account the contributions of the pore dimensions. The literature is silent on these aspects and a few works appeared reporting a detailed study of the impact of pore diffusion processes on heavy metals uptake and in particular, the effects of the pore radius and pore size distribution on the sorption kinetics (Wu et al., 2009a).

Boyd or Reichenberg model

The kinetic data were evaluated by the procedure given by Reichenberg (1953) and Walton (1962). For intraparticle diffusion-controlled adsorption, the following series solution was used:

$$\frac{q_t}{q_e} = 1 - \frac{6}{\pi^2}\sum_{n-1}^{\infty}\frac{1}{n^2}exp\left(-\frac{D_i n^2 \pi^2 t}{R^2}\right) = 1 - \frac{6}{\pi^2}\sum_{n-1}^{\infty}\frac{1}{n^2}exp(-n^2 Bt) \quad (2.11)$$

Where q_t and q_e are respectively instantaneous (at time t) and the equilibrium adsorbed phase concentration (adsorbed amount per unit mass of adsorbent), R the adsorbent radius, D_i the effective intraparticle diffusion coefficient. B is a parameter defined by:

$$B = \frac{\pi^2 D_i}{R^2} \quad (2.12)$$

Reichenberg (1953) showed that Eq. (1) can be well approximated by

$$Bt = \pi\left(1 - \sqrt{1 - \frac{\pi}{3}\frac{q_t}{q_e}}\right)^2 \text{ for } \frac{q_t}{q_e} < 0.85 \quad (2.13)$$

Or

$$Bt = -ln\frac{\pi}{6} - ln\left(1 - \frac{q_t}{q_e}\right) \text{ for } \frac{q_t}{q_e} > 0.85 \quad (2.14)$$

Banghan's model

Banghan's model can be represented by the following equation:

$$log\ log\left(\frac{C_i}{C_i - q_t m}\right) = log\left(\frac{K_0 m}{2.303V}\right) + \alpha\ log(t) \quad (2.15)$$

Where C_i is the initial concentration in the solution(mg/L), V (L) the volume of the solution, m(g/L), the mass of the adsorbent, q_t(mg/g), the amount of adsorbate retained at time t and K_0 the constant.

2.5.3.2 Reaction kinetic models

These models assume that the surface reaction is the controlling rate step. However, the surface reaction term does not necessarily imply that actual reaction that causes chemical bonds to form takes place on the surface but physical interactions such as the Van der Waals forces may also play a role (Largitte and Pasquier, 2016)

Pseudo 1st order model

Langmuir model this model was first proposed by Langmuir in 1918 for the description of the kinetics of gas adsorption onto solid surfaces and developed later for solution systems (Plazinski et al., 2009b; Sen Gupta and Bhattacharyya, 2011).

The differential form:

$$\frac{dq(t)}{dt} = k_1(q_e - q_t) \quad (2.16)$$

Where q_e and q_t are the values of the amounts adsorbed per unit mass at equilibrium and time t. the k_1 rate constant (min^{-1}). Integrating with respect to the boundary conditions: $q_t = 0$ at $t = 0$ and $q_t = q_t$ at $t = t$, yields:

$$q_t = q_e\,(1 - \exp(-kt)) \tag{2.17}$$

The linearized form can be expressed as

$$ln\left(\frac{q_e}{q_e - q_t}\right) = k_1 t \tag{2.18}$$

Or

$$ln(q_e - q_t) = ln\, q_e\, k_1 t \tag{2.19}$$

Equation 1 is rearranged to give

$$log(q_e - q) = log\, q_e - \frac{k_1}{2.303} t \tag{2.20}$$

The value of k_1 can be calculated from the slope of the $\ln(q_e - q_t)$ vs t. The influence of pH and temperature have not been studied theoretically because of their complexity. The wide application of this equation has been reported in literature however, there are a lot of problems associated its application (Tran et al., 2017): the first is the incorrect form of the linear equation (appendix A). The second is the calculation of the parameters (q_e and k_1). It is necessary to calculate q_e for fitting experimental data however, determining the value is a difficult task. This may be due to the fact that in many sorbate- adsorbate interactions chemisorption is very rapid at the initial stage and bad slows down, thus, is difficult to conclude if equilibrium has been attained (Sen Gupta and Bhattacharyya, 2011). Two methods have been proposed to calculate q_e to obtain an accurate estimation of the kinetic parameters and explained in detail in appendix A (Ho and McKay, 1998): trial and error and application of a non-linear optimization technique.

However, for this study and isotherm will be fitted first to obtain the required value of q_e as proposed by (2012). Furthermore, this equation is valid only for the initial 20-30 minutess of the contact time and not the entire range otherwise, they will not fit the data (Plazinski et al., 2009b). The value of k_1 depends on the initial concentration of the solution which differs for different systems. It is usually inversely proportional to the initial concentration of the adsorbate in the bulk phase (Sen Gupta and Bhattacharyya, 2011). Moreover, when considering the effect of temperature and pH on k_1 value, a general observation based on experiments indicate that the changes in k_1 cannot be accounted for by simply estimating by using an equilibrium data (Plazinski et al., 2009b)

.

Pseudo-second order equation

The most commonly used form is presented by (Foo and Hameed, 2010; Ho and McKay, 1998):

$$\frac{dq(t)}{dt} = k_2(q_e - q_t)^2 \quad (2.21)$$

Where k_2 is the rate coefficient. Separation of the variables followed by integration and application of boundary conditions (q_t = 0 at t = 0 and $q_t = q_t$ at t = t) yields a linear expression:

$$\frac{t}{q(t)} = \frac{1}{k_2 q_e^2} + \frac{t}{q_e} \quad (2.22)$$

The procedure for applying his equation is based on plotting $\frac{t}{q(t)}$ vs t that will give a linear relationship. After which, the parameters can be determined directly from the slope and y-intercept. k_2 depends on the applied process conditions. The factors that have been taken into account are initial concentration, pH of the solution, temperature and agitation of shaker rate (Foo and Hameed, 2010). The rate constant k_2 strongly depends on the initial concentration. The rate constant is inversely proportional to the initial concentration, this interpretation stems from k_2 being time scaling factor i.e. the higher the concentration, the longer it will take to reach equilibrium (Crittenden and Thomas, 1998). The influences of temperature and pH have not been studied theoretically due to their complexity. These factors are not restricted to the equilibrium features of the system but they lay a major role in the kinetics of the process

In this case, the significance of the transport of adsorbate on the surface region can be identified by varying the mechanical mixing rates. At higher agitation rates, the volume of the subsurface layer reaches a constant minimum while the rate of solute transport within it reaches a constant maximum value and can be neglected (Ho and McKay). As $t \rightarrow 0$, the initial adsorption rate, h, is defined as (Sen Gupta and Bhattacharyya, 2011):

$$h = k_2 q_e^2 \quad (2.23)$$

The initial adsorption rate, h, adsorption capacity, q_e, and rate coefficient, k_2, can be determined experimentally from the slope and intercept of the $\frac{t}{q_e}$ vs t plot. The pseudo-second order equation has been interpreted as a special kind of Langmuir kinetics (Ho and McKay, 1998; Plazinski et al., 2009b; Sen Gupta and Bhattacharyya, 2011): The line of interpretation assumes that (1) the adsorbate concentrations constant with time and (2) the total number of binding sites depends on the amount of adsorbate adsorbed at equilibrium.

2.5.4 Error Functions

The optimization of single solute isotherms requires an error function to be defined in order to be able to assess the fit of the isotherm to the experimental data. In this study, four different error functions were examined and in each case the isotherm parameters were determined by minimizing the respective error function across the concentration range studied using Microsoft Excel. In general, when values of errors function are low it means there is an agreement between the experimental and calculated data, and the model converges and is favourable (Benderdouche et al., 2018):

The sum of the squares of the errors (ERRSQ).

This error estimation method is represented by Equation 2.24:

$$SSE = \sum_{i=1}^{n} \left(q_{e,calc} - q_{e,meas}\right)_i^2 \quad (2.24)$$

This feature has significant drawbacks despite its significant use. Indeed, the calculated isotherm parameters resulting from such an error function will provide a better fit at the higher end of the concentration spectrum of the liquid phase. This is due to the magnitude of errors, and as the concentration rises, the number of errors will rise.

Where N is the number of experimental data points, $q_{e,calc}$(mg/g) is the theoretically calculated adsorption capacity at equilibrium, $q_{e,meas}$ (mg/g) is the experimental adsorption capacity at equilibrium and P is the number of parameters in each isotherm model.

Marquardt's percent standard deviation (MPSD)

This error function is similar to a geometric mean distribution which was modified to allow for the numbers of degrees of freedom of the system:

$$\sqrt[100]{\frac{1}{N-P}\sum_{i=1}^{n}\left(\frac{q_{e,calc}-q_{e,meas}}{q_{e,meas}}\right)_i^2} \quad (2.25)$$

The chai test

The chai test is the sum of the squares of the differences between the experimental and model theoretical data:

$$x^2 = \sum_{i=1}^{n} \frac{\left(q_{e,calc}-q_{e,meas}\right)^2}{q_{e,meas}} \quad (2.26)$$

The chi-square test measures the difference between the adsorbed quantities of experiments and calculated, $q_{e,\,exp}$ and $q_{e,\,cal}$, respectively. Also, the magnitude of the chi-square value depends on

the $q_{e,\ exp,}$ and $q_{e,\ cal}$ agreement: if the information assessed from the model is comparable to experimental information, it would be low and if they differ, it would be big (Dada et al., 2017).

The determination coefficient

The determination coefficient represents the percentage of variation explained by the regression line in the dependent variable. The value of the determination coefficient calculated from equation 2.27 may differ between 0 and 1.

$$R^2 = \frac{\Sigma(q_{e,calc} - \bar{q}_{e,meas})^2}{\Sigma(q_{e,calc} - \bar{q}_{e,meas})^2 + (q_{e,calc} - q_{e,meas})^2} \quad (2.27)$$

2.6 Conclusion

This chapter gave a review of the equilibrium isotherms and kinetic models. Theoretical aspects and governing processes of the models as well as other equations were provided.

3 Method and Materials

3.1 Introduction

In order to meet the set objectives of this project, this chapter will discuss or present the methods used the sample preparation, experimental methods and the analytical techniques as well as their limitations. The outline of the chapter is also presented in figure 3.1 and explained in detail in subsequent subsections.

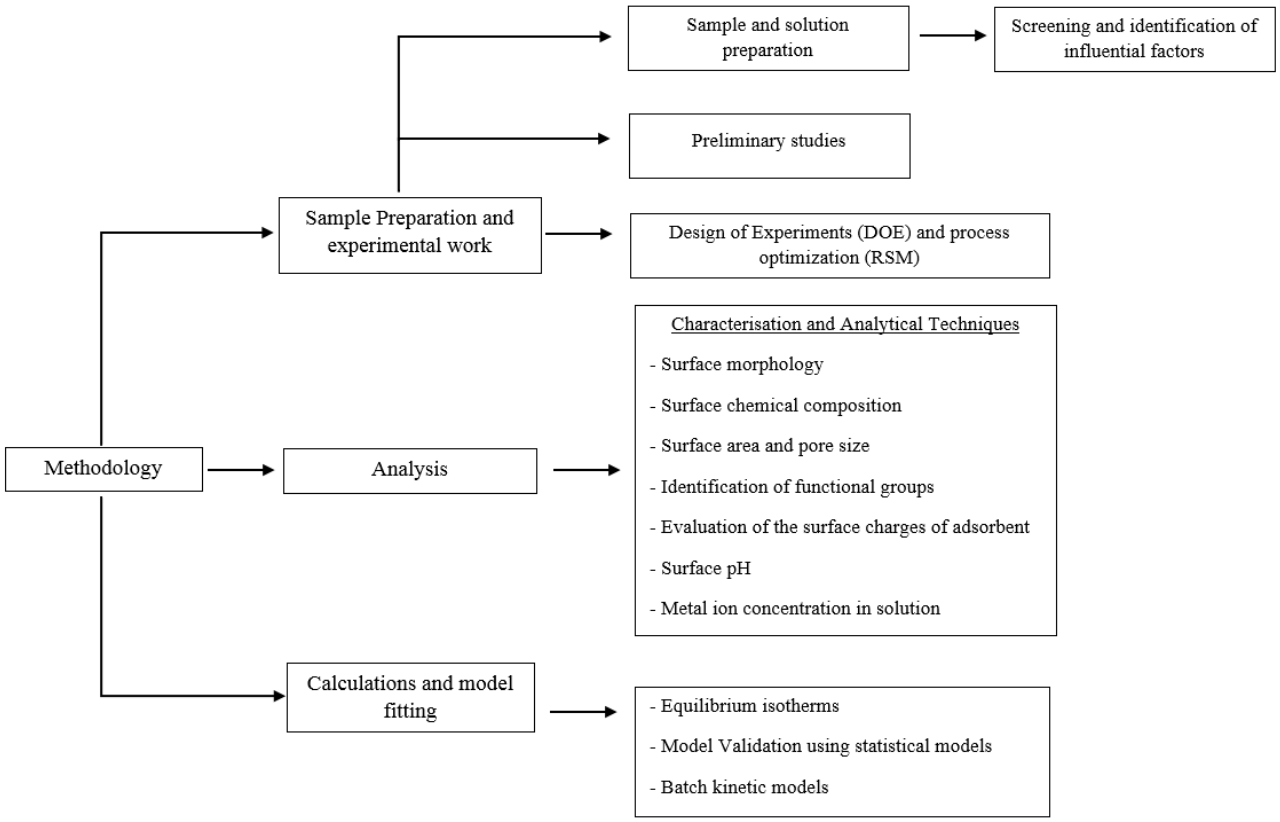

Figure 3.1: The outline of the experimental procedure.

3.2 Material preparation

3.2.1 Adsorbent preparation

The banana and orange peels were obtained from the local fruit market in central business district (CBD) Johannesburg, South Africa. Both the orange and banana peels were washed with distilled water to remove the particles that were adhered to the surface and water-soluble materials. To eliminate humidity and facilitate crushing, the drying process was done in two steps. Firstly, the peels were air-dried for 24 hours to reduce the moisture content so that they were not subjected to high temperatures in the oven that would affect their structure. Too high temperatures (150>) can cause some pores to close up which can reduce the available sites for binding (Chatterjee and Schiewer, 2014). The peels were further dried in an oven until they had reached a constant mass. From literature, the optimum drying temperatures for orange and banana peels are 85°C and 105°C, respectively (Mohamad et al., 2012). The dried peels were ground and sieved to obtain specified particle size ranges of $500 > x > 300$, $300 > x > 106$ and $106 > x$ microns, where x is the adsorbent.

3.2.2 Preparation of heavy metal solution

A synthetic solution that contains Cu metal ions was prepared by dissolving required quantities of $CuSO_4 \cdot 5H_2O$ in distilled water (see Appendix A). The same procedure was followed when preparing the other metal ions (Mn, Ni and Cr) that were used to conduct the preliminary study. In a study done by Sud et al. (2008), which was dealing with agricultural waste (banana peels, orange peels, fig leaves, etc) as adsorbents, the optimum range of pH values were reported as between 5 and 5.5 for copper adsorption. Thus, this range was used as the initial basis and the pH was adjusted by adding 0.1M of NaOH or HCl.

3.3 Experimental methods

3.3.1 Batch Experiments

Preliminary batch adsorption experiments were performed first to test the feasibility of using untreated banana and orange peels for the purpose of removing metal ions from single-solute solutions of synthetic water. These experiments were also used to determine the contact time and choose appropriate parametric conditions required for the DOE. After these parameters (i.e. temperature, initial metal concentration, bioadsorbent dosage, type of adsorbent and agitation rate) were established, a detailed adsorption study was performed.

For all batch experiments, a desired mass of the adsorbent was mixed with different concentrations of the synthetic solution in conical flasks at room temperature using a constant shaking speed at a specific pH. The HCl or NaOH was added to adjust the pH accordingly to the desired value (5-5.5). Even though, HCl and NaOH are the most commonly used reagents for pH adjustments, they were used because they are effective and relatively inexpensive. HCl and NaOH were also used in all titration experiments to determine the surface acidity and basicity. However, caution was taken

not to use too much because it would result in many free ions which would affect the results of the experimental tests (Fathy et al., 2013). The initial and final metal concentrations were analysed using the atomic absorption spectrometer (AAS). A discussion of each experimental procedure is provided below.

Preliminary experiments

The purpose of the preliminary experiments was to test the efficiency of the adsorbents that were prepared from banana and orange peels.

A 1000 ppm of stock solution of different metal ions was prepared as discussed in section 3.2.2. The experimental solutions of desired concentration of 10mg/L (see chapter 5 for details) were prepared by successive dilution of the stock solution. Eight conical flasks were filled with 100 mL of adsorbate solution with an initial concentration of 10 mg/L. The lowest concentration was chosen to perform the preliminary experiments because the adsorption process is believed to be most effect at low concentrations (Dursun, 2006). After adding 0.1 g of adsorbent, the conical flasks were shaken at 120 rpm in a thermostatic shaker at room temperature. The shaking rate was chosen based on literature from studies that used one-variable-at-a-time (OFAT) method to assess the effect of process variables (Mohamad et al., 2012). At defined time intervals of 10 minutes, one conical flask was removed and the residual concentration of the filtrate was analysed using AAS.

Isotherm and kinetic model application experiments

The purpose of this section was to investigate the equilibrium properties of the adsorption of Cu using banana and orange peels as adsorbents. The results from this chapter were later used to model the adsorption kinetics.

A solution with the desired metal ion concentration was prepared to cover the entire concentration range (from 5-100 mg/L). The experimental parameters (pH, shaking speed and temperature) were adjusted according to the specified values (Chapter 5). The adsorbate initial concentrations C_i (mg/L) in all liquid samples was predetermined. The amount of the bioadsorbent solids, m (g), that were used, were weighed for each test work and recorded. The bioadsorbent solids were added into each 100 mL sample solution that was contained in 250 mL conical flasks and the contents were mixed (through shaking) over a sufficient contact period until equilibrium was established, in this case, 120 minutes. At the end of the contact period, solids and liquids were separated by filtration. The liquid portion was analysed using (AAS). The adsorption isotherm (q_e, amount adsorbed (mg/g) vs C_f, final concentration (mg/L) was plotted. Thereafter, batch equilibrium models were applied (see Chapter 7).

In the above procedure, the initial sorbate concentration C_i was varied to obtain the points for the equilibrium isotherms plots. However, there is a variation of this method called the "tea-bag experiment" whereby a small amount of the sorbent is physically separated (contained in a permeable bag) in a large volume of solution that would not change its concentration, therefore, $C_i = C_f$ and only the solids are analysed (Volesky, 1990). However, this method is tedious and requires additional equipment for analysis. Hence, analysing the filtrate concentration through AAS was more desirable and efficient.

Lastly, the kinetic experiments were carried out by agitating ten 100 mL solutions in 250 mL conical flasks of constant Cu concentration with 3.5 g/L of adsorbents at a constant agitation speed of 120 rpm, a temperature of 35 °C and pH set between 5 and 5.5. The conical flasks were removed one at a time from the shaker at different time intervals and the last flask was removed after 120 minutes. After filtration, the liquid solution was analysed while the solid was discarded.

3.3.2 Design of experiments and process optimization

Two of the key objectives of the study can be summarised as follows: (1) screening and identifying the most statistically influential and favourable factors, and (2) optimizing the favourable parameters. Thus, DOE and RSM were used to execute these two objectives, respectively. DOE was used because it is a structured way of conducting experiments. Hence, by using DOE, more valuable and precise data about the process are obtained since the joint impact of all components is assessed (Jarrett, 2000).

Furthermore, the screening of variables (see Chapter 6) was done at the beginning of DOE in order to investigate the extent of influence of a few variables on the response (recovery of Cu) and to determine their suitable ranges. The statistical significance of each factor and associated interactive effects were evaluated using a two-level five-factor full factorial (2^5) and percent Cu removed was used as the measured response. The experimental results were analysed statistically for the significance of the factors using the probability plots, Pareto chart and statistical analysis principles (explained in Chapter 6).

3.3.3 Methodology for data analysis

The Pareto Chart

The Pareto chart is used to highlight and distinguish between the most important set of factors. The Pareto chart also shows the absolute values of the standardized effects from the largest effect to the smallest effect. The chart plots a reference line to indicate which effects are statistically significant; Bonferroni limit is the threshold above which the effects that appear at this level are significant (very important). The effect terms below the threshold of the t-limit are insignificant factors, while the effects that appear above the t-limit but are below the Bonferroni limit may possibly be significant (moderately important) depending on the line of work of the experimenter (Bhaumik and Mondal, 2016). The Pareto chart displays the absolute value of the effects thus, one can determine which effects are large but one cannot determine which effects increase or decrease the response. Therefore, to evaluate this effect, the normal probability plot of the standardized effects will be used to examine the magnitude and direction of the effects on one plot.

Normal Probability Plot

The normal probability curve is used to determine the direction, magnitude and the significance of effects. The data is plotted against a theoretical normal distribution in such a way that the points should form an approximate straight line. The effects that fall along the line are negligible, whereas significant factors will tend to depart from the line (Bhaumik and Mondal, 2016). Positive effects increase the response when the settings change from the low value of the factor to the high value. Negative effects decrease the response when their settings change from the low value of the factor to the high value of the factor (Jarrett, 2000). Effects further from zero on the x-axis have greater magnitude and thus, are more statistically significant.

The value of the effects due to a response to variation in an input parameter can be calculated mathematically using the following equation (Jarrett, 2000):

$$Effect = \frac{2}{m}\sum_{i=1}^{m}(algebric\ sign\ \times\ R_{i,observed}) \tag{3.1}$$

Where $R_{i,observed}$, is the ith observation in the experimental data and m is the number of runs. To draw the probability plot, the effects are rearranged in ascending order then numbered according to this order. Thereafter, a value of percentage is calculated based on equation (Jarrett, 2000):

$$P = \frac{(i-0.5)}{n} \times 100 \tag{3.2}$$

Where *n* is the total number of effects, P the probability of points and *i*, the order number.

Statistical Analysis Principles

The following principles are relevant for screening factors. They are an effective way to examine designed experiments (Yuan et al., 2007):

Effect of the hierarchy principle:

- Lower order effects are more likely to be more important than higher order effects and effects of the same order are likely to be equally important.
- In order for an interaction to be considered as significant, at least one of its parent factors should be significant.

The sparsity of effects principle:

The number of relatively important effects in a fractional experiment is small.

Normal plot of residuals

A residual plot is a graph that is used to assess the merit-of-fit in regression and analysis of variance (ANOVA). Analysing residual plots helps determine whether the ordinary least squares assumptions are being met. If these assumptions are satisfied, then ordinary least squares regression will produce unbiased coefficient estimates with the minimum variance (Yuan et al., 2007).

Residuals vs predicted plot

This plot is used to examine the extent of scatter around the zero lines for the entire range of the fitted values. A random pattern of residuals on both sides of 0 is favourable. Whereas non-random distinct patterns may violate the assumption that predictor variables are unrelated to the residuals. This implies that an incorrect functional for modeling the curvature may have been used (Jarrett, 2000).

After screening, factor optimization (see Chapter 7) was performed to predict the response values for all possible combination of factors within the experimental region and to identify an optimal experimental point. The RSM was used to optimize the significant factors. The design procedure for the RSM was as follows (Dutta et al., 2011): (1) designing and performing a series of experiments for the adequate and reliable measurement of the response (copper recovery), (2) developing a mathematical model, (3) finding the optimal set of experimental parameters, and (4) representing the effects of process parameters through three dimensional (3-D) plots.

In this research, the optimised results obtained by using RSM that were designed using a central composite design (CCD) and a quadratic response surface model (Equation 3.1) were fitted to the equation (Dutta et al., 2011):

$$Y = \beta_0 + \sum_{i=1}^{n} \beta_i X_i + \sum_{i=1}^{n} \beta_{ii} X_i^2 + \sum_{i=1}^{n} \sum_{j=i+1}^{n} \beta_{ij} X_i X_j + \varepsilon \quad (3.3)$$

In Equation 3.1**,** Y is the predicted response, β_0 is the coefficient for the intercept, β_i is the coefficient of linear effect, β_{ii} is the coefficient of quadratic effect, β_{ij} is the coefficient of interaction effect, n is the number of variables, and X_i and X_j are the coded independent variable.

After performing the experiments the regression coefficients were obtained and the adequacy of the model was checked using the ANOVA technique (Dutta et al., 2011). The methods that were used for analysis include Fisher's variance ratio test (F-test), model coefficient standard errors (t-test), and the correlation coefficient (R^2). Design Expert 11 (Stat-Ease, Inc.) software was used to obtain results for ANOVA, F-test, t-test and R^2.

3.3.4 Calculations and Model Fitting

Data evaluation

The removal efficiency (R) and adsorption capacity (q_e, mg/g) were calculated by Equations 2.1 and 2.2. (Defined in Chapter 2), respectively. The two equations are reproduced and given as follows

$$\%\text{Removal, R} = \left(\frac{c_0 - c_{eq}}{c_0}\right) \times 100$$

$$q_{eq} = \left(\frac{c_0 - c_{eq}}{m}\right) V$$

Isotherms and kinetic models

There is a large number of models that are available, which makes selecting a suitable model for testing mechanisms and kinetics of the adsorption process very challenging. Furthermore, the mathematical model should be consistent with the proposed mechanisms (Volesky, 2003b). In order to identify the mechanisms of the adsorption process, experiments to study system variables such as solution initial metal concentrations, sorbent particle size, and solution temperature were carried out (see Chapter 6). An adsorption model selection process for system design (Figure 3.2) was used. The linear modeling equations that will be used are explained in detail Chapter 2 Section 2.5.

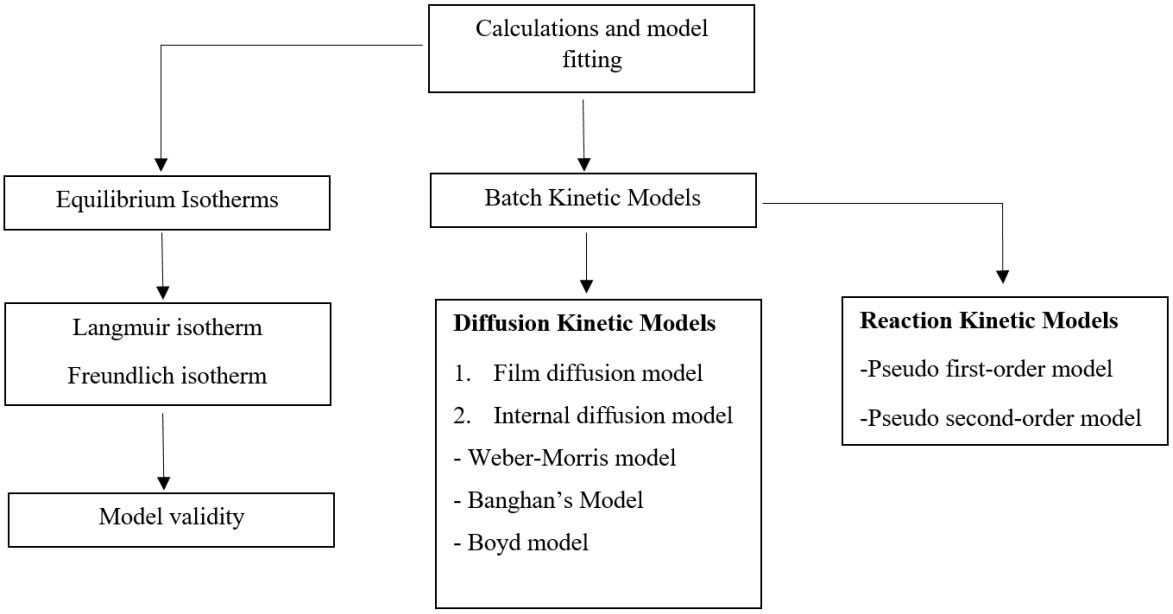

Figure 3.2: An adsorption model selection for system design.

Model Validity

The validity of a model may be quantitatively checked by statistical models (explained in Chapter 2, Section 2.5). Furthermore, the following algorithm (Figure 3.3) for linear regression was used (Kaushal and Singh, 2017):

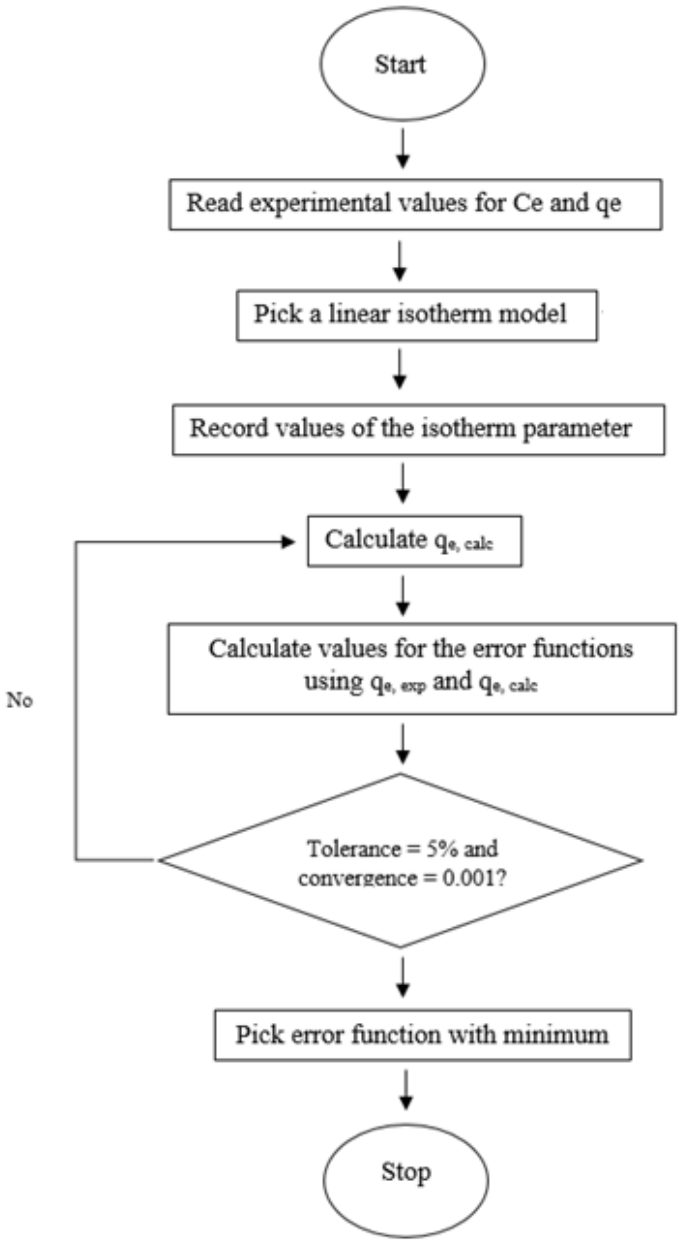

Figure 3.3: Algorithm for linear isotherm model regression using error functions(Kaushal and Singh, 2017).

3.4 Analytical techniques

The details of the equipment and analytical techniques that were used in this research project are discussed below.

3.4.1 Agitation and solution analysis equipment

All adsorption experiments were carried out in 250 mL conical flasks placed in the Labcon shaking incubator as shown in Figure 3.4 with speed and temperature adjustments made according to specific experiments.



Figure 3.4: Adsorption shaking test equipment (Labcon shaking incubator)

The Varian Spectra 200 series 240FS-AA AAS with an air/acetylene flame (Figure 3.5) was used to determine the metal concentrations of all samples using the conditions in Table 3.1 (Varian Techtron (Pty) Ltd., 1989).



Figure 3.5: Atomic Absorption Spectrophotometer (AAS) equipment for metal ion concentration analysis

Table 3.1: Metal sample conditions to determine concentration using the Atomic Absorption Spectrophotometer

Metal	Wavelength (nm)	Slit width (nm)	Lamp current (mA)	Range (ppm)
Copper(Cu)	222.6	0.2	4	1-280
Nickel (Ni)	341.5	0.2	4	1-100
Manganese (Mn)	403.1	0.2	4	0.5-60
Chromium (Cr)	428.9	0.5	7	1-100
Iron (Fe)	372.0	0.2	5	1-100

Modified from Varian Techtron (Pty) Ltd. (1989).

3.4.2 The emission scanning electron microscope

The transmission electron microscope (TEM) and scanning electron microscope (SEM) systems are the two most common types of electron microscopes. The SEM was used to study the surface morphology of the adsorbents before and after adsorption. This technique is used for high magnification of materials. TEM allows one to observe details at the highest possible resolution giving structural information about elements as small as individual atoms. It also provides information about internal structures as it passes through objects, which SEM cannot provide (Ebnesajjad, 2014). However, TEM is limited to samples that may be thin enough to allow electrons to pass through them. The thinning process is technically challenging and requires additional tools to perform (Bonnamy and Oberlin, 2016). Thus, SEM was used in the whole study because it is much faster, less restrictive and can sometimes be performed with reasonable sample preparation. It also provides well detailed three-dimensional and topographical imaging.

3.4.3 Energy Dispersive X-Ray Spectroscopy

Energy Dispersive X-Ray Spectroscopy (EDS or EDX) is a chemical microanalysis technique used in parallel with the SEM scans. The data produced by the EDX study comprises of spectra that show peaks that are related to the elements that make up the sample's true composition. Elemental mapping of the sample and image analysis can also be produced (Shrestha, 2016). Thus, while the SEM analysis was being conducted, EDX metal composition diagrams where generated for the sample banana and orange peels.

3.4.4 Brunauer-Emmett-Teller surface area

The Brunauer-Emmett-Teller (BET) method was used to determine the internal surface area of the bioadsorbent before adsorption. The standard method for determining the internal surface area is based on low-temperature gas adsorption (typically nitrogen adsorption) and the subsequent application of the BET isotherm (Lowell et al., 2004). Ideally the BET evaluation provides a particular surface area assessment of materials by way of nitrogen multilayer adsorption measured as a function of relative pressure using a totally automated analyser. The technique is made of an external area and pore region evaluations to decide the total specific surface area (in m^2/g). It yields essential information for studying the effects of surface porosity and particle measurement in many applications (Allen, 1981). As part of the BET analysis, Barrett-Joyner-Halenda (BJH) analysis was also used to determine the pore area and specific pore volume using adsorption techniques. This technique characterizes pore size distribution independent of the external area due to the particle size of the sample (Allen, 1981).

3.4.5 X-ray diffraction

X-ray diffraction (XRD) is a powerful non-destructive technique used to characterize crystalline materials. It gives information about the structures, phases, texture and other structural parameters such as average grain size, crystallinity and crystal defects. X-ray diffraction peaks are generated by the constructive interference of a monochromatic X-ray laser, dispersed from each set of lattice planes in a sample at different angles (Hafizovic et al., 2007).Therefore this analytical tool was used to determine whether the peels are crystalline in nature of amorphous.

3.4.6 Fourier transform infrared spectroscopy

There are several types of infrared spectrometers in the world, but the most widely used ones are the fourier transform infrared spectroscopy (FTIR). The FTIR spectrometers are more modern and have numerous performance advantages over dispersive instrumentation. Some of the advantages include spectral quality, data collection speed, and reproducibility of data (Rey et al., 1989). In this study, the FTIR was used for identifying the different functional groups present on the surface of the peels. It was also used to observe how the structure changed after the adsorption of heavy metal ions.

3.4.7 Determination of surface charges and pH

The following analysis was carried out using the method outlined by Fiol and Villaescusa (2009) and Pathak et al. (2016). Titration was used to determine the surface acidity and basicity of the banana and orange peels. This method assumes that protons (H^+) and hydroxyl groups (OH^-) determine whether the surface of the peels is acidic or basic. The functional groups on the surface accept or donate protons, therefore, the surface will be positively charged if it accepts protons from an acidic solution and negatively charged if it gives protons in a basic solution (Pashai Gatabi et al., 2016; Pathak et al., 2016a).

Surface acidity: To 50 mL of a 0.1 M solution of NaOH, 0.5 g of bioadsorbent material was added. The sample was shaken continuously in a thermostatic shaker for 24 hours to allow for sufficient mixing, after which it was filtered. The titrant, in this case, 0.1 M HCl, was added through a burette to the filtrate containing 0.1 M NaOH to determine the endpoint. Phenolphthalein was used as an indicator. After the endpoint was established, titration calculations (explained and illustrated in Appendix A) were performed to determine the surface acidity.

Surface basicity: To 50 mL of a 0.1 M solution of HCl, 0.5 g of bioadsorbent material was added. The sample was shaken continuously in a thermostatic shaker for 24 hours to allow for sufficient mixing, after which it was filtered. The titrant, in this case, 0.1 M NaOH, was added through a burette to the filtrate containing 0.1 M HCl to determine the endpoint. Phenolphthalein was used

as an indicator. After the endpoint was established, titration calculations (explained and illustrated in Appendix A) were performed to determine the surface basicity.

Surface pH: To 50 mL of distilled water, 0.5g of bioadsorbent material was added. The sample was shaken continuously in a thermostatic shaker for 24 hours to allow for sufficient mixing. This mixture was then filtered and the final pH was determined. Thus, giving the pH of the surface of the adsorbent.

3.4.8 The point of zero charge

The point of zero charge (pH_{pzc}) is an important adsorbent parameter that aids in understanding the adsorption of charged species and the influence of pH on the adsorption process (Bhaumik and Mondal, 2016). Several techniques such as potentiometric mass titration (PMT), and immersion technique have been used to determine the pH_{pzc} of many materials (Pashai Gatabi et al., 2016). However, for this study, the immersion technique was used because of its simplicity.

The procedure by Fiol and Villaescusa (2009) was followed. A solution of 50 mL of KNO_3 was each poured into 12 conical flasks. The pH of this solution was adjusted across a range of 2-12 by adding either 0.1 M HCl or 0.1 M NaOH. A mass of 0.5 g of the orange or banana peels was added to a series of these flasks containing different pH values. The flasks were then shaken for 48 hours in a thermostatic shaker at 30℃. The final pH (pH_f) of the solution was measured for each flask after 48 hours of shaking. A plot of ΔpH ($pH_f - pH_i$) vs pH_i was plotted and the value at which the graph cuts the x-axis gave the value of the point of zero charges.

3.5 Summary

The materials and methods used in the study were presented and discussed in this chapter. The chapter focused in particular on the following activities which constitute the study's laboratory testing aspect:

- Preparation of the adsorbent and synthetic solution
- DOE and RSM
- Batch experiments for preliminary studies, equilibrium isotherms and kinetic studies.

The next chapters (Chapter 4 through to 9) will focused on discussing the results obtained using the methods outlines in this chapter.

4 Characterization of Banana and Orange Peels

The characterization of the structure and the surface chemistry of biosorbents is important in the development of the adsorption process. Furthermore, the physical and chemical characteristics of bioadsorbents are pivotal in identifying and interpreting the metal binding mechanisms on the surface of the adsorbent. Thus, to obtain detailed information about the structure, morphology, and composition of the adsorbents, a combination of characterization techniques were used.

This section presents and discusses the results for the characterization of the adsorbents using Brunauer-Emmett-Teller (BET), Scanning Electron Microscope (SEM), X-ray Diffraction, Fourier Transform Infrared Spectroscopy (FTIR), and characterization based on titration methods (surface pH, Point of Zero Charge pH_{PZC} and surface charges).

4.1 Scanning Electron Microscopy

Characterization by SEM offers topological and elemental information of the solids. The surface morphology of the adsorbents before and after Cu adsorption was observed using the Carl Zeiss Field Emission SEM. The samples were coated with gold and palladium before the investigation to enhance electron conductivity. Therefore, in the study of copper adsorption onto banana and orange peels, the SEM was used to acquire surface topology of unloaded and loaded adsorbents.

The SEM micrograph (Figure 4.1A) of the banana peel before adsorption shows a heterogeneous, rough surface with crater-like features which indicates the presence of lignin, pectin, and other viscous compounds (Ali et al., 2016). The electron micrographs (Figure 4.1B) also revealed that the particles are of irregular but similar shape, and its surface exhibits a micro-rough texture, which can promote the adherence of Cu. Figures 4.1C and 4.1D are SEM characterization of the banana peel after adsorption, they showed a complete change in surface texture. After adsorption of Cu ions, the fibrous structures disappeared, and a smoother surface with bigger and agglomerated particles was observed (Figure 4.1C). These changes in the morphologies are in good agreement with the literature for various materials (Liu et al., 2012).

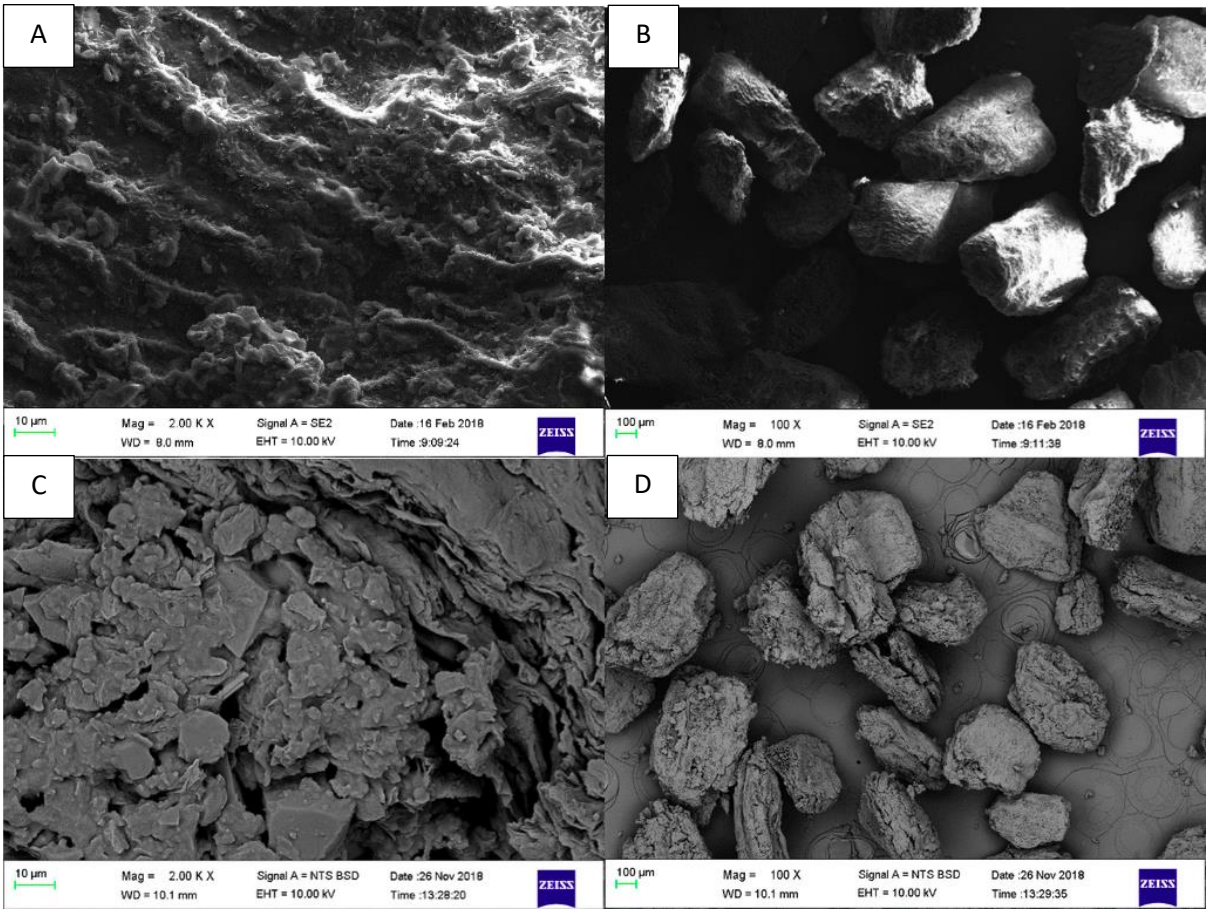

Figure 4.1: SEM of banana peels. The micrographs (A and B) depicts banana peels before adsorption at x 2.00 and x 100 magnification while the banana peel micrographs (C and D) were observed at x 2.00 and x 100 magnification after adsorption.

The micrographs displayed in Figure 4.2 showed the view of the orange peel before (Figures 4.2A and 4.2B) and after adsorption (Figures 4.2C and 4.2D). The surface of the orange peel was uneven and highly rough (Figure 4.2 A). In addition, sharp and irregular particles varying in shape and size can be seen distributed randomly on the surface of the orange peel. At a higher magnification, some pores can be observed in figure 4.2 B. The SEM image (Figure 4.2B) shows a heterogeneously porous structure. After adsorption of Cu ions, a significant change can be observed as depicted in figure 4.2C and 4.2D. The rough surface is now fuller and smooth with less irregular particles seen distributed on the surface (Figure 4.2C). Crater-like structures can be seen but no pores are observed (Figure 4.2D). Lastly, a hollow structure with valleys and a few protruding peaks can be noticed (Figure 4.2C and D). Dhal et al. (2018) also reported the same observations during adsorption of metal ions using orange peels.

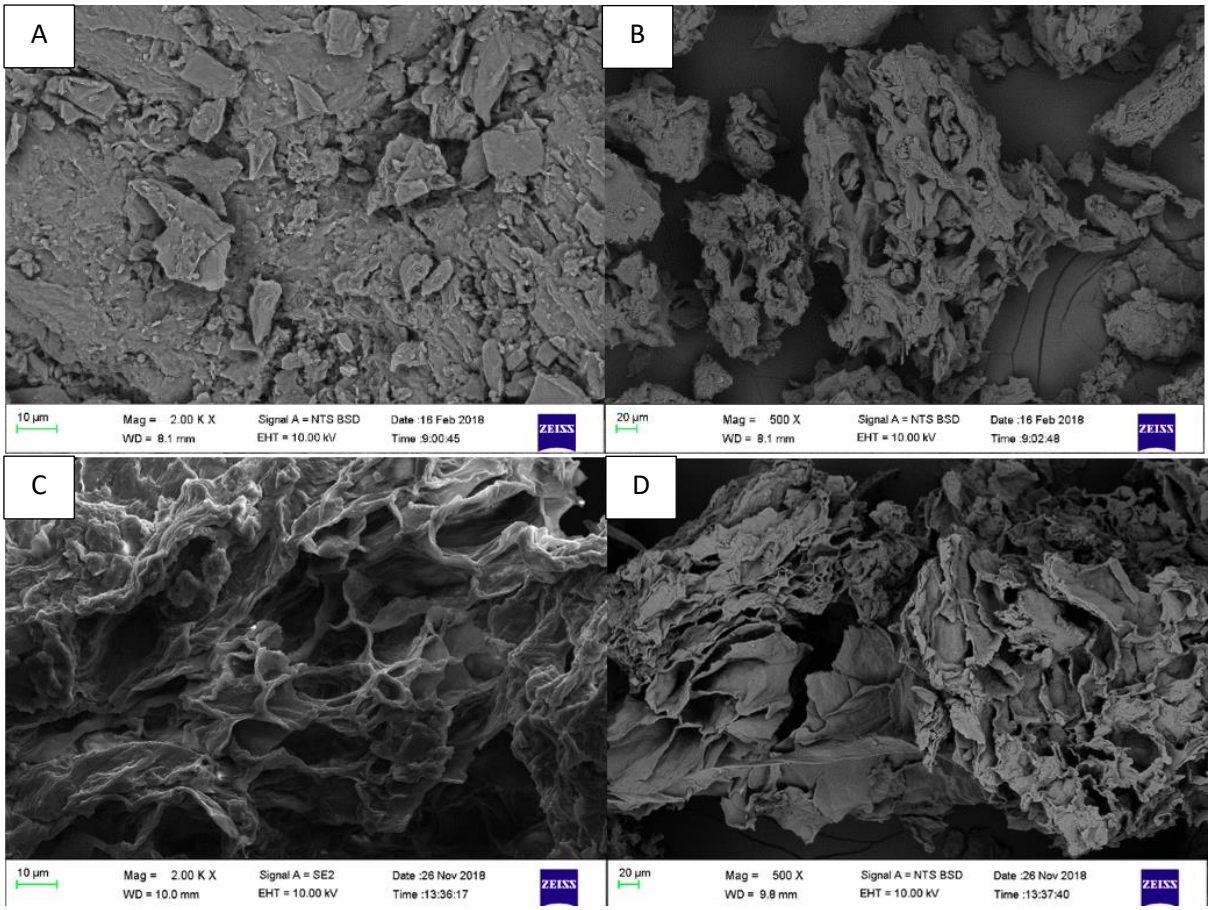

Figure 4.2: SEM of orange peels. The micrographs (A and B) depicts orange peels before adsorption at x 2.00 and x 500 magnification while the orange peel micrographs (C and D) were observed at x 2.00 and x 500 magnification after adsorption.

4.2 Energy dispersive X-ray spectroscopy

EDX is an analytical tool used to determine the elemental composition of materials. Thus, in order to know the composition of the fruit peels, the elemental analysis was done with the use of EDX analysis. The EDX analysis of the untreated banana peel as shown in figure 4.3A, indicated the presence of various elements (carbon, chlorine, oxygen, and silicon) along with a high amount of potassium, while EDX spectra of the copper-adsorbed banana peel (Figure 4.3B) showed an additional peak confirming the adsorption of copper onto the surface of the banana peel. After adsorption, changes in peak intensities were observed while the potassium and chlorine peaks disappeared. This can be attributed to the dissolution of KCl from the banana peel when in contact with the copper aqueous solution (Arunakumara et al., 2013).

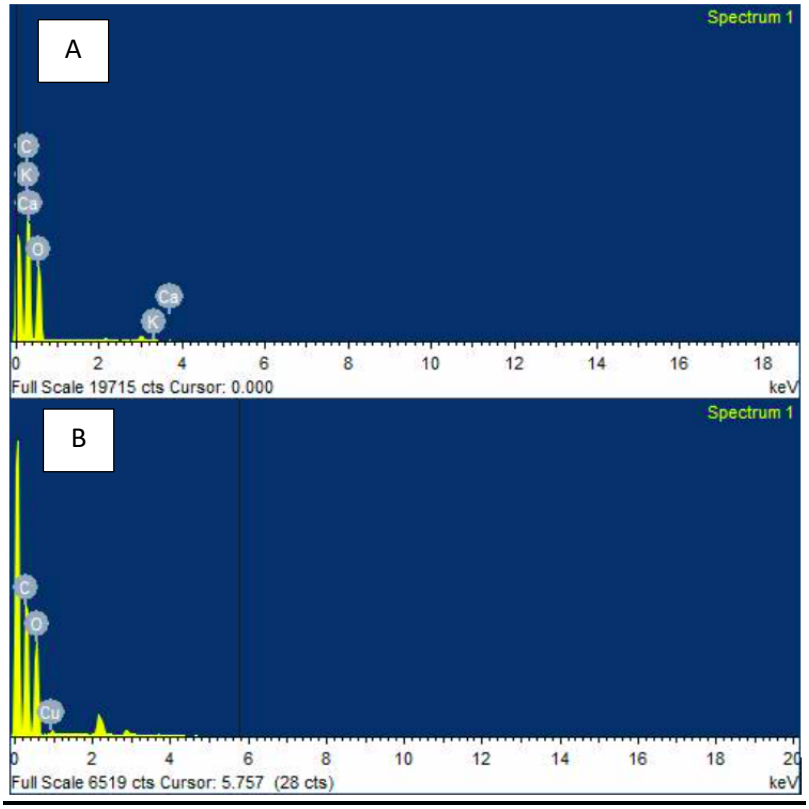

Figure 4.3: EDX image of banana peels before (A) and after (B) adsorption.

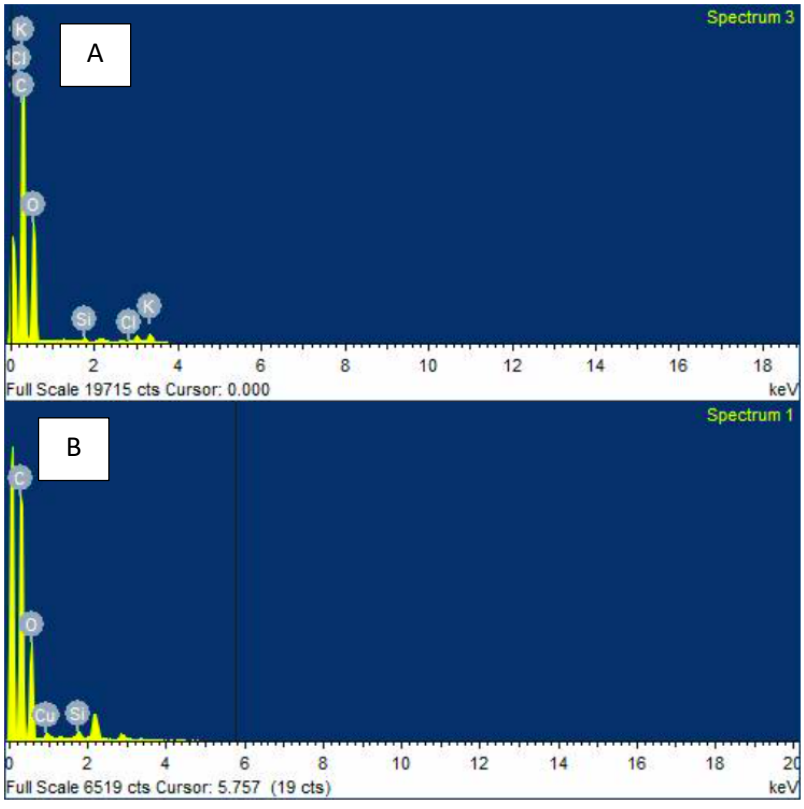

Figure 4.4: EDX image of orange peels before (A) and after (B) adsorption**.**

The elemental analysis of orange peel before and after adsorption can be seen in figures 4.4A and B, respectively. The presence of elements such as carbon, oxygen, calcium, and potassium were observed on the peels before adsorption (Figure 4.4A). However, due to adsorption of copper ions onto the orange peel, the calcium and potassium peaks disappeared suggesting the possibility of ion exchange between the sorbate and adsorbent (Figure 4.4b)(Feng and Guo, 2012).

From the data in the EDX figures above, it is apparent that hydrogen is not present in the spectra when it is expected to be as the peels are organic materials. he reason given for this observation by Stojilovic (2012) is that EDX is related to the non-valence shell K-shells. Hydrogen does not have a K shell but it only has a K shell in covalent bonding, and it only shares this electron. Therefore, the appearance of a signal can be observed from Na in energy dispersive SEM and the second-row elements in wavelength dispersive SEM (Stojilovic, 2012).

4.3 BET characterization

4.3.1 BET surface area and porosity

The pore-structure of a porous media influences most of its behaviour, such as elastic and mechanical behaviour, movement and flow of fluids, etc., which makes understanding and quantifying of the pore-structure parameters crucial in modeling the behaviour of porous media (Worch, 2012). Therefore, in this section, the bioadsorbents were characterized in terms of their surface properties such as surface area and pore volume. The properties were determined by using the nitrogen adsorption method fitted by the BET equation. The results are summarized in tables 4.1 and 4.2.

Table 4.1: Physiochemical properties of unmodified banana peels in their size ranges (106, 300 and 500 microns)

Measured parameters	Particle size (microns)		
	>106	106 < x < 300	300 < x < 500
External surface area (m^2/g)	0.4911	0.6751	0.4652
BET surface area (m^2/g)	0.4054	0.4142	0.7582
Pore volume (m^3/g)	0.000569	0.000422	0.000376
Pore size (nm)	5.61052	3.63072	3.63072

Table 4.2: Physiochemical properties of unmodified orange peels in three size ranges (106, 300 and 500 microns)

Measured parameters	Particle size (microns)		
	>106	106 < x < 300	300 < x < 500
External surface area (m^2/g)	16.9432	9.6383	4.5685
BET surface area (m^2/g)	11.9471	6.4530	3.0216
Pore volume (m^3/g)	0.011184	0.006962	0.004243

Pore size (nm)	3.74455	4.29318	5.61731

Surface area is an intrinsic quality of powdered and porous materials that gives critical information about the adsorption capacity and it is expressed as surface area per unit mass of sample or specific surface area (Liu et al., 2012). There are two types of surface areas that play important, but different roles in the performance of the adsorbents; (1) the external surface area which has a strong influence on the rate of mass transfer during adsorption based on Equation 4.1 (Worch, 2012), (2) internal surface area which is often referred to as the BET surface area. Moreover, the size of the internal surface area is related to the pore system. Typical ranges for BET surface area for common adsorbents are given in Table 4.3. However, according to Gregg & Sing (1983) the external sample specific surface areas are negligible and insignificant in comparison to that on the 'internal' pore wall. However, this cannot be the case for the banana and orange peels because the difference between the external and internal surface areas is very small (see Tables 4.1 and 4.2).

$$\text{Mass transfer} = \text{Mass transfer coefficient x area available for mass x driving force} \quad 4.1$$

From Tables 4.1 and 4.2, it can be seen that the orange peels have larger external and internal surface areas across all particle size ranges as opposed to the banana peels. Therefore, it can be assumed that orange peels are more porous than banana peels because in line with previous work that has been done (Hossain et al., 2012), porous materials tend to have bigger internal surface areas. Furthermore, porous adsorbents are used in water treatment and they have large surface areas (Leofanti et al., 1998).

Commercial adsorbents are also compared with bioadsorbents and it can be seen from the results presented in tables 4.1 and 4.2 that the surface areas of the fruit peels are very low compared to the engineered adsorbents (Table 4.3). According to Pathak et al. (2017), the low surface area can be caused by the operational complexity of degassing the lignocellulosic samples as it is a characteristic feature of carbonaceous materials. Similar results have been observed in previous studies (Lowell et al., 2004). However, the BET surface area can be improved by chemical washing as it is also capable of unclogging pores after they have been exposed to high temperatures (Jaria et al., 2017).

Table 4.3: Representative internal surface area ranges for different adsorbents**.**

Adsorbent	BET Surface Area (m^2/g)
Activated carbon	600 - 1200
Polymetric adsorbent	300 - 1400
Aluminium oxides	150 -330
Granular ferric hydroxides	150 - 350
Zeolites	400 - 900

Modified from (Worch, 2012)

4.3.2 Particle size

In this study, three different particle sizes were studied as presented in Tables 4.1 and 4.2. From the results, it can be seen that the surface area increased with decreasing particle size. Similar trend from previous studies exhibited the same relationship. For example, Martín-Lara et al. (2013) demonstrated that smaller particles generally show a higher surface area which in turn results in greater adsorption capacity and shorter equilibrium times. A study also conducted by Hossain et al. (2012) on the biosorption of Cu(II) from water using banana peel based biosorbents, showed an increase of 74 to 96% in the adsorption capacity when the size of the particles was decreased from 600 to 70 microns. An increase in surface area due to a decrease in the particle sizes was the reason for this observation. Studies by Martín-Lara et al. (2013) and Pathak et al. (2016) have equally confirmed this trend.

Therefore, it is always expected for smaller particles to remove more metal ions from a solution, however, contrary to these reports, Liu et al. (2012) suggests that relatively small different sized particles do not show a significant difference in their surface area thus, the difference in adsorption capacity will not be significantly different. The main explanation given by Liu et al. (2012) was that the different powdered particles still had similar thickness implying that they have similar surface areas and interactions between the particles and the sorbate solution.

4.3.3 Pore size, shape and distribution

The pore size is an important adsorbent parameter. As discussed in Section 4.3.2, the surface area of the adsorbent directly affects the analyte retention. Pore size defines an ability of the analyte molecules to penetrate inside the particle and interact with its inner surface as most surface molecular interaction mainly occur on the inner particle surface (Sing, 2001). Furthermore, the pore shape is mostly unknown, but it could be approximated by the model. Three basic pore models exist (Leofanti et al., 1998): (1) cylindrical pores, circular in cross-section, (2) ink-bottle pores having a narrow neck and wide body, and (3) slit-shaped pores with parallel plates. The decision on the choice of which model is appropriate for a particular adsorbent is usually based on the cross-calculations of pore volume and surface area, and comparison with the experimentally measured

values. In this work, the Barrett-Joyner-Halenda (BJH) method was used. The model is based on the assumption that pores have a cylindrical shape and that pore radius is equal to the sum of the Kelvin radius and the thickness of the film adsorbed on the pore wall (Dias and Ciminelli, 2000). Thus, the pore shape was assumed to be cylindrical based on the used BJH model.

Most engineered adsorbents contain large internal surface areas with a large number of pores with different shapes and sizes. Referring to the International Union of Pure and Applied Chemistry (IUPAC) classifications in Table 4.4, there are three types of pores that can be identified. The results presented in Tables 4.1 and 4.2 show that the pores of the banana and orange peels can be classified as mesopores (1< x <25 nm). Macro and mesopores are typically applicable in mass transfer operations that take place in the inner particles of the adsorbent whereas the micropore volume is mainly used to determine the internal surface which is related to adsorbent capacity (Haul, 1982).

Table 4.4: IUPAC classification of pores

Pore Class	Range of the pore (nm)
Macropore	> 25
Mesopore	1<x<25
Micropore	<1

Modified from (Worch, 2012)

Lastly, pore diameter and volume also influence adsorption because they determine the extent of diffusion of the pollutant molecules into the pores (Rangabhashiyam et al., 2014c). The pore volume and diameter were also determined and presented in Tables 4.1 and 4.2. From this data, we can see that the peels have relatively small pore sizes. Their pore volume also increased with a decrease in particle size for both peels. This may be due to the increased surface area; the more area of the surface that is exposed, the more pores are available for interactions.

The pore size and volume structure are very important, but the measured number is not always an indication that the volume of pores identified will all participate in the adsorption process (Rangabhashiyam et al., 2014c). This means that the amount and distribution of pore sizes in a given adsorption preparation may be such that some of the internal surface areas are completely inaccessible to large ion molecules and may restrict the rate of adsorption by impeding the diffusion of ions throughout the porous medium (Leofanti et al., 1998). Thus, the availability of pores does not necessarily mean they are active and ready to receive ions. In addition, the adsorbent peels exhibit multiple scale pore-structures that are more complex than those of conventional adsorbents which means the small pores may affect the assumption of standard

continuum approach which may result in a change of the physics of transport mechanisms (Hubbe et al., 2011). However, further investigation is needed.

4.4 X-Ray Diffraction Spectroscopy

XRD uses destructive and high accuracy rays to detect single crystals, polycrystalline to amorphous materials (Jaishankar et al., 2014). From the XRD pattern, you can determine what crystalline phases or amorphous materials are present in the adsorbent (Speakman, 2016). Thus, the XRD was used to investigate the type of phases that are present in the peels as well as suggest how each phase will affect the adsorption of Cu. This analysis was only done before adsorption.

The results obtained from the XRD analysis of orange and peels are shown in Figures 4.5 and 4.6, respectively.

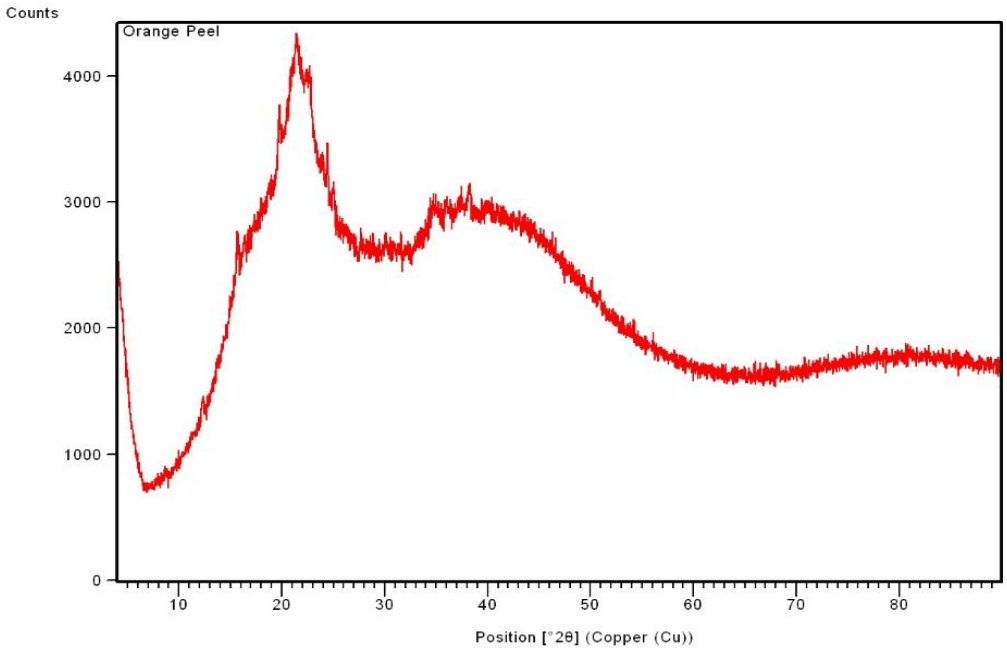

Figure 4.5: A diffractogram of an XRD analysis of orange peels before adsorption showing the intensity as a function of the diffraction angles.

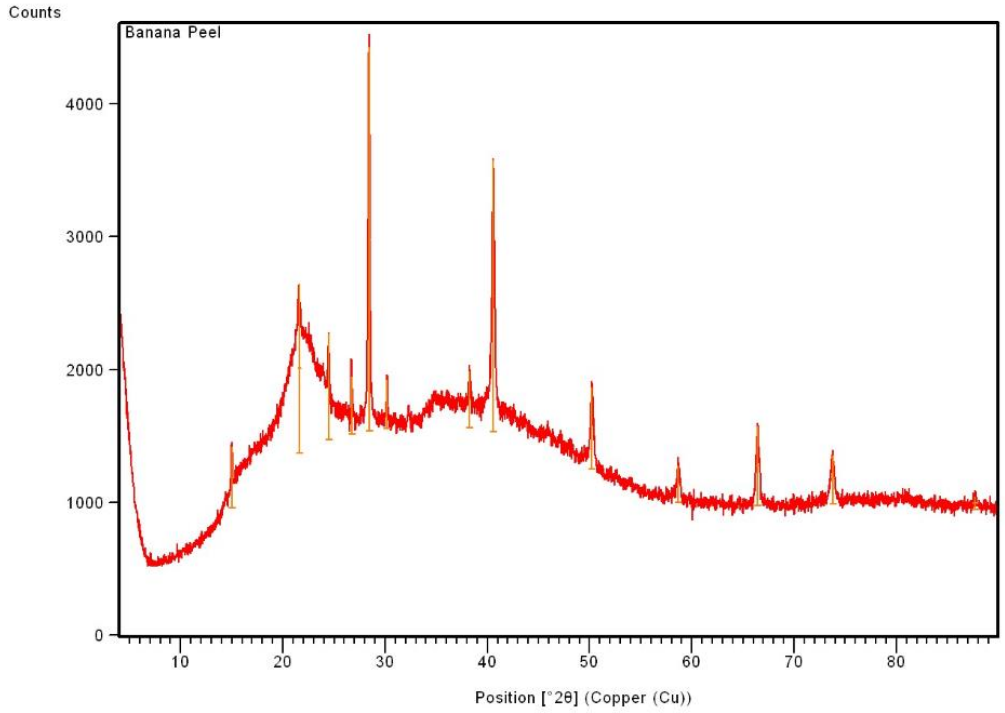

Figure 4.6: A diffractogram of an XRD analysis of banana peels before adsorption showing the intensity as a function of the diffraction angles.

The diffractogram of the orange peel (Figure 4.5) shows a broadband between 30° and 50° and a low-intensity band characterized by a wide bump consisting of scattered X-rays. Furthermore, the X-ray diffraction spectrum (Figure 4.5) did not exhibit well-defined peaks in any region, which indicated that no discrete mineral phase was detected. Thus, the orange peel has a completely amorphous structure. From the diffractogram presented in Figure 4.6, it is apparent that the banana peels are characterized by a broad hallow band that contains within its high-intensity peaks seen as the narrow distinct peaks. Therefore, it can be assumed that the broadband in the structure contains smaller crystallites and this can be seen by the regions of regular arrangements present in Figure 4.1 B from the SEM results. Hence, from the figures above, it can be seen that banana peels contain both amorphous and crystalline phases while orange peels contain mainly amorphous phases.

The degree of adsorption is influenced by the arrangement of the structure of the adsorbent. Structural phases form when bundles of cellulose aggregate together to form microfibrils in which highly ordered (crystalline) regions exist with less ordered (amorphous) regions (Demirbas, 2008). Interestingly, this can be observed in the SEM section where the banana peels (Figure 4.1) exhibit a surface morphology consisting of particles arranged in an orderly pattern whilst the orange peels (Figure 4.2) consist of particles that are less ordered. Furthermore, the quantity and distribution of crystalline and amorphous regions in the peels vary depending on the type of sample and the method of measurement (Young and Rowell, 1986). During adsorption, when the solution is in contact with the adsorbent, adsorbents containing more amorphous regions tend to have better

adsorptive capacities because the aqueous solution is able to come into contact with the large surface. This is due to its disordered structure thus, making reaction sides more accessible (Acemioglu and Alma, 2001). Hence, the adsorption capacity depends on the degree of crystallinity, amorphous regions and void regions of an adsorbent (Lee et al., 1983). Therefore, based on the results obtained, orange peels are expected to be a better adsorbent because they are amorphous in structure.

The relationship between adsorption and crystallinity has been widely investigated. For example, Xie et al. (2014) used activated carbon from orange peels. He explained that the whole wall of activated carbon is composed of graphite crystallite that decreased in scale due to the widening of the internal structure disordered so as to form a larger specific surface area. Thus, the lower the crystallinity, the larger the specific surface area. The same trend can be observed when one compares the results obtained from the BET and XRD analysis for both the peels. From the reported results, banana peels had lower surface areas compared to the orange peels and according to the XRD results obtained (Figure 4.5), they are also crystalline in structure thus, confirming this statement. The opposite applies for the orange peels.

4.5 Fourier transform infrared spectroscopy

Surface functional groups are one important characteristic of an adsorbent which is largely characterized by the FTIR. However, this method is only able to provide a qualitative description of the surfaces of the adsorbents. Thus, the FTIR was used to identify functional groups present on the surface of adsorbents. It was further used to compare and evaluate surface changes after adsorption.

4.5.1 Identifying the peaks on the peels

The aim of this subsection is to identify the functional groups that are present on the surface of the adsorbents and discuss how these would affect the performance of the material.

Figure 4.7 shows the FTIR spectra of the banana and orange peels between 4000 and 500 cm^{-1}. The ascending and descending patterns of the spectrum, the number of peaks and their sharpness indicate the presence of the functional groups. From the results obtained, it can be seen that both spectrums of the peels (Figure 4.7) show similar features. When analysed further between the wavelength range of 1000 and 1800 cm^{-1} distinct high-intensity peaks start to form. However, as the wavelength approaches 2000cm^{-1}, the number of low-intensity peaks start to form and the strength starts to decline only to form three observable distinct peaks between 2800 and 3500 cm^{-1}. After which, the spectrum starts to increase forming low-intensity peaks near the end of the spectrum. The assignments of these bands for both banana and orange peels are discussed below.

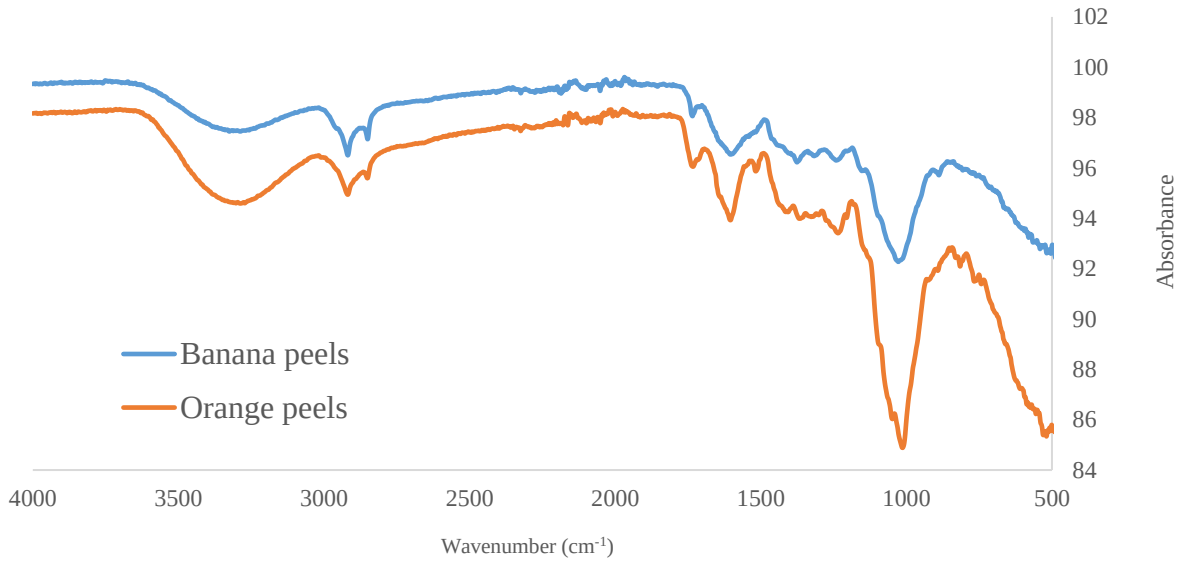

Figure 4.7: FTIR spectrum of dried banana and orange peels before adsorption.

The spectrum presents the characteristic band corresponding to the cellulose besides lignin (Liang et al., 2010). Therefore, in figure 4.7 the FTIR spectrum of the dried banana peels shows the stretching absorption band centred at 3341cm^{-1} that represents OH groups in the banana peels while the band observed at the 2891cm^{-1} was assigned to the stretching vibrations of C-H stretching of alkanes. The band appearing at 2856 was assigned to the C-H stretching of carboxylic acids. The C=O of esters and the anion COO^- stretching were assigned to 1734 and 1613.6 cm^{-1} vibrational modes respectively. The peak appearing at 1035cm^{-1} was assigned to C-O stretching of ethers/esters and 884.6 to N-H deformations of amines (Noeline et al., 2005; Kamsonlian et al., 2011a).

In figure 4.7 looking at the orange peel spectrum, the most intense peak in the high energy region around 3413 cm^{-1} is due to the long O-H stretching of alcohols, phenols and carboxylic groups, as in pectin, cellulose and lignin. Thus, indicating the availability of "free" hydroxyl groups on the surface (Liang et al., 2011). The intense band at 1045cm^{-1} corresponds to C-O-H/C-O-R (alcohols or esters) while the distinctive band at 2925cm^{-1} 1860cm^{-1} is related to the presence of the symmetric and asymmetrical C-H stretching vibration of aliphatic acids. Aliphatic chains (-CH_2- and –CH_3-) which form the basic structure of this lignocellulosic material (Feng and Guo, 2012). Bending vibrations around 1736 cm^{-1} are due to non-ionic carbonyl groups (-COOH, -$COOCH_3$) and it may be assigned to carboxylic acids or their esters. The signals at 1648 and 1442 cm^{-1} can be assigned to symmetric and asymmetrical stretching vibrations for C=O in carboxylic groups (-COO^-), respectively. Finally, the band around the 1068 cm^{-1} can be attributed to stretching vibrations of C-OH of alcoholic and carboxylic acids.

The FTIR gave a qualitative description of the surface of adsorbents i.e. the type of functional groups that are present. With this information, one will be able to hypothesize about the adsorption rate and mechanisms based on the type of functional groups present on the surface of the adsorbents. Thus, the aim of the next part is to describe the changes that took place after the adsorption of Cu ions onto the two adsorbents.

4.5.2 Results after adsorption

The FTIR spectra of the banana and orange peels after the adsorption of Cu ions relative to the untreated banana and orange peels are shown in figures 4.8 and 4.9, respectively. The changes caused by adsorption in the presence of functional groups are of particular interest because they show the changes that have occurred when the sorbate and adsorbent were in contact, and gives rise to a new spectrum. Furthermore, the effectiveness of the adsorbent depends largely on their chemical composition, particularly the functional groups present on the surface (Liang et al., 2010).

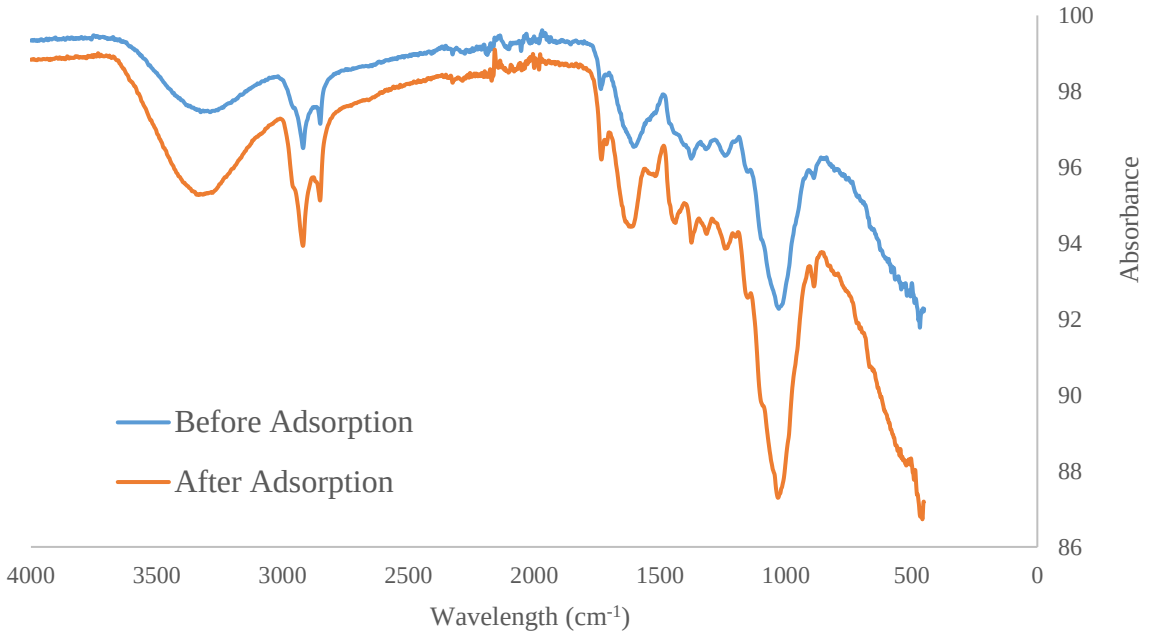

Figure 4.8: FTIR spectrum for the banana peel after and before adsorption

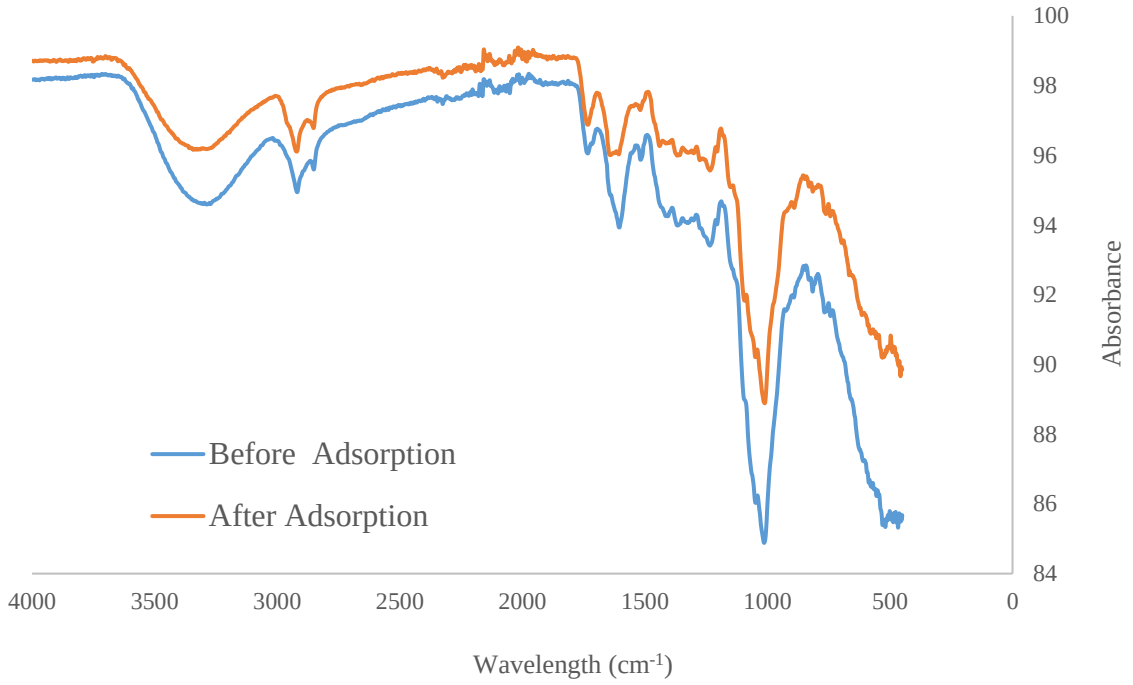

Figure 4.9: FTIR spectra of the orange peel before and after adsorption.

It can be seen that for both peels that there is no transformation of the shape of the spectra, just a shift up or down. This could be an indication that no chemical transformation has taken place and this would be in line with previous studies (Kamsonlian et al., 2011a; Feng and Guo, 2012). Hence, the shifting of the peaks was due to the binding of metals to the surface of the adsorbent but the intensity depends on the type of metal or complexations that are formed (Liang et al., 2010). This can be observed in both figures, where the shift for banana peels (Figure 4.8) is downwards and that of orange peels (Figure 4.9) is upwards. The shift observed in Figure 4.8 confirms that there was a decrease in the number of available functional groups on the surface of the adsorbent (Lu et al., 2009). An explanation for this shift to lower wavelengths after adsorption is that there was a chemical interaction between metal ions and hydroxyl groups (-OH) (Thirumavalavan et al., 2011). The orange peel spectra after adsorption shifted upwards. Similar results were observed in the literature (Feng et al., 2010; Liang et al., 2010; Pathak et al., 2016b). As an example, Pathak et al. (2016a) studied the adsorption of metal ions onto fruit peels, orange peels included. The results displayed an upward shift in the FTIR spectra with carboxylic functional groups identified as the main active ones.

Fruit peels are made of complex organic compounds such as cellulose, lignin, proteins and lipids (Das et al., 2008) as well as inorganic elements like potassium as observed in the EDX results (Section 4.2). Some authors (Thirumavalavan et al., 2011), claim that the shift in wavelength is

mainly due to pre-treatment, pH of the solution and metal binding. They further argue that the pH, unlike the pre-treatment, does not cause radical structural changes but merely alters the -OH bonds due to H^+ ions binding to functional groups. However, it is still unclear to which degree this is the main cause of the high intensity peaks. As a result, other authors have suggested using an ATR-FTIR or Raman spectra to analyse the changes (Shrestha, 2016).

4.6 Point of zero Charge and Surface Charges

The pH at which the surface of the adsorbent has a zero net charge is called the point of zero charge (pH_{pzc}) (Pashai et al., 2016). The pH_{pzc} was measured using the immersion technique following the procedure by Fiol and Villaescusa (2009). Changes in the final and initial pH values indicate the process of adsorption by dissociation of functional groups behaving as active sites on the adsorbent surface (Bhaumik and Mondal, 2016). The surface of the adsorbent is negatively charged in solutions with a pH value higher than the pH_{pzc} which causes interaction with cationic species while at solution pH values lower than pH_{pzc}, the surface becomes positively charged, attracting anionic species (Pagnanelli et al., 2003). The results are presented in figure 4.10.

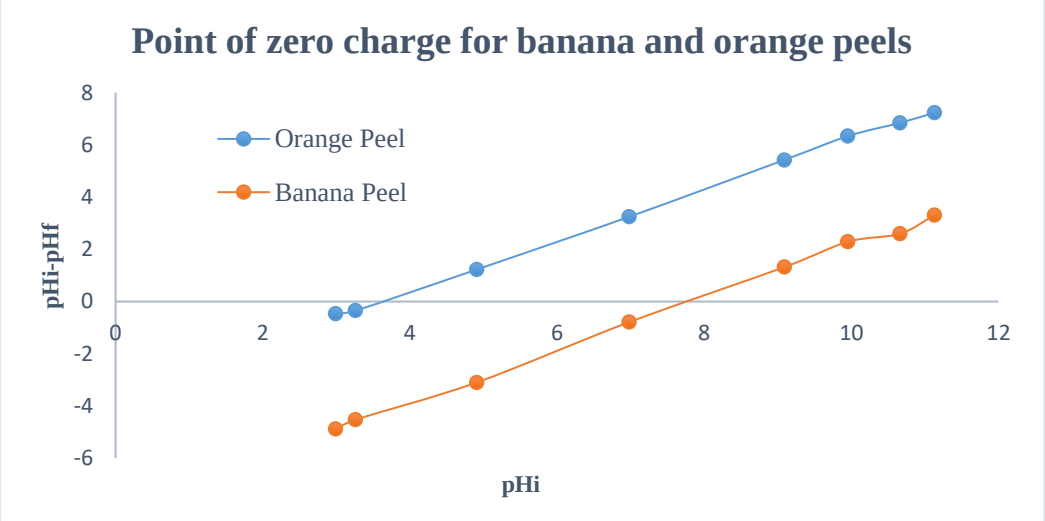

Figure 4.10: Point of zero charge of fruit peels in 0.1M KNO_3.

The surface pH is the property of the adsorbent that gives information about the change of the pH of water when a known amount of adsorbent is added to it. The pH changes due to some compounds contained on the surface of the adsorbent leaching into the solution (Kosmulski, 2002). The charges present on the surface of the adsorbent also help determine whether the peel is acidic or basic.

In addition, by calculating the net charge amount of basic and acidic sites available on the surfaces of the peels, the type of impurity that can be adsorbed can be determined. To determine net surface charges, the ratio of basic to acid sites (B/A) was calculated according to Pathak et al. (2017). The

ratio of the acid to basic sides is presented in table 4.5. The surface has more basic charges if B/A >1, the net acidic and basic sites are equal and the surface is neutral if B/A = 1, and the surface has more acidic sites (positive) charges if B/A < 1 (Pathak et al., 2016a). Figure 4.10 and table 4.5 were used for the analysis of pH_{pzc} and surface charges.

Table 4.5: Surface Charge of fruit peels.

Fruit Peel	Surface pH	Available sites(mmol/g)		Basic/Acidic sites
		Acidic	Basic	
Banana	7.79	1.09	8.58	7.89
Orange	3.75	3.19	2.61	0.82

The pH_{pzc} (Figure 4.10) of orange peels and the surface pH (table 4.5) are 3.81 and 3.75, respectively. Therefore, orange peels can be classified as a bioadsorbent with an acidic character. The concentrations of adsorption sites of acidic type and basic type corroborate this result; that is, the concentration of acidic sites was higher than that of basic sites, i.e. 3.19 and 2.61 mmol/g, respectively. Also, it is well known that acidic surfaces favour adsorption of anions whereas basic surfaces favour adsorption of cations (Pashai Gatabi et al., 2016; Pathak et al., 2016a). Thus, these peels would be best suited for the removal of anionic species. However, a cation is often complexed with ligands, some of them being negatively charged. Therefore, in such a case, the cation is, in fact, a negative complex, which may adsorb very well on a positively charged surface (Gutierrez et al., 2018). Thus, explaining the reason orange peels are capable of adsorbig metal ions. Moreover, if the pH of the solution is above the pH_{pzc} which is the case for this system as explained in Chapter 5, the surface of the absorbent is negatively charged due to the acid groups being de-protonated thus, attracting cations. Hence, according to these results, orange peels could be a low-cost bioadsorbent to remove metal ions from industrial wastewater.

The zero-charge point of banana peels is 7.89 (Figure 4.10). This result is of the same order of magnitude as that reported in the literature (Palma et al., 2011b; Pathak et al., 2016a). This shows that there are more basic sites than acidic sites making it basic in nature. The amount of basic sites is three times higher than the acidic sites, i.e. 8.58 and 1.09 mmol/g, respectively. The surface pH value of banana peels is 7.79 and the B/A ratio is >1 (table 4.5), which also confirms that banana peels are basic in nature.

4.7 Summary

The structure, physical and chemical properties of banana and orange peels were studied in order to obtain information about how the material is expected to behave during the adsorption of metal ions. Due to the complicated nature of biosorption mechanisms, the combination of characterization techniques such as FTIR, SEM/EDX, XRD, BET and titration methods were used to identify the dominant mechanisms for the adsorption of Cu ions onto banana and orange peels. A summary of the findings is given below (table 4.6):

Table 4.6: A summary of the physical and chemical properties of the adsorbents**.**

Parameter	Value/Description	
	Banana peel	**Orange peel**
Physical nature	A heterogeneous, rough surface with crater-like features.	A heterogeneously porous structure with sharp and irregular particles distributed randomly on the surface.
External surface area (m^2/g)	0.68	9.64
BET surface area (m^2/g)	0.41	6.45
Pore volume (m^3/g)	0.000422	0.006962
Pore size (nm)	3.63	4.29
Phase identification	Crystalline	Amorphous
Point of zero charge	7.89	3.81
Surface charges	Basic	Acidic
surface pH	7.79	3.75

* For the surface area, pore size and pore volume, the particle size used $300 < x < 500$ microns

- Topographic features of the prepared adsorbents were determined and revealed that the surfaces of fruit peels were naturally porous and rough as evident from the SEM images.
- The FTIR technique was used to qualitatively determine characteristic functional groups which may be responsible for the adsorption of metal ions. It was further applied to confirm the removal of metal ions from the solution by distinguishing the peak position and intensity.
- Specific surface area (SSA) and pore structure of the adsorbents were examined using N_2 sorptometry using Brunauer-Emmett-Teller (BET) theory. Pore sizes were calculated from the adsorption branch isotherms using the Barrett-Joyner-Halenda (BJH) method.
- The surface chemistry was determined by the acidic or basic character of their surface. The surface charge of the material in the aqueous media is important, especially in adsorption studies because for example, one may produce high surface area material, but if the surface charge of the material is opposing the adsorption due to it being the same charge as the

adsorbate, then the material needs to be modified and the right pH conditions found that would contribute to the best adsorption.

5 Selectivity Effects on the Adsorption of Heavy Metal Ions onto banana and orange peels

The main goal of this study was to investigate the efficiency of prepared untreated banana and orange peels for removal of metal ions from artificially contaminated water samples. This study was also used to establish the equilibrium time and choose the appropriate particle size for the process. Furthermore, the choice of the factors that will be held constant throughout the project will be explained after which, the removal percentage of metals will be discussed and the choice of the modeling metal will be explained based on the experiments performed. Also, unless otherwise stated, the shaking speed and temperature values are from literature.

5.1 The controlled operating conditions

The toxic effects of metal ions that make up part of the products and by-products of our technologies and processes have become increasingly worrisome in recent years. Volesky (2003c), divided the toxic metal ions into two groups: “the big three”, i.e. mercury, lead and cadmium, and the “second-tier toxic heavy metals” that include copper, zinc, nickel, manganese, chromium, arsenic, selenium and vanadium. In this work, second-tier metals were chosen for this section as they form part of the acid mine drainage problem that is currently prevalent in South Africa. The concentrations of concern are not from the point source but rather those found in traces in potable water. Furthermore, controlled adsorption process parameters, in particular, the selection of the process equilibrium time, particle size and operative pH will be discussed.

5.1.1 Operative pH

Previous studies on the adsorption of bio-peels have reported on the importance pH has on the adsorption of metal ions; it affects the arrangement of active exchange sites as well as the ionic strength of the adsorbate solution (Dursun, 2006; Rao et al., 2010; Iftekhar et al., 2018). However, for the purpose of this study, the pH will not be studied but rather be kept constant at pH 5.5-6 because the ultimate goal is to treat portable water that still contains metal traces. In addition, this is a plausible pH range to be used as pH 4-6 is usually reported as the optimum bioadsorption operating range to avoid micro-precipitation and other metal uptake contributions (Nurchi and Villaescusa, 2008; Iftekhar et al., 2018).

5.1.2 Equilibrium time

The contact time has a significant impact on the process of biosorption and it can also influence the processes' economic efficiency as well as the kinetic adsorption (Iftekhar et al., 2018). To establish the equilibrium time of any given system at a given temperature, the equilibrium time depends on the ratio of C_{eq} / C_0, the particle radius, and the specific rate coefficient limiting mass transfer (Crittenden and Thomas, 1998). Therefore, it would be more accurate to calculate the time based on experimental observations rather than to estimate it. The reason for this is that if the right time is not established, one runs the risk of not reaching equilibrium or running it for too long which may result in the degradation of the adsorbent and occurrence of side reactions (Dursun, 2006). Thus, equations 5.1 and 5.2 can be derived from the model solutions for surface diffusion (Liang and Tsai, 1995a) and for pore diffusion (Tsukamoto and Ohe, 1991) were proposed to calculate the minimum equilibrium time, t_{min}: $t_{B,min} = \frac{T_{B,min} r_p^2}{D_s}$ *(5.1)*

$$t_{B,min} = \frac{T_{B,min} r_p^2 \rho_p q_0}{D_s} \quad (5.2)$$

Where r_p is the adsorbent particle radius, D_S is the surface diffusion coefficient, D_p is the pore diffusion coefficient, ρ_p is the particle density, q_0 is the adsorbent loading in equilibrium with C_0, and $T_{B,min}$ is the minimum dimensionless time necessary for approaching the equilibrium.

However, despite the availability of such equations, their applicability to estimate the equilibrium time is limited as the diffusion coefficients are not known at the time the isotherms are measured. The equilibrium load for C_0 must also be known in the case of pore diffusion but equilibrium loads are obtained from the isotherm measurement results and are not known prior to measurement (Tsukamoto and Ohe, 1991; Worch, 2012). For these reasons, a simple preliminary adsorption test was performed in order to determine the exposure time needed for the system to reach equilibrium. The synthetic solutions were prepared as discussed in Chapter 3. The experiments were conducted at 25^0C at a shaking speed of 120 rpm with an initial metal concentration of 10mg/L, adsorbent dosages of 2mg/L (the values were taken from literature as they were the set optimum concentration for adsorption using biosorbents) and pH 5.5-6. From the results that are presented in Figures 5.1 and 5.2 it can be seen that the equilibrium time was established between 100 and 110 minutes. Therefore, 120 minutes was used as the time for adsorption. The extra 10 minutes were a safety measure for the approximate value.

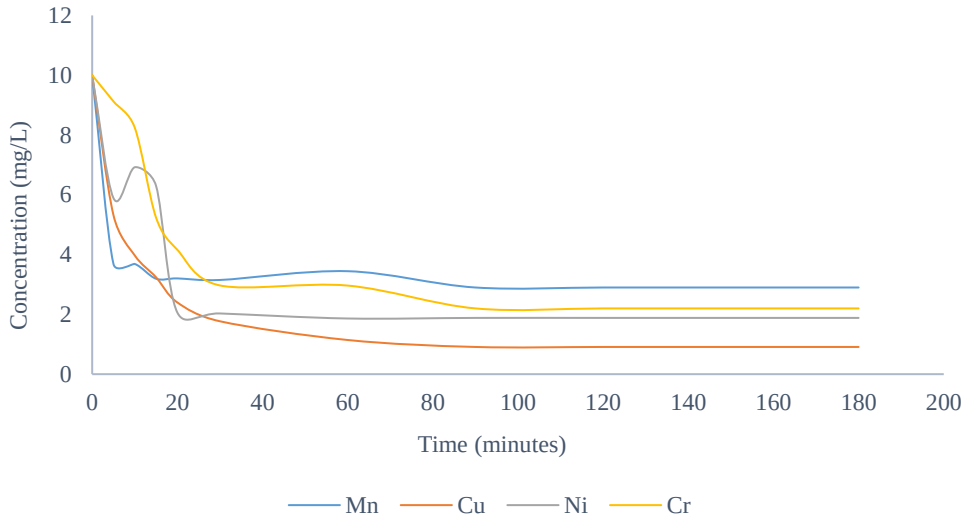

Figure 5.1: Adsorption of metal ions onto banana peels**.**

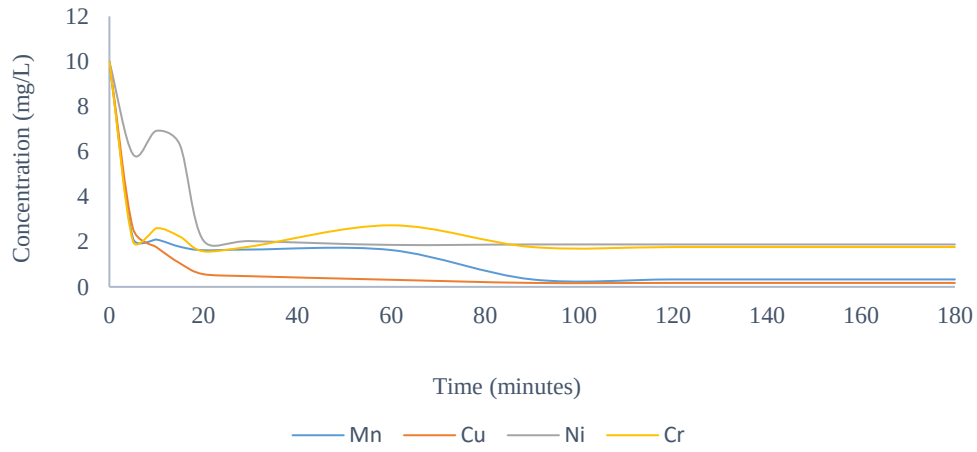

Figure 5.2: Adsorption of metal ions onto orange peels.

5.2 Particle size

The effect of particle size on the removal of heavy metals was investigated using banana and orange peels having the following particle size ranges; X <106, 106 < X < 300 and 300 < X < 500 microns (µ). The dosage was set at 1g/L with an initial 5ppm concentration, pH between 5.5-6 range and 120rpm shaking rate. The process was performed at room temperature i.e. the thermostatic shaker was set at 25°C. See figures 5.3 and 5.4.

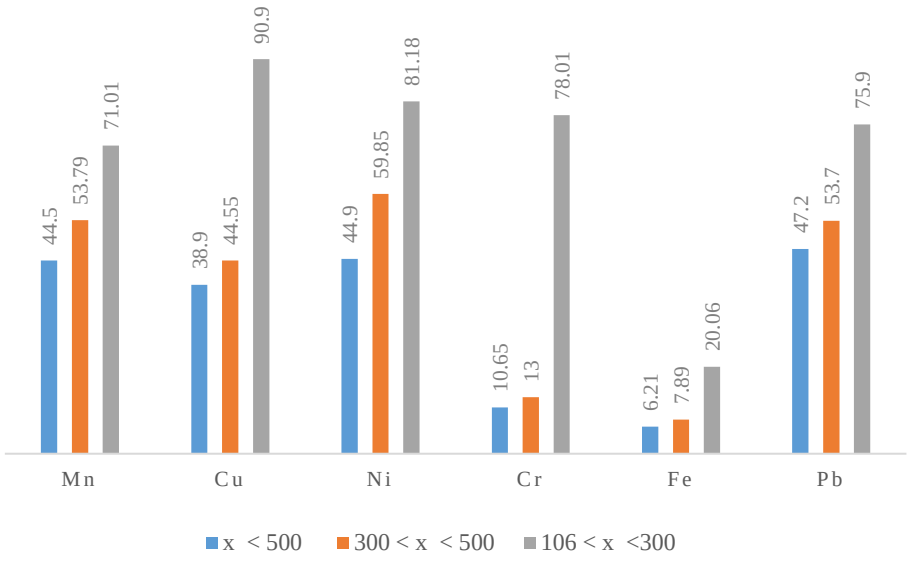

Figure 5.3 Effect of particle size on % heavy metals removed using banana peels.

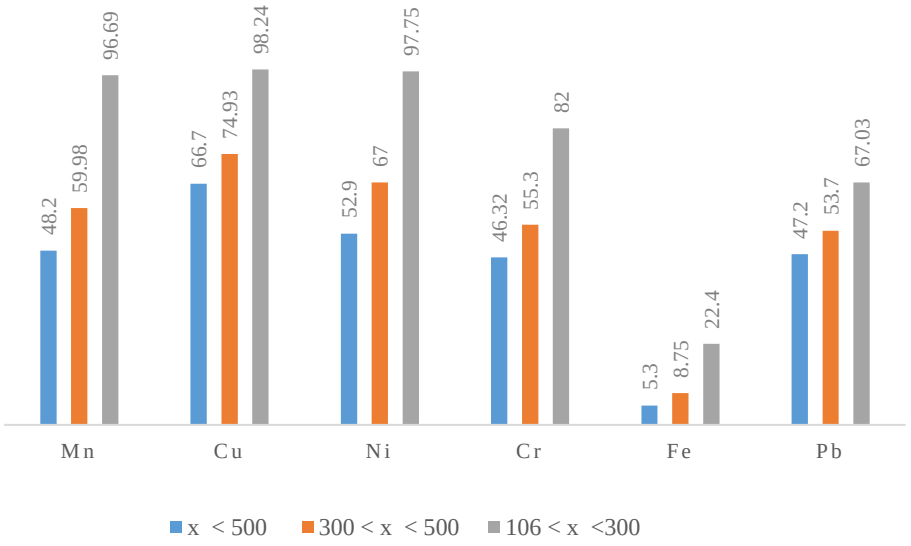

Figure 5.4 Effect of particle size on % heavy metals removed using orange peels.

Making reference to the results, it can be seen that heavy metals removal increased with particle size reduction. In principle, a finer ground particle is expected to adsorb more metal ions compared to coarser particles under specified conditions. These results are consistent with those of other studies (Abdi and Kazemi, 2015; Amarasinghe and Williams, 2007) and in a few studies this is usually explained in terms of surface area, i.e. if the surface area of adsorbents is high, the exposure of adsorbent sites to solid-metal ion interaction is high (Hubbe et al., 2011). Therefore, this implies that, the smaller the size of the particle, the higher the surface area per adsorbent unit weight. Hence, it is expected that a higher percentage will be removed by smaller sized adsorbents.

On that account, milling to a particle size of 300-500 microns seemed to be more suitable for the process for both the peels. The second particle size range was selected for easy filtration and to minimize filtration related errors. Furthermore, in addition to energy requirements, especially if smaller particle sizes are to be achieved, one can anticipate increased problems with handling very fine material, including greater difficulty in later separation from the water phase, filter blockage and even dust hazard (Amarasinghe and Williams, 2007). Therefore, the particle size range of 300-500 microns was used for all the batch experiments.

5.3 The efficiency of untreated peels for removal of metal ions

Studying the rate of adsorption and efficiency of adsorbents to adsorb metals is important to understand because it aids in better process design. Thus, batch experiments were carried out to determine the adsorption percentage of heavy metals (Cu, Ni, Cr, and Mn) using banana and orange peels. Figures 5.5 and 5.6 show the relationship between the percentage of metal ion removal and the time of contact in fruit peels.

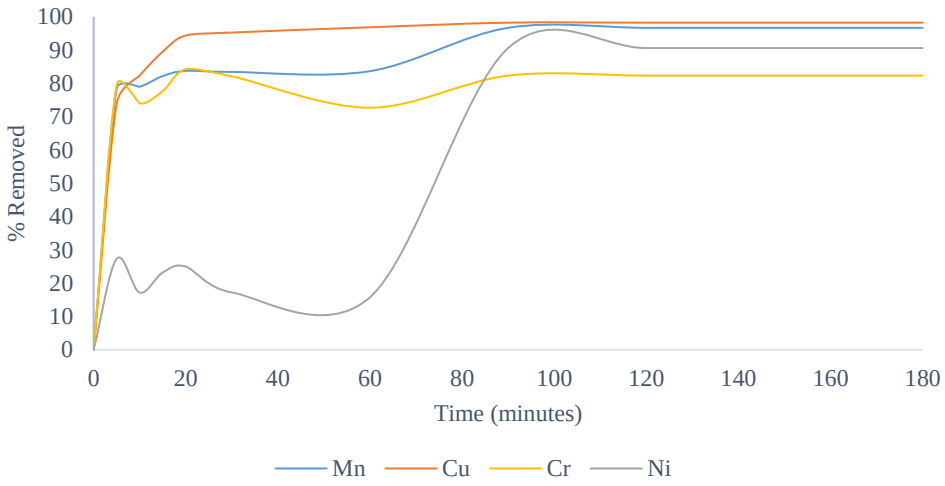

Figure 5.5: Percentage removed of metal ions using orange peels.

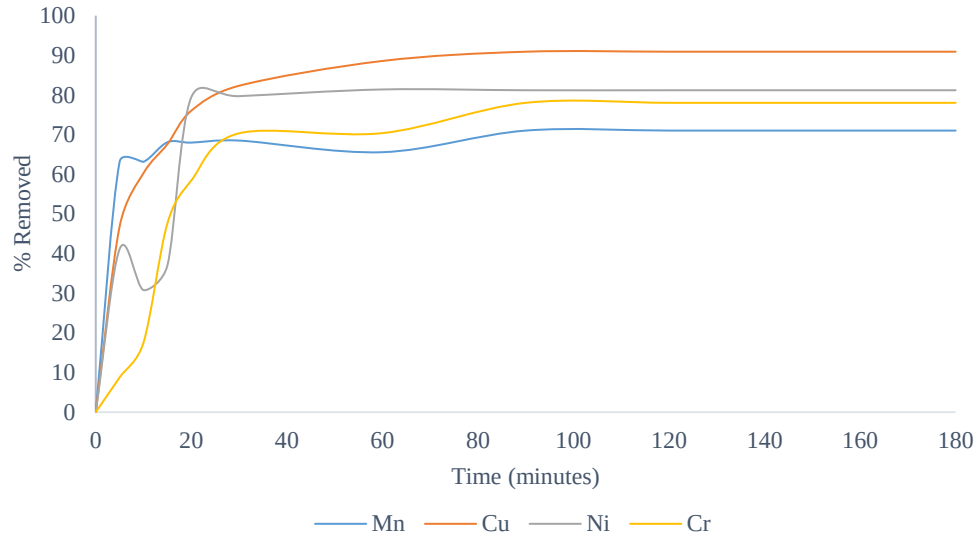

Figure 5.6: Percentage removed of metal ions using banana peels.

According to the results shown in both figures above, the process of removing metal ion from the fruit peels can be divided into two stages; a rapid stage in the first 20 minutes in which the diffusion of metal ions from the bulk of the solution to the adsorbent surface was high (Annadurai et al., 2003). Approximately 25-89% of metal ions were removed by orange peels while at this stage 35.1 - 80% were removed by banana peels. This rapid stage was followed by a gradual phase from 20 to 100 minutes of removal in which the diffusion of the pollutant ions to the pore structure and the adsorbent's internal surface was slow due to the activated sites becoming engaged and unavailable (Wu et al., 2009a). In previous studies (Faria et al., 2004; Xie et al., 2014) that used activated carbon derived from the peels, the samples showed a higher percentage of metal ions removal than their untreated fruit peels at the contact times investigated. Activated carbon samples from banana peels showed the highest percentage of removal (about 92% of copper ions are removed after an hour) between the fruit peels that were studied, while carbon samples from orange peels showed a comparable removal percentage of about 84%. Furthermore, based on the overall mean percentage removal of heavy metals (87.6–92.2%), the heavy metal adsorbing capacity of the natural adsorbents is of the order: orange peels > banana peels. Also, the efficiency of heavy metal removal by the natural adsorbents is affected by many factors which will be discussed in later chapters. However, according to Yang (2003), selectivity on adsorbents can manifest in any particular separation process in one or several ways, for example:

- There may be differences in thermodynamic balance for each adsorbent-adsorbent interaction; this is often referred to as the effect of equilibrium.

- There may be differences in the rates at which various adsorbents travel into the adsorbent's internal structure; this is often referred to as the kinetic effect.
- Pore openings may be too small to allow one or more adsorbents to penetrate; this is known as the molecular sieving effect and may be regarded as an extreme kinetic effect.

Hence, coupling this explanation with the observation in figures 5.5 and 5.6, to some extend this may explain the irregularities in the curves as the adsorption process proceeds along the allowed contact time. However, investigations into further explaining this effect was not done in this study.

The percentage removal of metal ions on orange peels can be ordered as Cu> Mn >Ni > Cr while that of banana peels can be ordered as Cu > Ni > Cr > Mn. The results obtained do not agree with some found in literature (Amarasinghe and Williams, 2007; Annadurai et al., 2003), but this can be due to the fact that the materials were prepared differently and the operating conditions differed greatly. Furthermore, the amount of metals removed by a particular adsorbent strongly depends on their surface acidity including the presence and amount of functional groups available (Nurchi and Villaescusa, 2008). Also, it is evidence from previous studies (Kamsonlian et al., 2011a; Lu et al., 2009) that some metal ions tend to be more interactive with some functional groups. As a result, in this work copper was selected as an analyte because it was the most stable based on the observed results. In addition, Cu is a common environmental pollutant and most of the released Cu into the environment is a result of the drainage of acid mine and leachates from landfills (Cheah et al., 1998).

5.4 Summary

This chapter investigated the efficiency of prepared untreated banana and orange peels for removal of metal ions from artificially contaminated water samples. The results showed that most of the studied metals had a high affinity to the adsorbents however, Cu was chosen because of its chemical properties and the fact that it is one of the common pollutants that result in AMD.

6 Identification of Significant Factors

6.1 Introduction

Design of experiments is a structured and organized way of conducting and analysing controlled tests to evaluate the factors that are influencing a response variable. It is a multivariate method that involves varying several factors simultaneously. This is a direct contrast of the traditional one-factor-at-a-time (OFAT) method which requires changing one factor at a time (Volesky, 2007). When one factor is changed at a time, the detection and evaluation of the interaction of combined factors is reduced and limited (El-Azazy et al., 2019). Therefore, DOE was used to perform justifiable and efficient experiments that would produce informed results.

The purpose of this chapter was to investigate and identify factors that significantly influence the adsorption of Cu using banana and orange peels. The study used a DOE method as a research tool to develop an experimentation plan for determining the significant factors affecting the copper adsorption process. The significance of each factor and associated interactive effects were evaluated using a two-level five-factor full factorial statistical design of experiments (2^5) and percent Cu removed was used as the measured response. For the data used in this section, reference should be made to Appendix B.

6.2 Materials and methods

6.2.1 Bio-adsorbent samples and solution preparation

The preparation of the materials and a detailed explanation of the method is given in chapter 4.

6.2.2 Experimental Plan for Statistical Design of Experiments (DOE)

An experimental design matrix was used in order to change several factors in a systematic way to ensure a reliable and independent study of main factors and their interactions. At this identification stage, the study looked at the influence of the main factors- adsorbent type, adsorbent dosage, temperature, initial Cu concentration and shaking speed. The main intention was to identify the key factors that affect the response and the interactions among them. Adsorption experiments were carried out at low and high factor values represented by -1 and +1, respectively were investigated.

6.3 Results and discussion

6.3.1 Influence of factors

Influence of adsorbent type

Some crop-based waste materials have been recognized as cost-effective and highly efficient adsorbents from aqueous solutions for removing and recovering various types of heavy metals. Outside process parameters, the ability is strongly attributed to the physiochemical properties of the fruit peels. The present work was aimed at assessing which of the two adsorbents would be the better adsorbent and the results are presented in figure 6.1. In figure 6.1 orange peels had a higher Cu removal as opposed to the banana peels. This is because orange peels are amorphous materials characterized by small particle sizes and high specific surface areas (discussed in Chapter 4) which increases its absorption capacity. Furthermore, they have a larger pore volume which increases the availability of pore structures that are accessible for metal uptake.

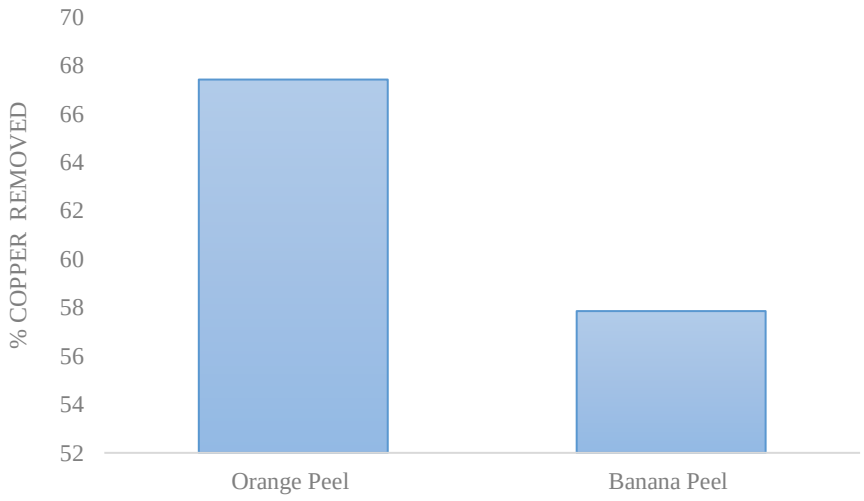

Figure 6.1: Effect of adsorbent type on the recovery of Cu ions.

Although, orange peels have an acidic surface, the point of zero charge that was calculated in Chapter 4 allowed orange peels to adsorb metal ions once they were placed in the Cu synthetic solution with pH value within the range of 5.5-6. This made the conditions favourable because according to the literature, if the point of zero charge of an adsorbent is less than that of the solution, then the adsorption of cations is favoured. The results presented in chapter 5 exploring the efficiency of the bioadsorbents, also revealed that orange peels adsorbed more metal ions as opposed to the banana peel. As a result, these characteristics make orange peels a better adsorbent as seen in figure 6.1.

Temperature

A large number of studies on the effects of temperature on metal uptake using biomaterials have been performed. The change in the temperature of the solution affects both the diffusion rate and solubility of metal ions. Furthermore, the type of functional groups present on the surface of the adsorbent also contributes to the metal uptake capacity at a given temperature (Park et al., 2010; Abbas et al., 2014). The effect of temperature is shown in figure 6.2.

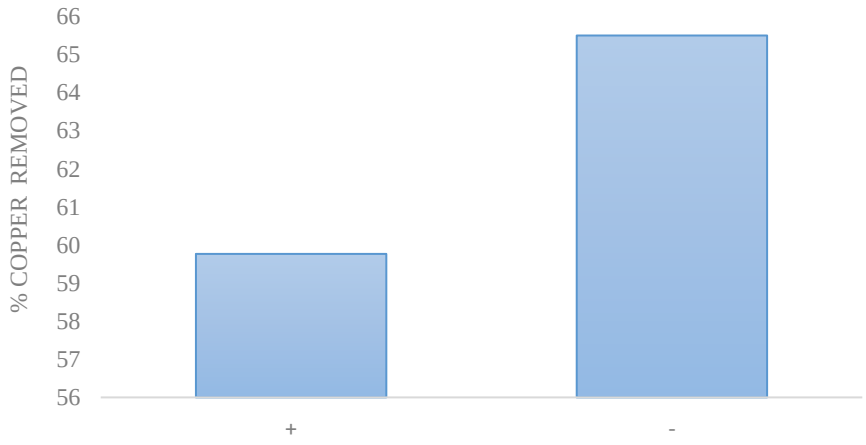

Figure 6.2: Effect of temperature on the percentage of Cu ions removed.

The figure shows that in the studied range of 25-50 ºC, lower temperatures favour the rate of recovery of Cu ions from the solution. Many researchers have reported the biosorption process as being exothermic thus, lower temperatures are favourable to attaining high removal percentages (Park et al., 2010). In contrast, some authors have urged that higher temperatures improved the elimination of heavy metals owing to an increase in its surface activity and kinetic energy (Abbas et al., 2014). Malkoc and Nuhoglu (2006) reported similar observations in the case of adsorption of Cr (VI) by tea waste. They attributed this to either an increase in surface activity or decrease in the boundary layer surrounding the adsorbents (Nguyen et al., 2013). Nevertheless, Park et al. (2010) explained that high temperatures tend to damage the active sites causing metals to escape from the adsorbent surface back into the solution. For this reason, room temperature is commonly used in biosorption experiments because temperatures in the range of 20-35 ºC do not seem to affect the biosorption efficiency (Das et al., 2008).

Effect of adsorbent dosage

The amount of adsorbent determines the degree of available binding sites which in turn determines the rate and extent of adsorption (Salman H Abbas et al., 2014). Thus, the adsorbent dosage was studied at 2-5mg/L. It can be seen from figure 6.3 that when a higher amount of adsorbent was

used, more Cu was removed from the water. The removal efficiency is generally increased as the concentration dose is increased. This is due to the fact that there is more mass available so more contact surface and binding sites available (Rao et al., 2010). However, contrary to this some studies have found that at dosages higher than 5g/mL, the rate of adsorption and the number of ion metals removed decreased. The reason for this is not clear but it may have something to do with the partial aggregation of active binding sites at high adsorbent dosages (Abdi and Kazemi, 2015).

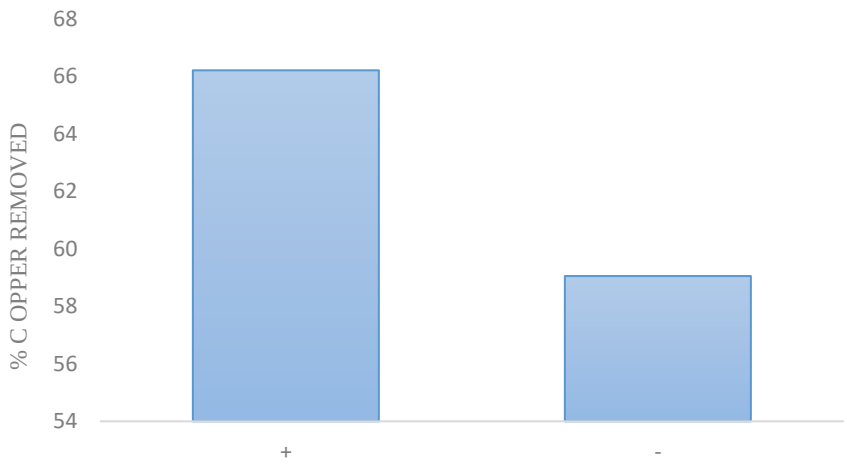

Figure 6.3 Effect of temperature on the percentage of Cu ions removed.

Initial Cu concentration

The influence initial Cu concentration has on the percentage removal of Cu ions was investigated. The experiment was carried out at a fixed adsorbent dosage and temperature at a pH in the range of 5.5- 6. The results in figure 6.4 show that the Cu metal removed decreased with an increase in initial metal ion concentration. The decrease in the percentage removed of Cu ions is expected as it is attributed to the lack of sufficient active sites to adsorb more metals available in the solution (Rao et al., 2010). According to Rao et al. (2010) at lower concentrations, Cu ions present in the solution have the potential of interacting with the binding sites and thus, the percentage was higher than those at higher initial Cu ion concentrations.

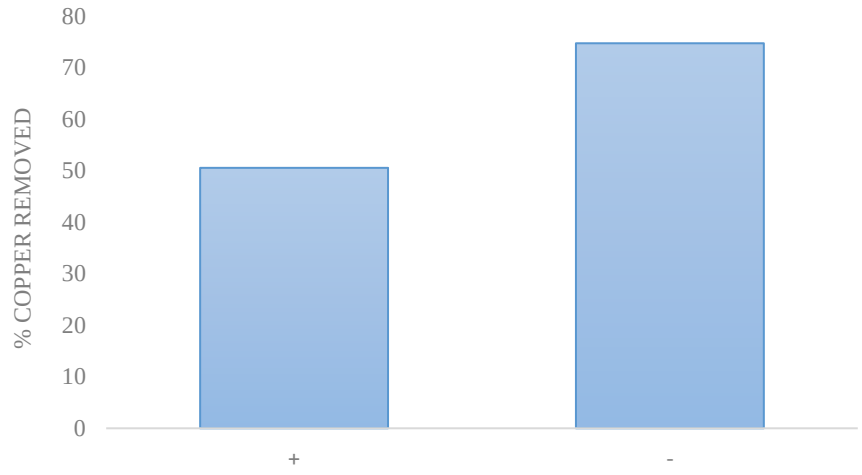

Figure 6.4: Effect of initial concentration on the recovery of Cu ions.

Influence of shaking speed

To increase the efficiency of adsorption, agitation is very important and helps speed up the process. Form the results shown in figure 6.5, it was observed that at lower shaking rates the best adsorption was found. Although contradictory to the fact that increasing agitation rate increases the diffusion of metal ions to the adsorbent surface and also reduces the film boundary layer around the adsorbents, resulting in increased adsorption, the decrease in the percentage of adsorbed metal ions as the agitation rate increases may be due to desorption from the adsorbent surface of certain metal ions (Amarasinghe and Williams, 2007). Some studies (Mohamad et al., 2012; Batagarawa and Dayo, 2017) also showed similar findings where the adsorption rate decreased as agitation rates increased. Other studies (Batagarawa and Dayo, 2017) however, were concerned that at lower shaking speeds, the adsorbent would accumulate at the bottom of the flask but this was not the case. The adsorption experiments at low shaking speeds were not hindered and good results were obtained.

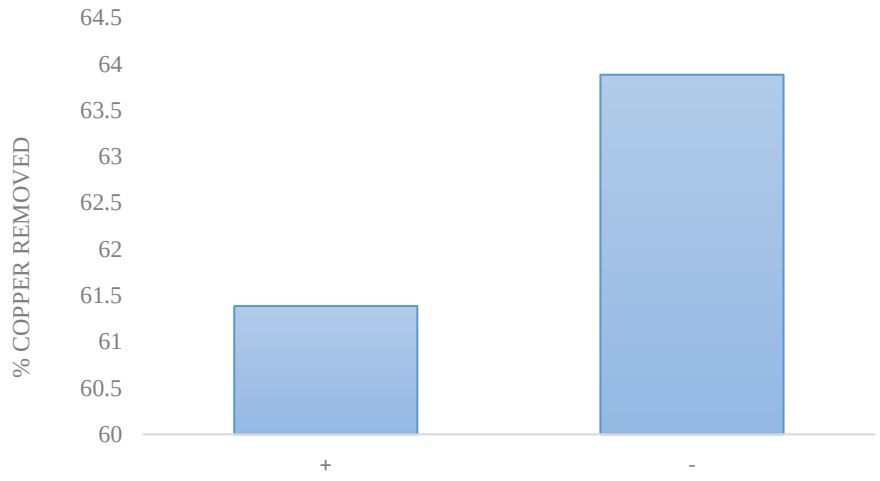

Figure 6.5: Effect of shaking speed on the removal of Cu ions.

6.3.2 Significant factors

The Cu extracted was calculated as % Cu removed from the metal solution and the normal probability plot were used to identify significant main effects and interactive effects as plotted in figure 6.6. The methodology for analysing the data is explained in detail in Chapter 3.

In DOE, factors can be classified as controlled factors and held constant factors. The controlled factors are the independent factors that will be chosen for the study (Table 6.1). The held constants (Table 6.2) are those that exert an effect on the response but are not of interest for this study. Thus, they will be held constant at a specific level.

Table 6.1: Experimental factors and levels for controlled factors.

Controlled factors	Level 1	Center point	Level 2
A: Temperature (°C)	25	30	35
B: Initial concentration (mg/L)	10	55	100
C: Adsorbent dosage (g/L)	1	3	5
D: Shaking speed (rpm)	100	125	150
E: Adsorbent type (BP/OP)	BP	OP	OP

BP: Banana Peel; OP: Orange Peel

Table 6.2: Experimental factors and levels for held factors.

Held Factors	Level
Solution pH	5.5
Particle size range (µm)	300< x < 500

At this diagnostic stage, the use of two levels for each factor allows for simplification of the analysis and provides a substantial reduction in the number of runs required (Garg et al., 2009). Furthermore, to simplify calculations and for uniform comparison, controlled factors were studied with their codified values of +1 (high level) or -1 (low level). The levels of controlled variables in coded units were obtained using the following formula (Witek-Krowiak et al., 2014):

$$coded\ value = \frac{X - X_0}{0.5(X_1 - X_2)} \quad (6.1)$$

Where, x = actual, x_0 = mean, x_1= lowest, x_2 = highest

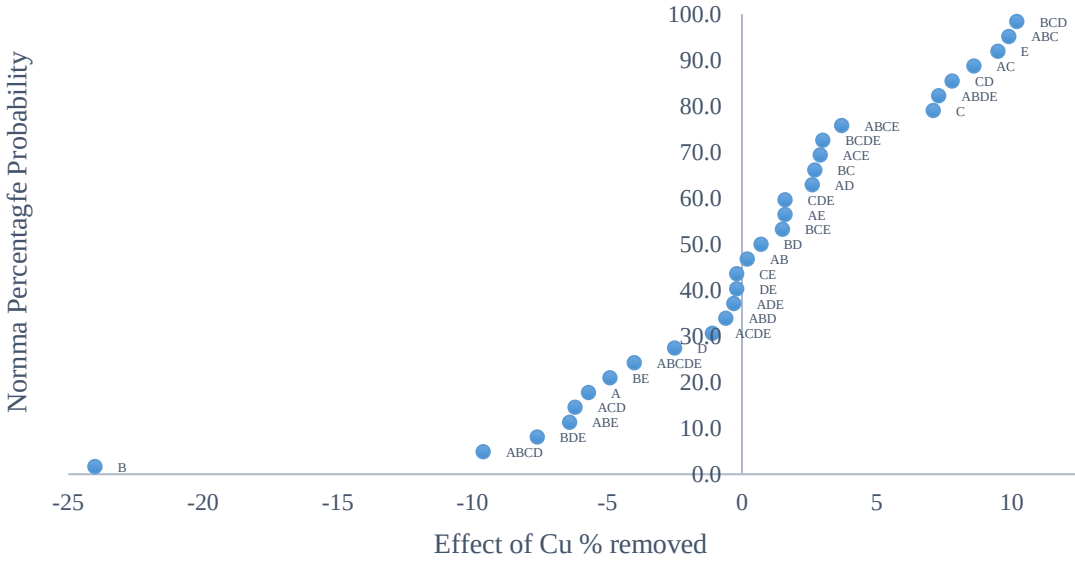

Figure 6.6: The normal plot of main factors and factor interactions from the 2^5 full factorial design**.**

Analysis of the individual factors show that initial concentration (B) was statistically significant because it is further away from the zero mean. Temperature (A), Adsorbent dosage (C), shaking speed (D) and Adsorbent type (E) were found to be statistically insignificant. However, further analysis showed that the interaction among factors B, C, and D was found to be statistically significant. To investigate this, screening principles and the Pareto chart were used to identify the most significant interaction (explained in Chapter 3).

According to the effect hierarchy principle, lower order effects are more likely to be more important than higher order effects i.e. the system is usually dominated by main effects and low-order interactions. Thus, the analysis of interactions was reduced to three factors. Furthermore, the effect heredity principle states that, in order for an interaction to be significant, at least one of the parent factors should be significant. Therefore, BCD was identified as the most significant effect because it is a three-factor interaction and two of the main factors are significant.

The Pareto chart shows the standardized effect from the largest to the smallest and a line is plotted to show which factors are statistically significant. The effects above the Bonferroni limit are definitely significant whilst those above the t-value limit could possibly be important depending on the line of work of the experimenter (Box et al., 2005). From figure 6.7, BCD is above the t-line therefore, it will be included as a significant interaction. Further, from the principles explained in Chapter 3, it can be seen in figure 6.7 that none of the two-level interactions cross the t-value thus, making three-level interactions the next low interactions. Additionally, BCD also contains factor B which is very significant as seen on the chart.

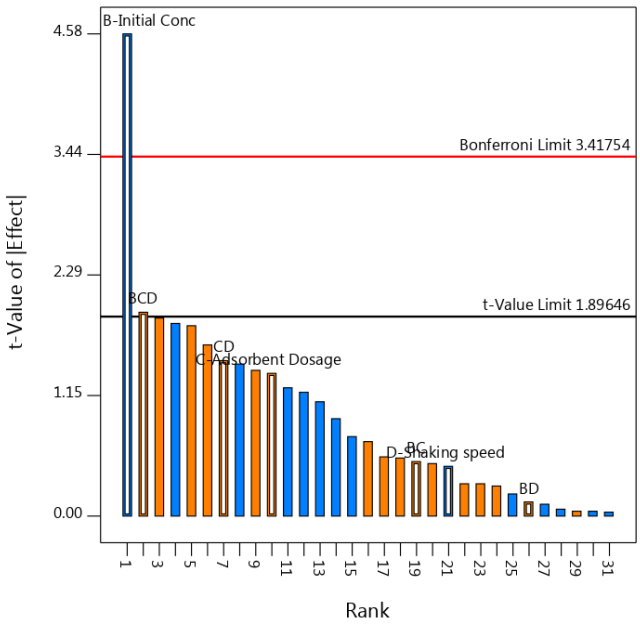

Figure 6.7: Pareto chart

Figure 6.8 is a normal plot if residuals. As can be seen, the residuals lie on a straight line with a linear correlation of 99% which shows that the residuals were normally distributed. Furthermore, figure 6.9 shows that the residuals are scattered around the zero lines for the entire range of the fitted values. Therefore, the satisfaction of this assumption means that the regression model is reliable and valid for this set of data.

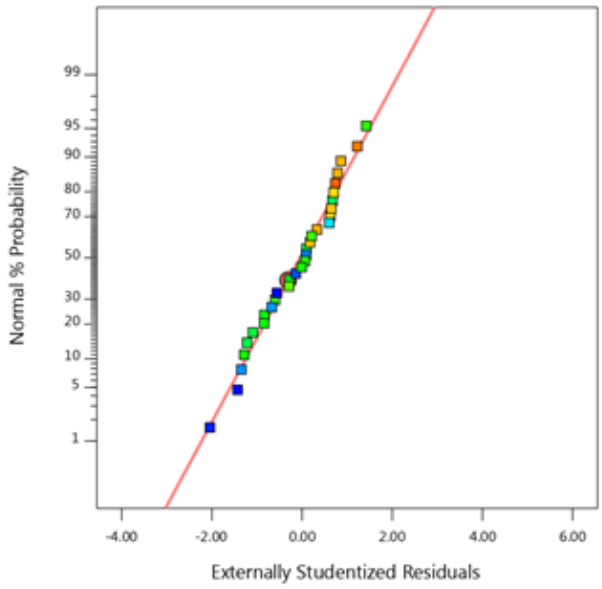

Figure 6.8: Normal plot of residuals.

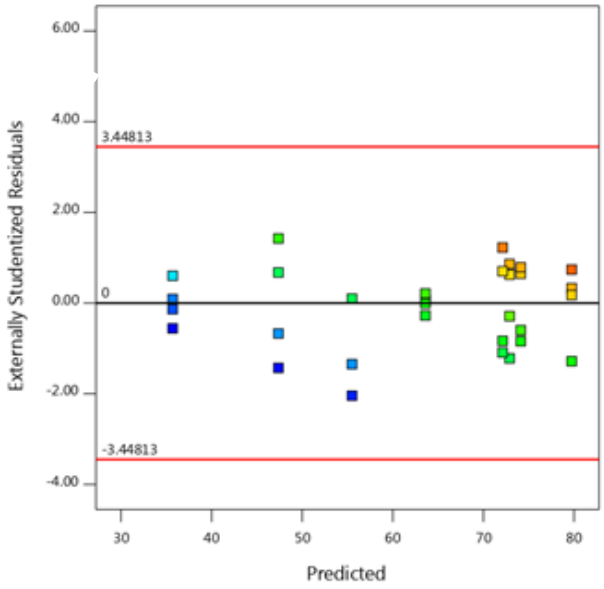

Figure 6.9: Plot of residuals- Externally Standardized Residuals vs Predicted.

6.4 Summary

The purpose of this chapter was to obtain experimental data to serve as an initial approach to the final optimization subsequently presented in Chapter 7 by identifying which factors had a significant effect on the response (copper recovery) effects and whether these were positive or negative. Initial Cu concentration, temperature, type of adsorbent, adsorbent dosage and shaking speed were the factors investigated. Factors have been studied at their maximum and minimum levels at this stage. The experimental results were statistically analysed using the probability plots for the significance of the factors.

Furthermore, the statistical method and experimental design approach selected have been able to satisfactorily help in determining statistically significant and insignificant factors. The results obtained indicate the following:

- Initial Cu concentration, adsorbent dosage and shaking speed were statistically significant.
- Under the ranges studied, the interaction between most of the variables was found to be statistically insignificant, except one that included initial Cu concentration, temperature, type of adsorbent, adsorbent dosage and shaking speed, which showed a marked influence on the copper recovery process.
- The results also showed that copper recovery was maximized at low initial concentration, low shaking speed, low temperatures, high adsorbent dosages and that orange peels were the better adsorbent.

Having identified the most influential factors the study in the next chapter will make use of a statistically-based optimization strategy called Response Surface Methodology.

7 Optimization of influential factors

Design optimization forms an important part of any design problem in engineering and in industry. The motivation behind numerous simulation functions in design is to build up a prescient model that can be used to improve a procedure, and the improvements mainly depend on optimizing techniques that are used in a particular procedure. Optimization can be defined as a procedure of improving a current framework, gadget, or process, for example, a metallurgical procedure (Chen et al., 2007).

In this section, parametric optimization was done using RSM to decide the ideal states of initial metal concentration, adsorbent dosage and shaking speed. RSM is the most prevalent procedure used to identify the ideal conditions by using a quadratic polynomial model and its application is a result obtained from screening tests (Myers et al., 2016). The central composite rotatable design (CCRD) was utilized to gather the information for fitting the second order response. The CCRD requires much fewer tests than the full factorial and has been proven to be adequate to represent most experimental designs (Simate et al., 2009). Furthermore, optimization work was done using design expert software. For the data used in this section, reference should be made to Appendix C.

7.1 Methods and materials

7.1.1 Adsorbent and adsorbate preparation

The preparation of the adsorbent and adsorbate were discussed earlier in chapter 3.

7.1.2 The experimental design for central composite design and response surface methodology

A CCRD consists of *2k* factorial or a fractional factorial points (coded ±1), augmented by *2k* axial or star points [(±λ,0,0,…,0), (0,±λ,0,…,0), …, (0,0,…, ±λ)] and n_c replicate points at the center [(0,0,0,…,0)] where *k* is the number of factors studied, λ is the distance of an axial point from the center. To ensure a constant variance of the predicted response at all points equidistant from the design center, the number of center point replications, n_c, for the three factors studied was calculated using the following equation (Witek-Krowiak et al., 2014):

$$n_c \approx 0.8385 \left(2^{\frac{k}{2}} + 2\right)^2 - 2^k - 2k \quad (7.1)$$

To simplify the calculations and for uniform comparison, coded values were used for the study shown in Tables 7.1 and 7.2.

Table 7.1: Relationship between coded and actual values of the variable**.**

Code	Actual value
-α	ξmin
-1	(ξmax + ξmin)/2 - (ξmax-ξmin)/2α
0	ξmax-ξmin)/2
+1	(ξmax + ξmin)/2 + (ξmax-ξmin)/2α
+α	ξmax

Table 7.2: Experimental layout and runs for the central composite rotatable design.

Factor Levels						Standard Run
Coded			Actual			
B Initial Cu Concentration	C Adsorbent dosage	D Shaking speed	B Initial Cu Concentration	C Adsorbent dosage	D Shaking speed	
-1	-1	-1	26.3	2.0	104.0	1
+1	-1	-1	88.7	2.0	104.0	2
-1	+1	-1	26.3	5.0	104.0	3
+1	+1	-1	88.7	5.0	104.0	4
-1	-1	+1	26.3	2.0	145.8	5
+1	-1	+1	88.7	2.0	145.8	6
-1	+1	+1	26.3	5.0	145.8	7
+1	+1	+1	88.7	5.0	145.8	8
-α	0	0	5.0	3.5	125.0	9
+α	0	0	110.0	3.5	125.0	10
0	-α	0	57.5	1.0	125.0	11
0	+α	0	57.5	6.0	125.0	12
0	0	-α	57.5	3.5	90.0	13
0	0	+α	57.5	3.5	160.0	14
0	0	0	57.5	3.5	125.0	15
0	0	0	57.5	3.5	125.0	16
0	0	0	57.5	3.5	125.0	17
0	0	0	57.5	3.5	125.0	18
0	0	0	57.5	3.5	125.0	19
0	0	0	57.5	3.5	125.0	20

The experimental results were analyzed statistically by ANOVA using Fisher's variance ratio test (F-test), standard errors of model coefficient (t-test), the coefficient of determination (R^2) and the absolute average deviation (AAD).

7.2 Results and discussion

In previous studies, pH, initial metal concentration, agitation speed, adsorbent dosage, adsorbent type, particle size and temperature have been identified as significant process parameters for the adsorption of metal ions. However, for this study, only initial ion concentration, adsorbent dosage and shaking speed where studied. The reasons for this choice are discussed in chapter 6 and adsorbent dosage, shaking speed and initial metal concentration were identified as statistically significant. Experiments also showed that orange peels were better at adsorbing copper ions as opposed to banana peels. Thus, in this chapter, CCRD and RSM were used to determine the optimal conditions of initial Cu concentration, adsorbent dosage and shaking speed using orange peels as an adsorbent.

7.2.1 Development of the fitted model and validation

Using the results of the randomized set of experiments, the regression model was fitted with the help of a statistical software - Design Expert 11.

Table 7.3: Observed values for Cu recovery**.**

Standard Run	Actual			% Recoveries
	B Initial Cu Concentration	C Adsorbent dosage	D Shaking speed	Observed
1	26.3	2.0	104.0	51.7
2	88.7	2.0	104.0	66.1
3	26.3	5.0	104.0	46.1
4	88.7	5.0	104.0	50
5	26.3	2.0	145.8	61.5
6	88.7	2.0	145.8	51.1
7	26.3	5.0	145.8	87
8	88.7	5.0	145.8	53
9	5.0	3.5	125.0	62
10	110.0	3.5	125.0	50.4
11	57.5	1.0	125.0	57.1
12	57.5	6.0	125.0	50.8
13	57.5	3.5	90.0	69.2
14	57.5	3.5	160.0	80.1
15	57.5	3.5	125.0	80.6
16	57.5	3.5	125.0	81.3
17	57.5	3.5	125.0	82.1
18	57.5	3.5	125.0	81
19	57.5	3.5	125.0	69.2
20	57.5	3.5	125.0	81.3

7.2.2 Derivation of the model

$$y = 77.61 - 3.34x_1 + 4.18x_3 - 8.41x_1^2 - 9.2x_2^2 - 4.26x_1x_2 - 7.84x_1x_3 + 6.14x_2x_3 \quad (7.2)$$

Where y = the response (% Cu removed), x_1= initial concentration, x_2= adsorbent dosage and x_3= shaking speed within the limits: $-\lambda \leq x_i \leq +\lambda$; i = 1, 2, 3; where x_i is the coded levels of process variables and $\lambda = 1.682$ is the distance of the star points from the center of the CCRD that gives the limits of the valid region under experimentation.

7.2.3 Checking for adequacy for the developed model

The adequacy of the fitted model was evaluated using Fisher's variance ratio test known as the F-test and the Student t-tests. The ANOVA and individual terms in the response surface model are shown in Table 7.4.

Table 7.4: ANOVA for the quadratic model**.**

Source	Sum of Squares	df	Mean Square	F-value	p-value	
Model	3404.46	7	486.35	22.87	< 0.0001	significant
A-Conc	152.32	1	152.32	7.16	0.0202	
C-aqitation	238.17	1	238.17	11.20	0.0058	
AB	145.35	1	145.35	6.83	0.0226	
AC	491.41	1	491.41	23.10	0.0004	
BC	301.35	1	301.35	14.17	0.0027	
A^2	1029.26	1	1029.26	48.39	< 0.0001	
B^2	1233.20	1	1233.20	57.98	< 0.0001	
Residual	255.23	12	21.27			
Lack of Fit	132.82	7	18.97	0.7750	0.6345	not significant
Pure Error	122.41	5	24.48			
Cor Total	3659.69	19				

The ANOVA table shows the regression model 'p' value less than 0.0001. Since the 'p' value is less than 0.05, this shows that the model is significant. The model F-value of 22.87 implies that the model is significant. There is only a 0.01% chance that an F-value this large could be due to noise. Furthermore, the lack of fit of 0.78 (Table 7.4) implies that the lack of fit is not significant relative to the pure error. Non-significant lack of fit is good.

From table 7.5, the coefficient of determination of 93% shows that the model is plausible, from a statistical point of view to define the true behaviour of the experimental system. Furthermore, the predicted R^2 of 0.81 is in reasonable agreement with the adjusted R^2 of 0.89. Adequate precision measures the signal to the noise and a ratio greater than 4 is desirable. The ratio obtained is 12.87 which indicates an adequate signal. Therefore, this model can be used to navigate the design space.

Table 7.5: Model fit of statistics.

Std. Dev.	4.61		**R^2**	0.9303
Mean	65.58		**Adjusted R^2**	0.8896
C.V. %	7.03		**Predicted R^2**	0.8146
			Adeq Precision	12.8705

Experimental (observed) results and predicted values obtained using the fitted model are presented in figure 7.1. As it can be seen from Figure 7.1, the predicted values are comparable to the experimental values, with the linear correlation coefficient (R^2) of 0.93. Statistically, this means that 93% of the sample variation can be explained by the independent variables.

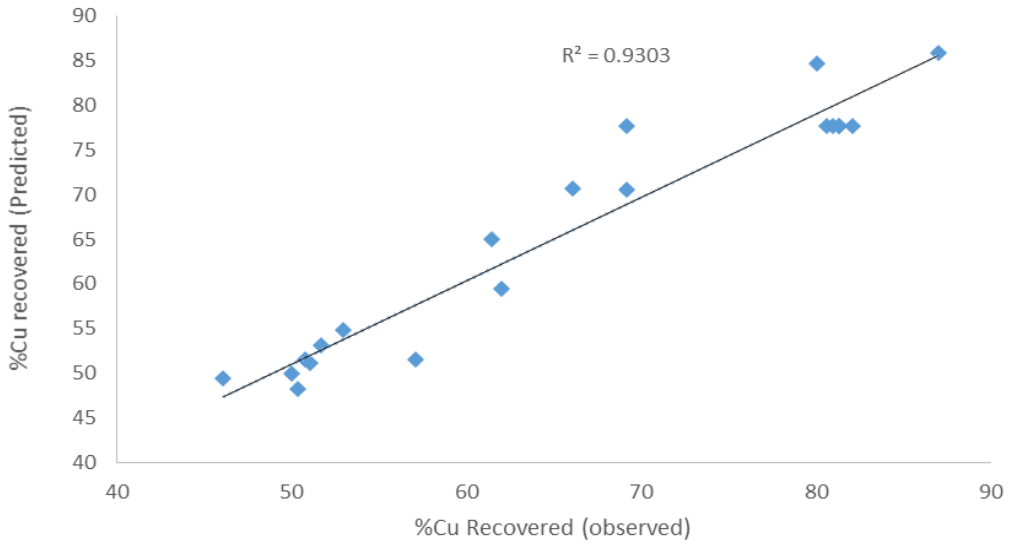

Figure 7.1: Relationship between experimental and predicted copper recovery.

7.2.4 Response Surfaces

Figures 7.2 through 7.4 show the three-dimensional surfaces as well as contour plots of the relationship between adsorbent dosage and initial concentration, shaking speed and initial concentration and, shaking speed and adsorbent dosage when one of the factors is kept constant. Detailed explanations of the effect of the factors were provided in Chapter 6.

Figure 7.2 shows the effect of adsorbent dosage and initial metal concentration on Cu recovery at constant shaking speed. The figure shows that as the dosage increases, the Cu recovery increases with a decrease in metal concentration.

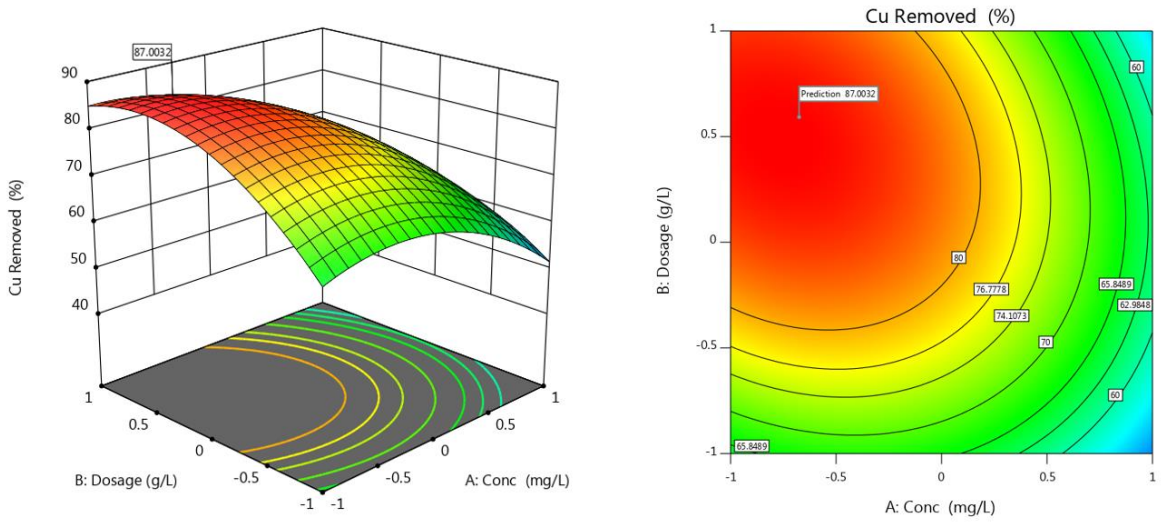

Figure 7.2. Response surface and contour plots at a constant shaking speed.

Figure 7.3 shows the effect of agitation and initial metal concentration on Cu recovery when the adsorbent dosage is held constant. As the figure shows, Cu recovery increases with a decrease in initial metal concentration and an increase in agitation rate.

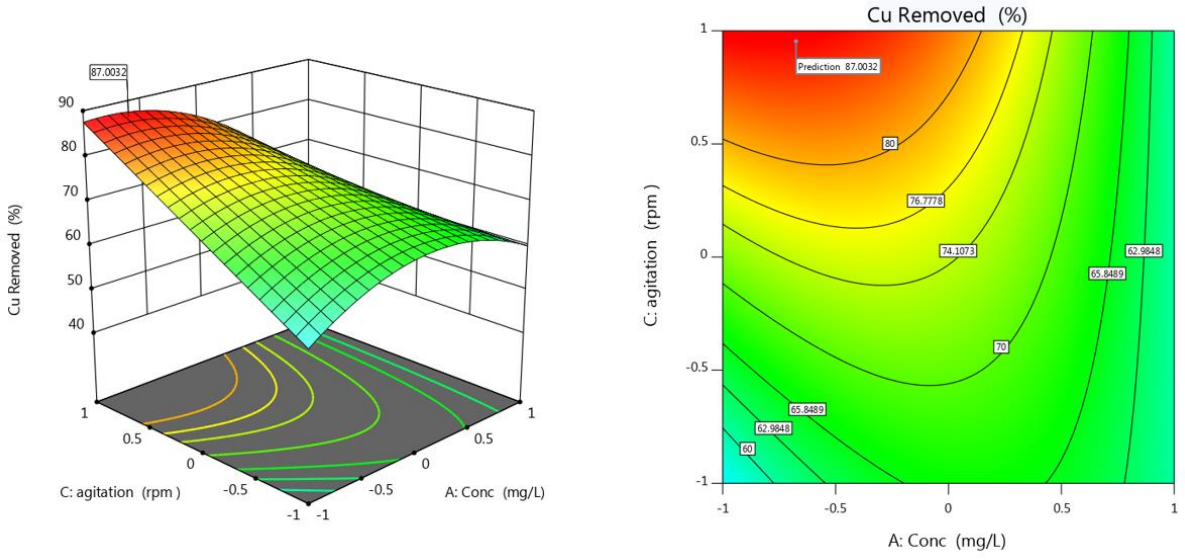

Figure 7.3: Response surface and contour plots at constant adsorbent dosage.

Figure 7.4 shows the effect of agitation and the adsorbent dosage on the Cu recovery when initial metal concentration is held constant. As the shaking speed increased the recovery also increased with an increase in adsorbent dosage. However, it should be noted that there was an optimal point of the adsorbent dosage that aided in maximum Cu recovery before it started decreasing again past the optimum value (refer to Chapter 6 for an explanation).

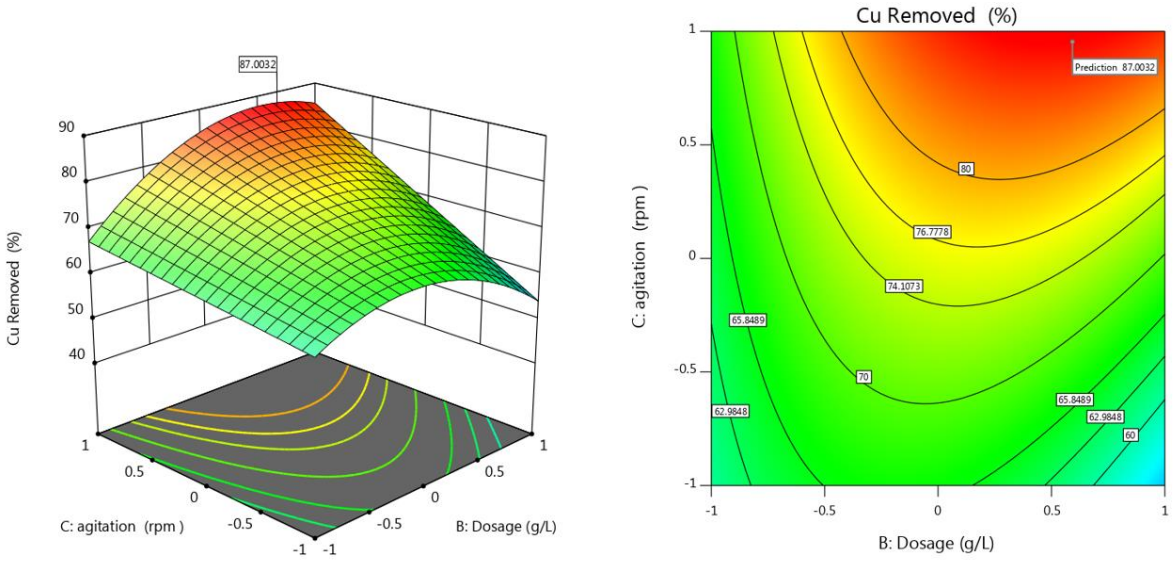

Figure 7.4: Response surface and contour plots at a constant initial metal concentration.

7.2.5 Determination of optimum conditions

As mentioned above, the objective of this chapter was to determine how to maximize the amount of Cu recovered. Hence, after the fitted model was checked for adequacy and was observed to be sufficient, the design software was used to find the stationary points. The following coordinates were calculated by the software:

Initial Cu concentration (A): -0.68

Adsorbent dosage (C): 0.59

Shaking speed (D): 0.95

The actual values were then calculated using the following equation;

$$X_i = X_{iH} - \frac{(X_{iH} - H_{iL})(x_{iH} - x_i)}{(x_{iH} - x_{iL})} \quad (7.3)$$

Where X_{iH} and H_{iL} are the actual high and low levels of X_i, respectively. x_{iH} and x_{iL} are the coded values of X_i. X_i is the coded variable that is being converted. The converted points are as follows: initial Cu concentration (A) was 51.6mg/L, adsorbent dosage (C) was 3.5g/L and shaking speed (D) was 146rpm.

7.2.6 Confirmatory Experiments

Reference should be made to the experimental information in Appendix C for the results mentioned in this chapter. The findings mentioned are an average of runs under similar conditions of experimentation (Table 7.6).

To test the validity of the model's optimized conditions, an experiment was conducted with the model's suggested parameters. The conditions used were as follows in the confirmatory experiment: initial Cu concentration at 51.6mg/L, adsorbent dosage of 3.5g/L and a shaking speed of 146rpm.

Table 7.6: Copper recovery at optimal conditions

Parameter	Initial concentration	Adsorbent dosage	Shaking speed	% Cu removed
Model	51.6	3.5	146	87%
Confirmation tests	51.6	3.5	146	82.13%

The %Cu removed was 82.13% after 120 minutes which is close to the model predicted value of 87%, with an error margin of only 4.87% Thus, the model can be considered to fit the experimental data very well. The designed model is therefore applicable.

7.3 Summary

The objective of this study was to explore optimal process conditions using RSM from a synthesized solution to sequester Cu using untreated orange peels. By reducing the number of experiments, RSM has proven to be a very effective and time-saving model for studying the influence of process parameters on the response. The effect of initial metal concentration, adsorbent dosage and shaking speed on Cu recovery using the response surface methodology and rotatable central composite design was investigated in this chapter. Using statistical software, design expert, a second order model representing the Cu recovery expressed as a function of these three variables was developed. The effects of individual variables as well as their combined interactive effects on the recovery of Cu were performed by statistical analysis (ANOVA). Using F-distribution tests, standard coefficient errors (student t-tests) and determination coefficient (R^2) the model was validated. This guaranteed that convergence at the actual optimum experimental conditions was achieved.

The study has shown that high shaking speed plus low adsorbent dosage and metal initial concentration resulted in higher yields of Cu recoveries. Under the experimental conditions considered, the set of conditions that produced the optimum copper recovery (87%) were found to be an initial Cu concentration of 51.6 mg/L, an adsorbent dosage of 3.5g/L and shaking speed 146rpm.

8 Adsorption isotherms and statistical validity

In the development of adsorption processes, the equilibrium isotherms are important and can also be used to describe how molecules interact with the active sites of the adsorbent during adsorption. The purpose of this study was to investigate the mathematical and statistical properties of two well-known linear isotherms and to compare different statistical criteria to specify the best linear curves fitted to experimental data. Thus, in this chapter, the results of the isotherms were discussed. Then, the best-fitting model was determined using the most commonly used error functions. After this, the applicability of the proposed suitable isotherm function was discussed using the governing assumptions and compared to the adsorbent properties to explain possible mechanisms involved in the process.

8.1 Analysis of Adsorption isotherms

Equilibrium isotherms were measured to determine the capacity of the biosorbents for metal ions and adsorption parameters that would be used for the kinetic studies. In the present research, the adsorption equilibrium data of Cu onto biosorbents prepared from ground banana and orange peels were analysed in terms of two common Langmuir and Freundlich isotherm models. The biosorbents were agitated with fixed volumes of metal ion solutions of varying concentrations until equilibrium was reached (Chapter 4). Table 8.1 summarizes the isotherm models used to fit the experimental data, which were explained and defined in chapter 2.

Table 8.1: The linear modeling isotherm equations that were used.

Isotherm	Equation	Plot	Equation number
Langmuir Isotherm	$\frac{C_e}{q_e} = \frac{1}{bQ_0} + \frac{C_e}{Q_0}$	$\frac{C_e}{q_e}$ vs $\frac{C_e}{Q_0}$	2.4
Freundlich Isotherm	$\ln q_e = \ln Kf + \frac{1}{n}\ln C_e$	$\ln q_e$ vs $\ln C_e$	2.7

8.1.1 The effect of isotherm shape

The impact of isotherm shape has been considered with the view of predicting whether an adsorption system is ‘favourable’ or ‘unfavourable’ (McKay et al., 1982). Also, the data from these experiments were studied using adsorption isotherms on arithmetic graphs drawn by plotting metal ion concentration C_e (mg/L) against adsorbent load q_e (mg/g) (refer to Figure 2.3 in Chapter 2) (Liang et al., 2010). Presented below (Figure 8.2 and 8.3), are the plots of the adsorption of copper onto banana and orange peels.

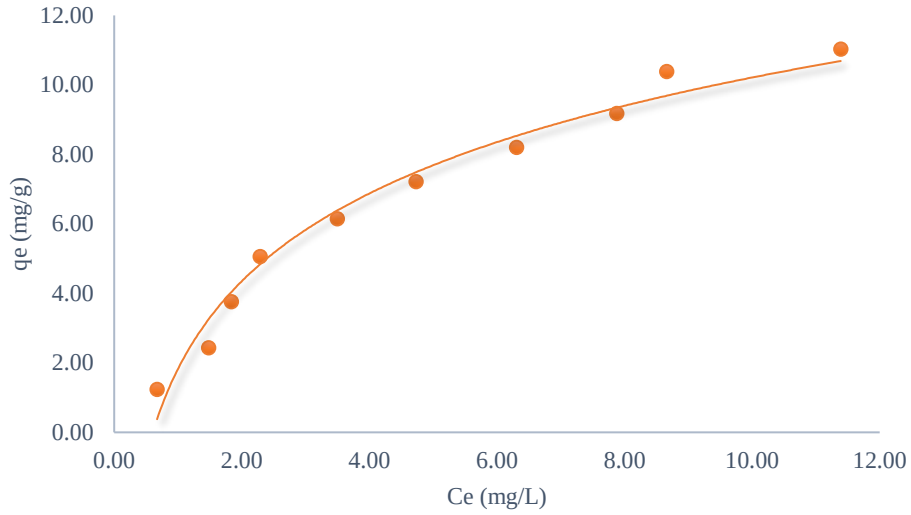

Figure 8.1: Arithmetic plot of metal ion concentration C_0 (mg/L) vs adsorbent loading q_e (g adsorbed/g solid) of orange peels at an initial concentration range of 5 – 50 mg/L at a constant mass dosage of 3.5g/L.

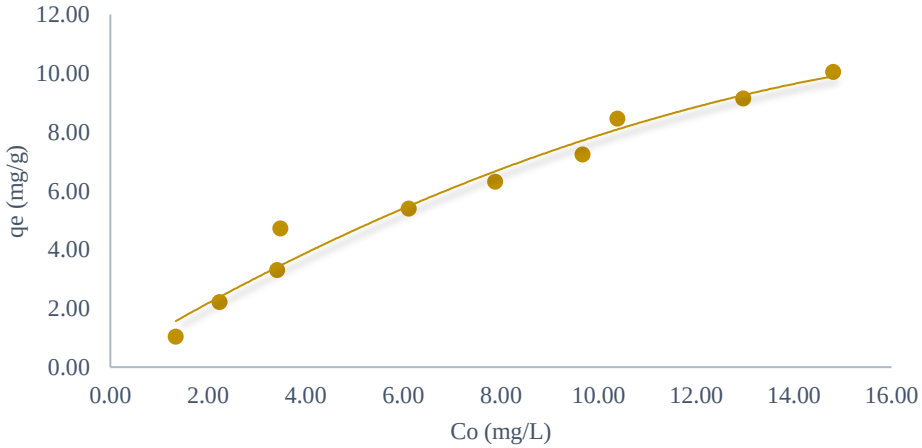

Figure 8.2: Arithmetic plot of metal ion concentration C_0 (mg/L) vs adsorbent loading q_e (g adsorbed/g solid) of banana peels at an initial concentration range of 5 – 50 mg/L at a constant mass dosage of 3.5g/L.

It can be seen that when the plots in figure 8.2 and 8.3 are compared to those in figure 2.3 (refer back to Chapter 2), the orange peels plot is similar to the 'strongly favourable' plot while the banana peels plot closely resembles the adsorption system labeled 'favourable'. Thus, both experimental data sets adequately represent the adsorption systems and therefore, can be subjected to further analysis.

8.1.2 Langmuir isotherm

Langmuir isotherm model is a semi-empirical isotherm obtained from a suggested kinetic system based on the assumption that the surface is energetically homogeneous and that there is no interaction between adjacent adsorbed species (Dada et al., 2017). The adsorption data for both

orange and banana peels were analysed using equation 2.5 (Table 8.1) and the isotherm parameters are presented in table 8.2. The linear isotherm plots for the adsorption of copper onto the prepared adsorbents are also presented in figures 8.3 and 8.4.

Table 8.2: Adsorption isotherm model parameters for the adsorption of Cu ions on banana and orange peels as adsorbents.

Model	Parameter	Adsorbent Type	
		Banana peel	Orange peel
Langmuir	q_{max} (mg/g)	33.33	20
	K_L (L/mg)	0.03	0.12
	R_L	0.39	0.15
Freundlich	K_f (mg/g)	1.09	1.9
	n	1.16	1.35

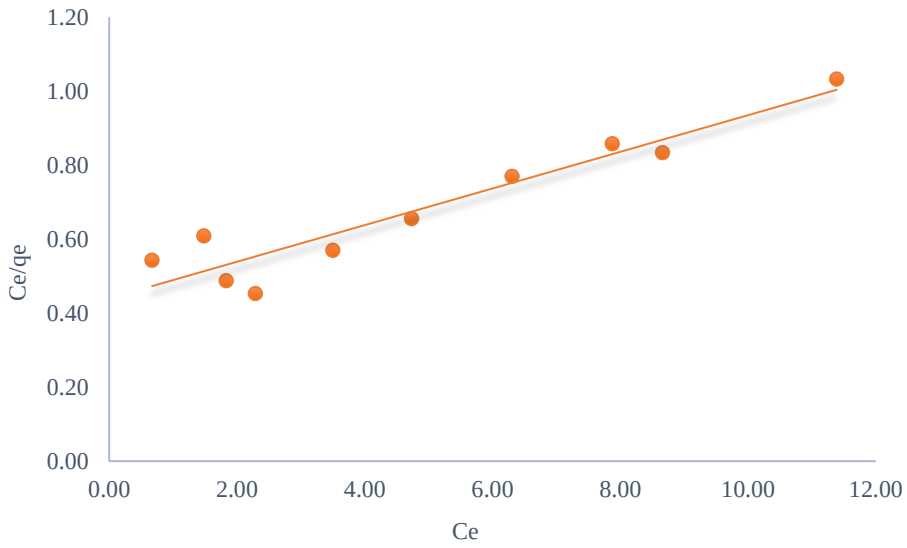

Figure 8.3: Langmuir adsorption isotherm for copper adsorption on orange peels at an initial concentration range of 5 – 50 mg/L at a constant mass dosage of 3.5g/L.

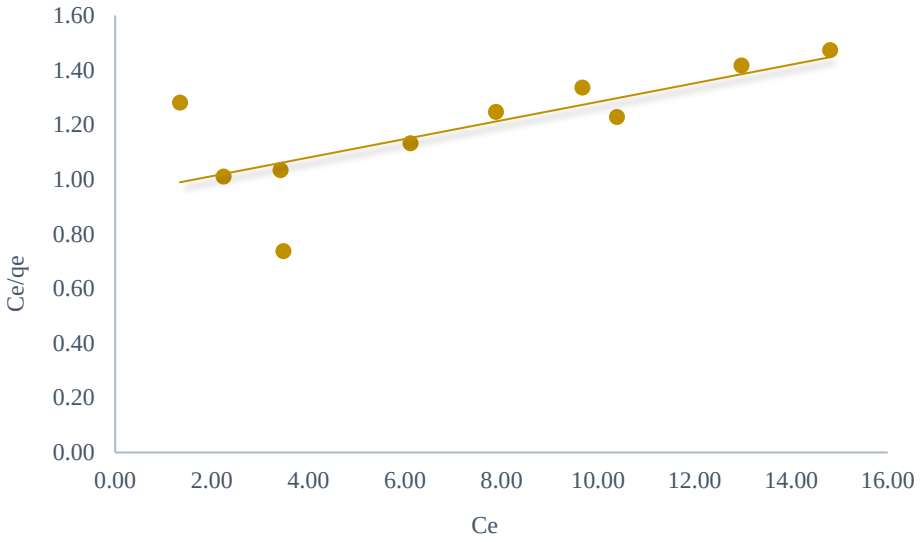

Figure 8.4: Langmuir adsorption isotherm for copper adsorption on banana peels at an initial concentration range of 5 – 50 mg/L at a constant mass dosage of 3.5g/L.

As presented in table 8.1, the maximum Langmuir monolayer adsorption capacity for the orange and banana peels were calculated as 20 and 33.33 mg/g, respectively, suggesting that the copper ions have preferential uptake towards the banana peel as compared to the orange peel. This can be attributed to the characteristics of the adsorbents as extensively explained in Chapter 4; according to one of the assumptions of this model, the surface of the adsorbent is uniform (Shanavas et al., 2011). Therefore, the banana peels were expected to perform better under this model because they are crystalline in nature as compared to the amorphous orange peels.

Another essential feature of the Langmuir isotherm can be expressed in terms of the dimensionless factor R_L (as defined in Table 8.3) also referred to as the separation factor. The separation factor, R_L of the adsorption of Cu onto both the banana and orange peels falls within the range of $0<R_L<1$, suggesting that adsorption of the metal ions is favourable within the studied concentration range. Hence, both peels are suitable for the adsorption of Cu ions from aqueous solutions.

Table 8.3: The effect of the separation factor on the adsorption of Cu on banana and orange peels.

Parametric conditions	Type of system
$R_L > 1$	Unfavourable
$R_L = 1$	Linear
$0 < R_L < 1$	Favourable
$R_L = 0$	Irreversible

8.1.3 Freundlich isotherm model

Freundlich isotherm mainly describes heterogeneous and multilayer adsorption (Liu and Liu, 2008). Figures 8.5 and 8.6 shows the plots of the experimental data modeled using equation 2.7 and the calculated parameters are presented in table 8.2. The K_f and n are the Freundlich isotherm constants describing adsorption capacity and intensity, respectively, were determined from the intercept and slope of the plot of lnq_e against lnC_e (figures 8.6 and 8.7).

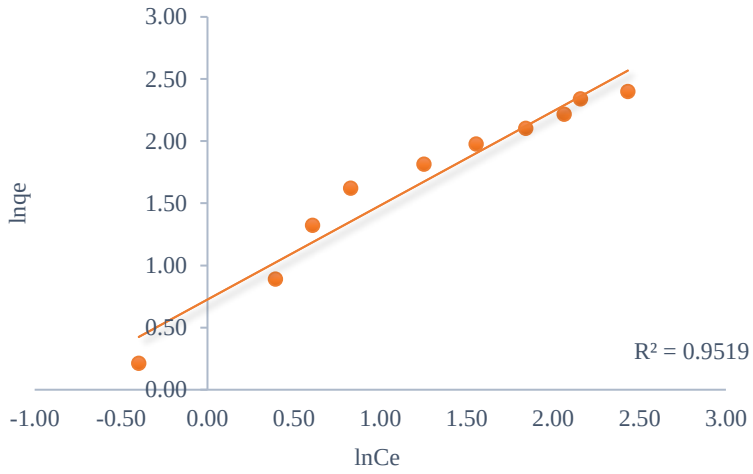

Figure 8.5: Freundlich adsorption isotherm for copper adsorption on orange peels at an initial concentration range of 5 – 50 mg/L at a constant mass dosage of 3.5g/L.

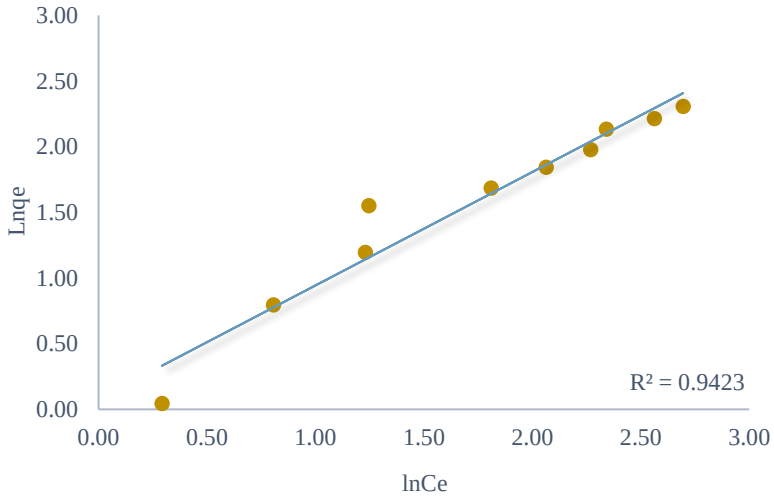

Figure 8.6: Freundlich adsorption isotherm for copper adsorption on banana peels at an initial concentration range of 5 – 50 mg/L at a constant mass dosage of 3.5g/L.

The magnitude of the exponent n indicates the adsorbent-sorbate system's favourability and capacity (McKay et al., 1982). The values of n are defined in table 8.4. The n values (table 8.2) for both adsorption peels are greater than 1 and lie in the range 1< n < 10 which is indicative of a favourable adsorption. Furthermore, 1/n values of the banana (0.86) and orange (0.03) peels are also less than one indicating that the systems are good and that there are greater bonds that exist between adsorbent and adsorbate due to the occurrence of chemisorption reactions.

Table 8.4: Parametric conditions of the Freundlich constant, n.

Parametric conditions	Type of system
n > 1	Favourable
1 < n < 10	Favourable
1/n < 1	Highly chemisorption
1/n ≈ 1	Heterogeneous
1/n > 1	Cooperative adsorption

8.1.4 Experimental vs Predicted

The experimental and predicted equilibrium data that was modeled with Langmuir and Freundlich are both depicted in figures 8.7 and 8.8. From the figures below, the results obtained are well fitted in the linear forms of Freundlich and Langmuir.

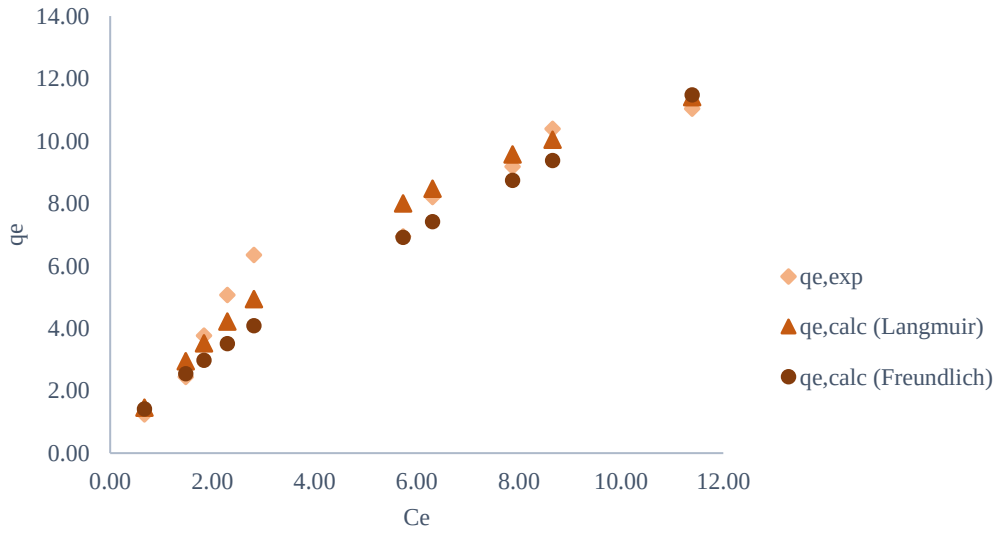

Figure 8.7: Experimental and predicted equilibrium isotherm data by both Langmuir and Freundlich models for the adsorption of Cu ions on orange peels.

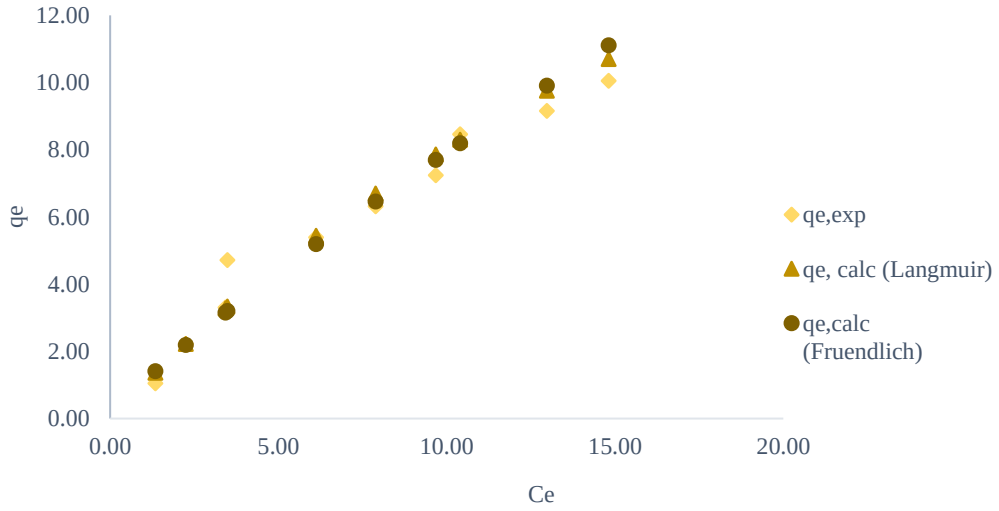

Figure 8.8: Experimental and predicted equilibrium isotherm data by both Langmuir and Freundlich models for the adsorption of Cu ions on banana peels.

These plots show how similar the experimental data is to the data predicted using both the Langmuir and Freundlich isotherms. According to linear regression and model assumptions of the Langmuir isotherm (Das et al., 2008; Rangabhashiyam et al., 2014a), there is: (1) monolayer adsorption, (2) adsorption occurs at specific homogeneous adsorbent sites, (3) no additional adsorption occurs once a pollutant occupies an adsorbent site, and (4) no interaction on adjacent sites between adsorbed molecules. On the other hand, the Freundlich isotherm was initially applied in non-ideal and reversible adsorption systems not restricted to monolayer formation. The empirical expression can be applied to multilayer adsorption with non-uniform distribution of adsorption heat and affinities over the heterogeneous surface (Rangabhashiyam et al., 2014a). However, all these assumptions are seldom true because there is the existence of heterogeneity in the adsorbent surface (explained in Chapter 4). Also, in many cases, the restriction of monolayer coverage or non-interaction between adsorbed species is not strictly followed (Ghosal and Gupta, 2017). Therefore, it is possible that they show the same trend because they obey some of the assumptions in both isotherms that were used to model the equations.

It is also known that the nature of the attractive forces holding the molecules on the adsorbent surface in adsorption is classified into physisorption and chemisorption (see Chapter 2). Physical adsorption is a process that is fast and reversible, influenced by the solution temperature and concentration. Additionally, layers of the adsorbate can be formed on the surface resulting in multilayer adsorption whereas, the adsorbent is chemically bound to the adsorbent in chemisorption. Therefore, in chemisorption, only one monomolecular layer is produced, whereas in physisorption, multilayer formation is possible (Bradshaw, 1977). Also, while physisorption and

chemisorption may occur at the same time at intermediate temperatures, at extreme temperatures they can be easily distinguished (Achife and Ibemesi, 1989; Bradshaw, 1977). For this study, intermediate temperatures were used, which may explain why both the plots using the different isotherms exhibit a similar trend.

Solid-liquid systems involving bioadsorbents are dynamic and complex, and obeying the isotherm does not necessarily reflect the validity of the aforementioned assumptions. In such systems the isotherm may not adequately describe the process and can be seriously affected by the experimental conditions, in particular, the range of concentration of the solute/adsorbate (Rangabhashiyam et al., 2014a). For example, in this study, both Langmuir and Freundlich isotherms adequately described the same set of liquid-solid adsorption data at a concentration range of 5-50 mg/L based on the relatively similar plots observed in figures 8.7 and 8. Therefore, another tool was required to assist in the selection of a model to predict q_e values that will be used in modeling kinetics later on in the study. In this case, statistical methods were applied as discussed in the next section.

8.2 Statistical validity

This section examined the mathematical and statistical characteristics of two well-known linear isotherms and compared distinct statistical criteria to identify the best linear curves for experimental information. Four different error functions have been examined in this study and the isotherm parameters have been determined (algorithm presented in Chapter 3). In the following subsections, the error functions studied were defined in Chapter 2 and are summarised in table 8.5 below. The best-fit isotherm was selected based on the error function that gave the minimum distribution of error between the experimental and predicted values while selecting a maximum for the coefficient of determination.

Table 8.5: Error functions used to statistically determine the best adsorption isotherm for the experimental data studied.

Error Function	Abbreviation	Model Equation
Chai-square test	χ^2	$x^2 = \sum_{i=1}^{n} \frac{(q_{e,calc} - q_{e,meas})^2}{q_{e,meas}}$
Sum of squares of the errors	SSE	$SSE = \sum_{i=1}^{n} (q_{e,calc} - q_{e,meas})_i^2$
Coefficient of determination	R^2	$R^2 = \frac{\sum(q_{e,calc} - \bar{q}_{e,meas})^2}{\sum(q_{e,calc} - \bar{q}_{e,meas})^2 + (q_{e,calc} - q_{e,meas})^2}$
Marquardt's percent standard deviation	MPSD	$MPSD = \sqrt[100]{\frac{1}{N-P}\sum_{i=1}^{n}\left(\frac{q_{e,calc} - q_{e,meas}}{q_{e,meas}}\right)_i^2}$

Where N is the number of experimental data points, $q_{e,calc}$(mg/g) is the theoretically calculated adsorption capacity at equilibrium, $q_{e,meas}$ (mg/g) is the experimental adsorption capacity at equilibrium and P is the number of parameters in each isotherm model.

The values of regression statistics are shown in table 8.6. According to the values presented in table 8.6, the Langmuir isotherm is statistically suitable to describe the biosorption of copper onto both the banana and orange peels. The highest R^2 values and lowest SSE, MPSD, and x^2 were found when modeling the equilibrium data using the Langmuir for linear regression analysis. The Langmuir isotherm constants have been commonly used in research to illustrate the adsorption ability and thermodynamic energy parameters (Dada et al., 2017). Therefore, it is an acceptable model to predict the equilibrium data for both systems at the specified process conditions (Explained in Chapter 4) and will be used to model q_e values that will be used for the kinetic study.

Table 8.6: The calculated values of the respective error functions.

Isotherm model	Adsorbent Type	Error Function			
		SSE	MPSD	X	R
Langmuir	Banana	3.37	0.9638	0.6678	0.9605
	Orange	4.6	0.9629	0.82255	0.9551
Freundlich	Banana	4.51	0.9862	0.84656	0.9477
	Orange	10.24	0.968	1.6945	0.9099

8.3 Summary

In this research, the adsorption of Cu ions onto banana and orange peels was carried out. The related results were modeled using the Langmuir and Freundlich isotherms through linear regression and, the best-fitting model was evaluated by using four different error functions. The values of the error functions were calculated using Microsoft excel. The analysis of the values showed that the Langmuir isotherm equation was statistically the best-fit equilibrium model for the adsorption process using both the peels as adsorbents. Hence, this adsorption isotherm model will be used to model the kinetic data in the next chapter.

9 Adsorption Batch kinetics and mechanisms

It is important to establish the rate of adsorption of copper onto the bioadsorbents as it is vital in designing a fixed-bed column. The amount of Cu adsorbed onto the surface of the banana and orange peel can be estimated by using kinetic equations that are required to estimate the fluid phase concentration in fixed-bed column operation. The dominant design parameter of fixed-bed column operation, the breakthrough time and shape of the breakthrough curve are dependent on the rate of adsorption (Dursun, 2006). Thus, in this chapter, reaction and diffusion models (presented in Table 9.1 and explained in Chapter 2) were evaluated with experimental data from Chapter 8 to understand the kinetics of the removal of copper from water using banana and orange peels as adsorbents. Also, possible governing mechanisms are discussed later in the chapter.

Table 9.1*:* Reaction and diffusion kinetic models that were used to evaluate the experimental data of the adsorption of Cu ions onto banana and orange peels.

Kinetic model	Linear Equation	Plot	Equation number
Pseuso first-order	$\log(q_e - q) = \log q_e - \frac{k_1}{2.303}t$	$\ln(q_e - q_t)$ vs t	2.18
Pseudo second-order	$\frac{t}{q(t)} = \frac{1}{k_2 q_e^2} + \frac{t}{q_e}$	$\frac{t}{q(t)}$ vs t	2.20
Weber-Morris	$q_t = k' t^{0.5} + C$	q_t vs $t^{0.5}$	2.9
Banghan's model	$\log\log\left(\frac{C_i}{C_i - q_t m}\right) = \log\left(\frac{K_0 m}{2.303V}\right) + \alpha \log(t)$	$\log\log\left(\frac{C_i}{C_i - q_t m}\right)$ vs t	2.14
Boyd-Reichenberg model	$Bt = \pi\left(1 - \sqrt{1 - \frac{\pi}{3}\frac{q_t}{q_e}}\right)^2$ for $\frac{q_t}{q_e} < 0.85$	Bt vs t	2.12
	$Bt = -\ln\frac{\pi}{6} - \ln\left(1 - \frac{q_t}{q_e}\right)$ for $\frac{q_t}{q_e} > 0.85$	Bt vs t	2.13
Liquid film diffusion	$\ln\left(1 - \frac{q_t}{q_e}\right) = \ln\left(\frac{6}{\pi}\right) - \left(\frac{D_i}{r^2}\right)\pi t$	$\ln\left(1 - \frac{q_t}{q_e}\right)$ vs t	2.8

9.1 Kinetic reaction models

9.1.1 Pseudo first-order model

Isotherm models were evaluated in the previous section and the information was used to model the kinetics. Figures 9.1 and 9.2 show the plot of $\log(q_e-q_t)$ versus t for the two adsorbents which represent the pseudo first-order kinetics for the removal of copper using banana and orange peels at the initial concentration of 50mg/L. The rate constants were determined for each adsorbent from the slope of the corresponding plot (figures 9.1 and 9.2) and are listed in table 9.2. Also, the results obtained from adsorption isotherms were used to calculate the required values of q_e as proposed by Worch (2012) (see Appendix E).

Table 9.2: Model parameters for the adsorption of copper from using banana and orange peels

Parameter	Adsorbent	
	Banana peel	Orange peel
$q_{e,,calculated}$	10.06	11.03
$q_{e,calculated,1}$	10.70	11.40
$q_{e,calculated,2}$	8.79	2.13
K_1 (min^{-1})	0.0145	0.01359
R^2	0.96	0.83

Where $q_{e,calculated}$ (mg/g) was from the experimental data, $q_{e,calculated,1}$ was calculated using the Langmuir isotherm and $q_{e,calculated,2}$ was calculated using the pseudo-first order kinetic model.

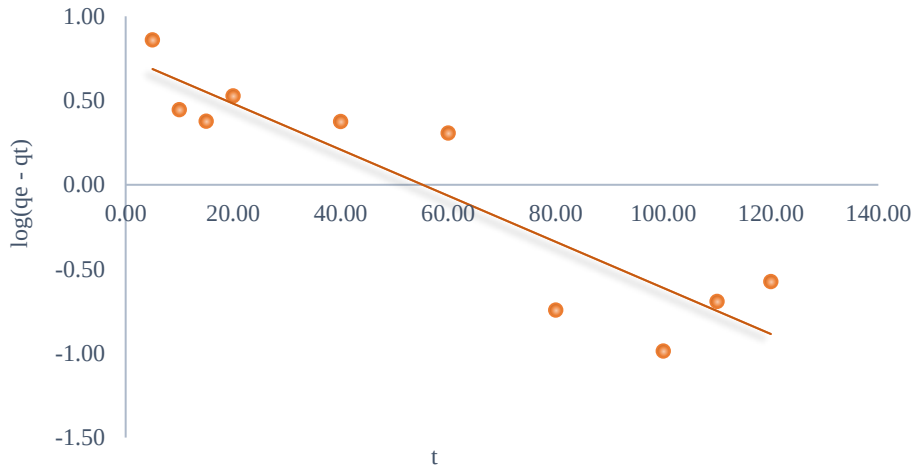

Figure 9.1: Experimental data fitted into the pseudo-first order kinetic model for the adsorption of Cu ions onto orange peels as an adsorbent at an initial concentration of 50mg/L.

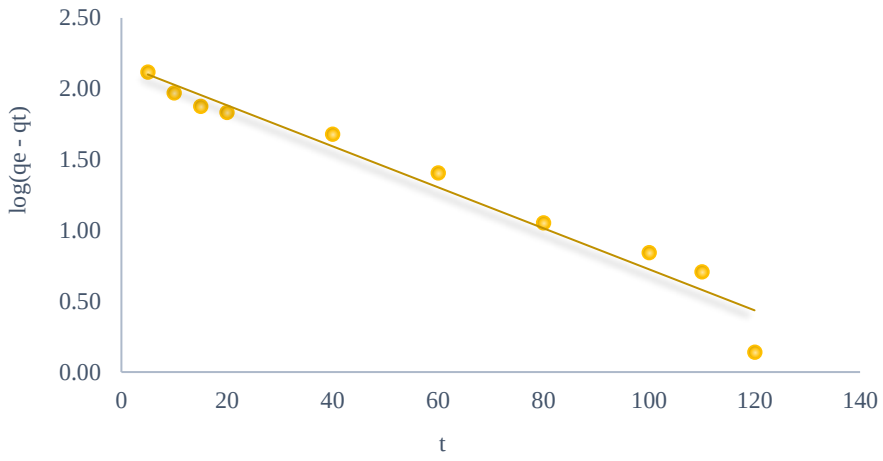

Figure 9.2: Experimental data fitted into the pseudo first-order kinetic model for the adsorption of Cu ions onto banana peels as an adsorbent at an initial concentration of 50mg/L.

The plot for the banana peels (Figure 9.2) had a good linear relationship with a coefficient of determination of 96.08% while that of the orange peels did not show a good linear relationship with a coefficient of determination of 83.16%. The maximum adsorption capacity of banana and orange peels was 8.79 and 2.13 mg/g, respectively. Researchers like Worch (2012), suggest that the model is suitable to describe only the first 20-30 minutes of the experimental data and not the entire range. Even so, the orange peels still do not fit the model well at this time interval (see Figure 9.1) and the differences in the theoretical and calculated q_e values (table 9.2) is very large. Therefore, it can be said that another model is required to model the kinetics of the adsorption of Cu ions using orange peels.

9.1.2 Pseudo second-order model

The adsorption kinetics were described as pseudo-second order using equation 2.8 (Table 9.1) . The plots of the t/q_t versus t for the two adsorbents are shown in figures 9.3 and 9.4. The results obtained yielded the second-order rate constant (k_2), estimated equilibrium capacity (q_e) and the coefficient of determination (R^2) for initial concentration of 50mg/L and adsorbent dosage of 3.5g/L, as shown in table 9.3. The plots were found to be linear with good correlation coefficients (± 0.99) indicating the possible applicability of the pseudo second-order kinetics in this study. Comparatively, in each case, the R^2 values were higher than those of the pseudo-first order model. This would suggest that the kinetics of the adsorption of Cu can be better described using pseudo-second order onto both biosorbents.

Table 9.3: Model parameters for the adsorption of copper from using banana and orange peels

Parameter	Adsorbent	
	Banana peel	Orange peel
$q_{e,,calculated}$	10.06	11.03
$q_{e,calculated,1}$	10.70	11.40
$q_{e,calculated,2}$	9.12	1.14
K_1 (g/mg.min)	0.014	0.677
h(mg/g.min)	1.17	1.44
R^2	0.995	0.997

Where $q_{e,,calculated}$ (mg/g) was from the experimental data, $q_{e,,calculated,1}$ was calculated using the Langmuir isotherm and $q_{e,,calculated,2}$ was calculated using the pseudo second-order kinetic model.

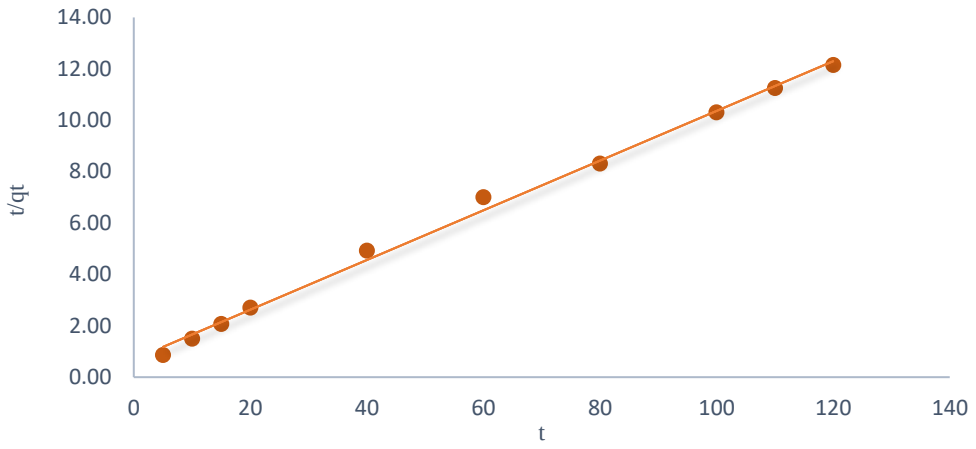

Figure 9.3*:* Experimental data fitted into the pseudo second-order kinetic model for the adsorption of Cu ions onto orange peels as an adsorbent at an initial concentration of 50mg/L.

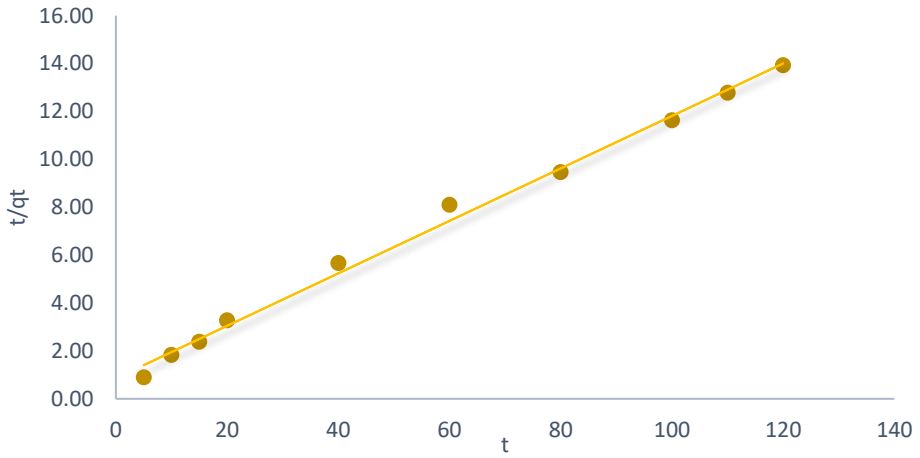

Figure 9.4: Experimental data fitted into the pseudo second-order kinetic model for the adsorption of Cu ions onto banana peels as an adsorbent at an initial concentration of 50mg/L.

Final remarks about reaction kinetics

The values of k_1 and k_2 are the time scaling factors that determine how fast a process would reach equilibrium. They are also usually dependent on process parameters such as initial concentration, adsorbent dosage, pH, temperatures, agitation speed, and particle size (Plazinski et al., 2009a; Chen et al., 2016, 2017). However, these are merely empirical constants with no specific physiochemical significance as they cannot be connected to the fundamental adsorption mechanisms (Tofan et al., 2008). As a result, for this study, there was no variation in the aforementioned process parameters. In this section instead, only the optimum values obtained in Chapter 7 were used to model the kinetics of the process under study.

The difference between the q_e values of both pseudo kinetic models for the adsorption of Cu ions on orange peels is too high when compared to the experimental and those predicted using the Langmuir isotherm (see Table 9.1). Therefore, the adsorption of metal ions onto orange peels does not follow pseudo first- or pseudo-second order kinetics. As such, some authors have made proposals to explain the deviations like the one exhibited by the adsorption of Cu ions on orange peels: (1) one argument for variations in the q_e values is that there is a time lag at the start of the adsorption method, potentially because of a boundary layer or external resistance control (McKay et al., 1982). It is also challenging to quantify this time lag and does little to aid in rationalizing the differences in experimental and theoretical q_e values (Ho and McKay, 1999). (2) Concerning the short time correlation between experimental and theoretical data for the pseudo-first order model, it was also suggested that another first order reaction dominates over the first or there is another reaction of another order (Liu and Zhang, 2009). Moreover, no mechanisms were suggested by any researchers for this phase.

However, it was discovered that the calculated q_e values for the adsorption of Cu ions on banana peels were close to the experimental q_e values calculated using the reaction kinetic models. Moreover, the value of the coefficient of determination (R^2) for the second-order kinetic model is higher than that of the pseudo first-order kinetic model at an initial copper concentration of 50mg/L. Even though banana peels fit both models well, Azizian (2004) found that for two cases, when the general analytical solution was obtained, the adsorption process obeyed pseudo first-order kinetics at high initial solute concentration, while it obeyed the pseudo second-order kinetics model at a lower initial solute concentration. This statement supports the findings of this section because it was used for an initial low concentration of 50 mg/L as opposed to other higher concentrations of 100-200 mg/L that were used in other studies that fit the pseudo first-order model well (Rengaraj et al., 2002; Tofan et al., 2008; Sen Gupta and Bhattacharyya, 2011). Thus, based on these results,

the kinetics of Cu adsorption using banana peels at a low initial concentration can be explained by the second-order kinetic model. This further assumes that chemisorption is the rate-controlling step which involves the presence and participation of valence forces generated when the adsorbent and sorbate exchange or share electrons (Tofighy and Mohammadi, 2011). Furthermore, in chemical adsorption, it is assumed that the adsorption capacity is proportional to the number of active sites occupied on the adsorbent surface. From the calculated qe values using both chemisorption models, banana peels exhibited better adsorption capacities which could imply that the peels have more active sites ready to participate in chemical reactions. The different mechanisms of adsorption are later explained (section 9.4) to elucidate the sorbent-sorbate interactions.

The pseudo first- and second-order have been empirical models until recently and thus, still lack a theoretical basis as they were not derived based on a pre-assumed reaction mechanism. However, they are largely associated with surface reaction controlled mechanisms. Even though this has been the case, some researchers have mathematically and experimentally illustrated that these models can fit another or a combination of other adsorption mechanisms: Rudzinski and Plazinski, (2007) demonstrated using a mathematical derivation that pseudo first and second-order can simulate the behaviour of intraparticle diffusion. The aforementioned interpretation indicate that pseudo first- and second-order kinetics are not models of defined mechanisms but, rather, highly flexible formulas that combine many different models with different controlling mechanisms. In short, efforts to determine the rate-controlling mechanism based on pseudo first- and pseudo second-order curve fit are essentially futile, as multiple conclusions are possible according to the existing theories of these two models. A better approach to getting better results according to Plazinski (2010), would be to carefully control experimental conditions to establish an appropriately controlled regime, which would obtain semi-empirical function yielding more meaningful, k_1 or k_2 values. Despite the fact that inconsistencies exist with these models, it is important to remember that empirical models are more descriptive than predictive. Therefore, to obtain good results, kinetic experiments for design purposes should be conducted under conditions as close as possible to the target large-scale operation (Foo and Hameed, 2010). Nonetheless, due to their practical significance, high curve-fitting capability, and easy manipulation, they will still have continued widespread acceptance in the modeling of liquid adsorption kinetics.

9.2 Diffusion models

Adsorption is an efficient technique of separation commonly used in the treatment of water purification and wastewater. Adsorption of metal ions using an adsorbent from a liquid solution usually includes three steps (Azizian, 2004; Yao and Chen, 2017): (1) diffusion of the adsorbate through the liquid film surrounding the adsorbent particle (internal film diffusion); (2) diffusion within the adsorbent particle (intraparticle diffusion) that may be due to pore diffusion or surface diffusion or a combination of both;(3) adsorption on the pore surface (surface reaction). In most adsorption systems, the surface reaction step is relatively fast and the control step is diffusion (film and/or intraparticle diffusion).

Adsorption response models such as the two pseudo models above, do not describe the above steps separately: when these models are used, they normally assume that the general adsorption rate is regulated solely by the adsorbent surface while intra-particle diffusion and external mass transport are ignored (Viegas et al., 2014). Therefore, this section aimed to use diffusion models to determine the rate-limiting step.

9.2.1 Weber-Morris

Weber-Morris Model (explained in Chapter 2) is a well-known approximate equation for intraparticle diffusion and this model can be expressed according to equation 2.15 in table 9.1. Where k' (mg/g $min^{1/2}$) is the intraparticle diffusion rate constant and C is the intercept that gives an idea about the boundary layer thickness, i.e., the larger the intercept, the greater the boundary layer effect. The values of k' and C were calculated from the slope and intercept of the linear plot of qt versus $t^{1/2}$ (Figure 9.5 and 9.6) and were listed in table 9.4. Equation 2.15 was used to plot the graphs presented in figures 9.5 and 9.6 at an initial concentration of 50mg/L.

Table 9.4 Diffusion model parameters for the adsorption of copper using banana and orange peels as adsorbents.

Parameter	Adsorbent	
	Banana peel	Orange peel
K'	0.0323	0.0356
C	4.68	5.54
R^2	0.925	0.9164

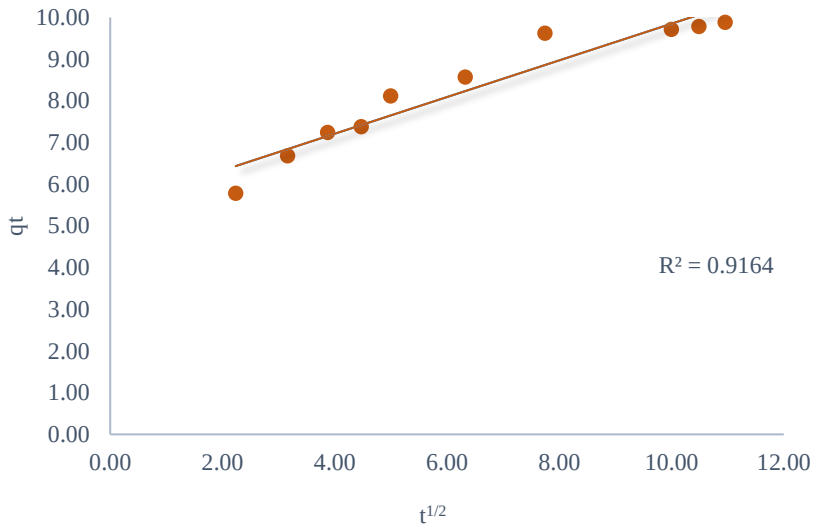

Figure 9.5: Intraparticle diffusion plots of the adsorption of Cu ions onto orange peels at an initial concentration of 50g/mL.

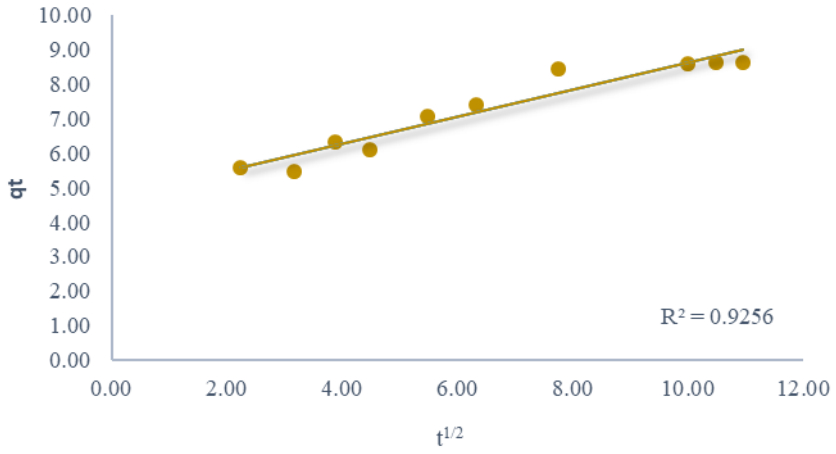

Figure 9.6: Intraparticle diffusion plots of the adsorption of Cu ions onto banana peels at an initial concentration of 50g/mL.

From the graphs presented above, it can be seen that the data points in both cases cannot be connected by a single straight line, which indicates that the adsorption of copper onto banana and orange peel adsorbents is not controlled by a single rate controlling diffusion step. However, like in most cases of some other adsorbents (Chakrapani et al., 2010; Ismaiel et al., 2014), there are multi-linear plots depicting the influence of two or more rate-controlling steps in the sorption process. Therefore, presented below (Figure 9.7 and 9.8) are the same but plotted to show the multi-linear plots that exist.

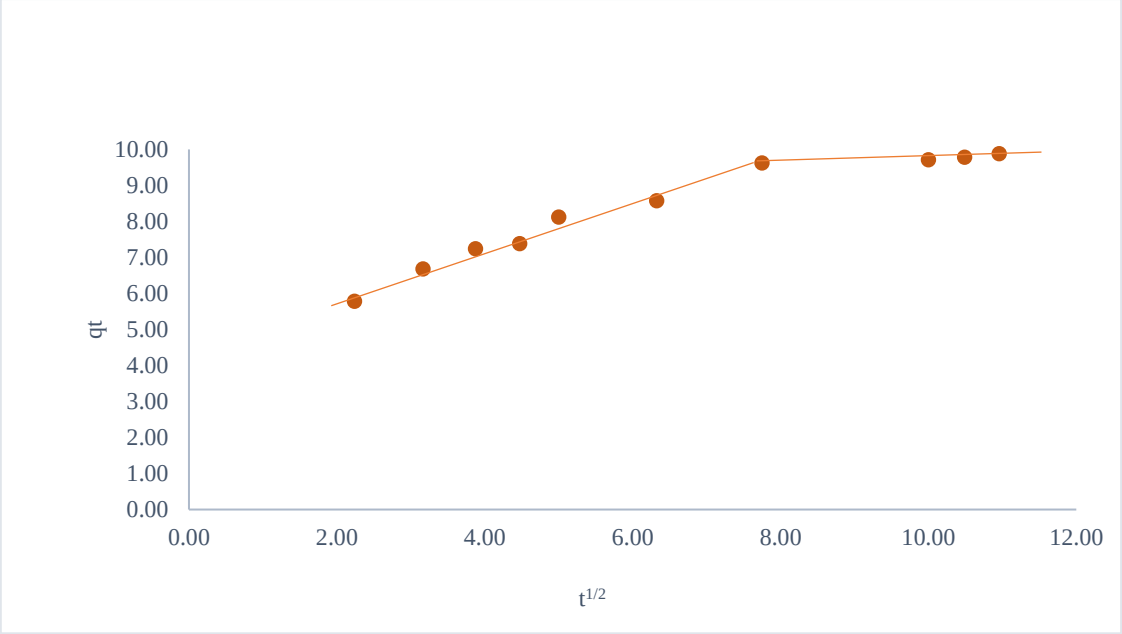

Figure 9.7: Intraparticle diffusion plots showing the dual nature of the kinetics of adsorption of Cu ions onto orange peels at an initial concentration of 50g/mL.

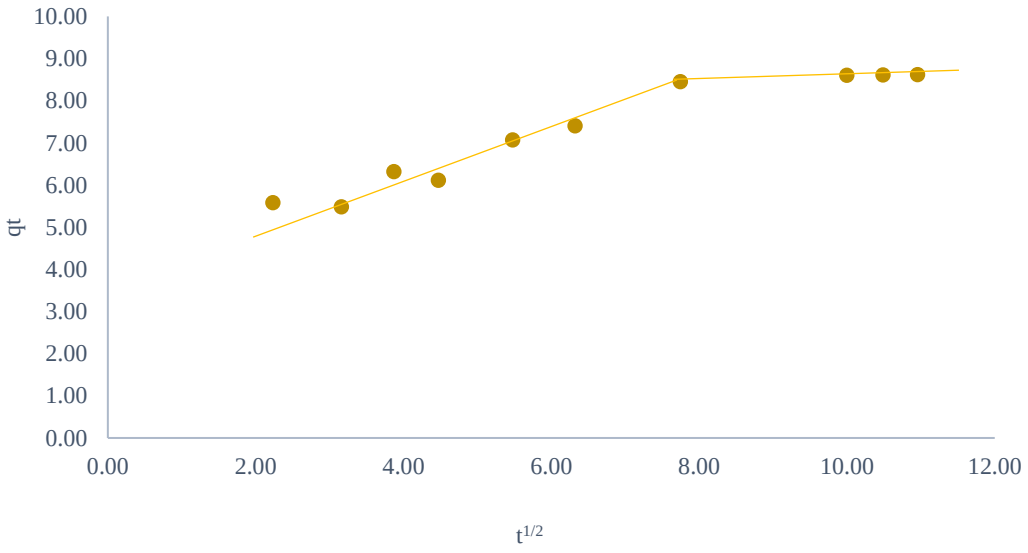

Figure 9.8: Intraparticle diffusion plots showing the dual nature of the kinetics of adsorption of Cu ions onto orange peels at an initial concentration of 50g/mL.

The intraparticle diffusion plots have a dual nature; the first portion of the plot indicates the first sharper portion which is the external surface adsorption or instantaneous adsorption stage (the initial stage of adsorption) and the second portion of the plot indicates an intraparticle diffusion effect (Chakrapani et al., 2010), see figure 9.7 and 9.8. In the aforementioned figures, two separate phases are apparent from the plots; first linear part (Stage I) followed by what almost resembles a plateau (Stage II). Over 50% of the Cu was quickly adsorbed by both the banana and orange peel

adsorbents in Stage I within eight minutes. This is due to the immediate adsorption of ions on the adsorbent surfaces of the most easily accessible adsorbent locations. The very slow diffusion of adsorbate from the surface layer into the internal pores is noted in Stage II. Thus, the original portion of Cu ion adsorption by banana and orange peel adsorbents can be controlled by the original intraparticle copper transport controlled by the mechanism of surface diffusion and the subsequent portion regulated by pore diffusion. Similar dual nature with initial linear and then plateau was found in the literature (Chakrapani et al., 2010; Ismaiel et al., 2014). Moreover, if the plots are linear and pass through the origin then the intraparticle diffusion is the sole rate-controlling step. If not, then some other mechanism along with the intraparticle diffusion is also involved (Lodeiro et al., 2007).

As can be seen from Figures 9.5 and 9.6, the intercept of the plots does not pass through the origin. This may be due to a difference in the rate of mass transfer in the initial and final stages of adsorption and indicates some degree of boundary layer control which implies that intraparticle diffusion is not the only rate-controlling step (Chakrapani et al., 2010). Similar observations were made by Yang et al. (2015) for their work on the biosorption of cadmium using biological materials. However, it should be noted that equation 2.15 approximates the pore diffusion kinetics without taking into account the contributions of the pore dimensions (Wu et al., 2009a). Also, the literature is silent on these aspects and not a lot of work reporting a detailed study of the impact of pore diffusion processes on heavy metal uptake in particular, the effects of the pore radius and pore size distribution on the sorption kinetics are available.

Thus, the lack of research regarding pore dimensions can be a possible contributing factor to the inability to provide reasons that could account for the data not passing through the origin; the characterization results from Chapter 4 of this work show evidence of pores together with their dimensions in the adsorbents. Thus, they may influence the mechanisms responsible for the adsorption of Cu ions. The following reasons could also explain why the data plots do not pass through the origin (Hanumantharao et al., 2012): (1) this model of intraparticle diffusion assumes that when the process approaches equilibrium, there is no change in solution concentration and, (2) the model of intraparticle diffusion is derived based on a constant diffusivity. However, conditions differ from system to system and the structure of bioadsorbents also makes it challenging to evaluate some changes or predict behaviour during adsorption. Hence, in an attempt to account for and learn about the intraparticle diffusion in the current adsorption system, the data were further evaluated using Banghan's pore diffusion model (section 9.2.2) and a third intraparticle diffusion model by Boyd was also applied (section 9.2.3).

Lastly, the intraparticle diffusion model parameters for the adsorption of Cu using banana and orange peels are given in Table 9.4 and it was observed that the values of C and k' were higher in the case for orange peels as opposed to those of obtained for the adsorption of copper onto banana peels. Thus, Weber's model would attribute stronger influence by external mass transfer effect in the adsorption process using orange peels as compared to banana peels because of the higher value of C. However, when agitation is introduced in the adsorptive system, the intraparticle diffusion of the solute that is adsorbed from solution to the sorbent sites could be a rate-controlling mechanism as opposed to film diffusion (Tsukamoto and Ohe, 1991; Viegas et al., 2014). Furthermore, it can also be observed in figure 9.8 that banana peels do not have a good linear correlation during the first stage of diffusion attributed to the boundary layer. Hence, film diffusion and the effects of operating conditions on the boundary layer are explained later in subsection 9.2.4.

9.2.2 Pore diffusion model – Banghan's model

The kinetic data for Cu adsorption onto the banana and orange peels were analysed by using the Banghan's equation to check if pore diffusion is the only controlling step in the adsorption process or not. $\log\log\left(\frac{C_i}{C_i - q_t m}\right)$ was plotted against log(t) (Figures 9.9 and 9.10) for the adsorption of Cu ions onto bananas and orange peels. The plots have high correlation coefficients greater than 90%. Thigh correlation coefficients confirm some conformity with the Banghan's equation. However, the experimental data put to representation by equation 2.14 (Table 9.1) did not yield a desired linear fit in the double logarithmic plot as shown in Figures 9.9 and 9.10. This indicates that the diffusion of the adsorbate into the pores of the adsorbents is not the only rate controlling step. Therefore, the contribution of pore diffusion to the adsorption of Cu ions using orange and banana peels could not be disregarded which means that during the various phases of the process, it could be a rate-limiting mechanism. Not a lot of work concerning the adsorption of metal ions has been done using this model. However, some authors like Chakrapani et al. (2010) have used it to account for and confirm the diffusion mechanism, which is the case in this work too.

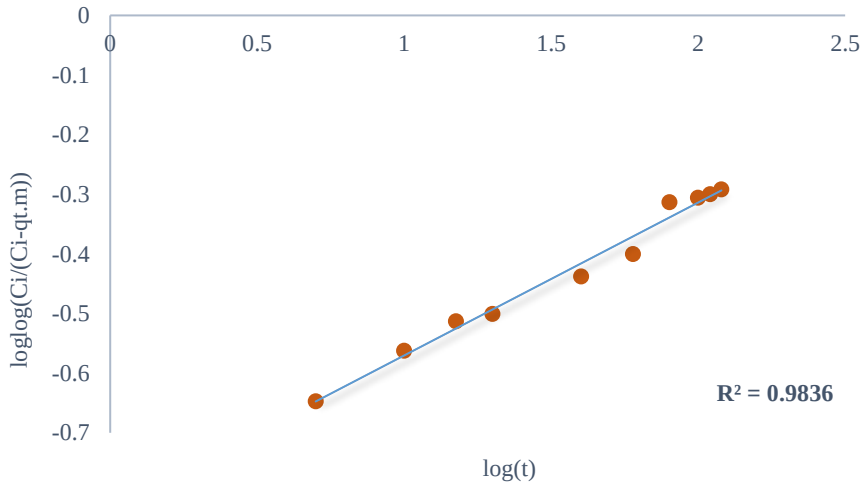

Figure 9.9: Experimental data of the adsorption of Cu ions onto orange peels fitted to the linear form of the Bangham's pore diffusion model at an initial concentration of 50mg/L with an adsorbent mass of 3.5g/L in a 0.1L solution.

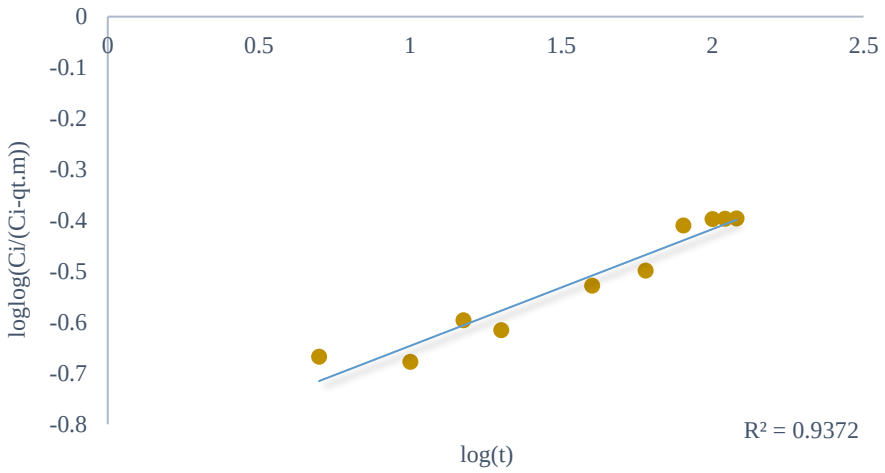

Figure 9.10: Experimental data of the adsorption of Cu ions onto banana peels fitted to the linear form of the Bangham's pore diffusion model at an initial concentration of 50mg/L with an adsorbent mass of 3.5g/L in a 0.1L solution.

9.2.3 Boyd model

To interpret the experimental information in determining the step governing the general rate of the adsorption of Cu ions using banana and orange peels, the kinetic data were evaluated by the procedure given by Reichenberg (1953) and Walton (1962) (see Chapter 2). Equations 2.12 and 2.13 (presented in Table 9.1) were used to evaluate the data and the plots are presented in figures 9.11 to 9.14. The linearity test for the possibility of pore diffusion being the rate-limiting step was tested by plotting Bt vs t (having a slope B). Also, according to this model, if the line passes through the origin then the process is governed by intraparticle diffusion.

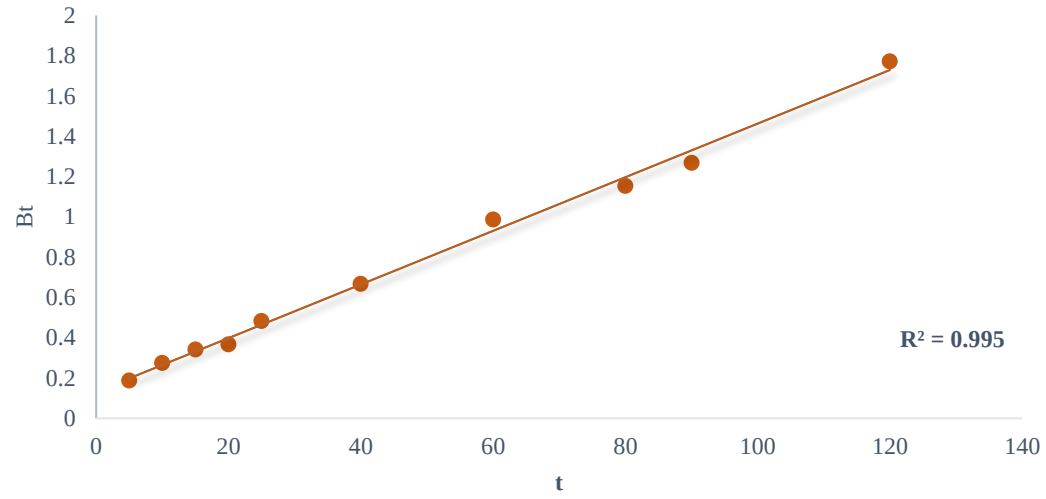

Figure 9.11: Adsorption of copper using orange peel by equation 2.12 of the Boyd and Reichenburg kinetic model at an initial concentration of 50mg/L.

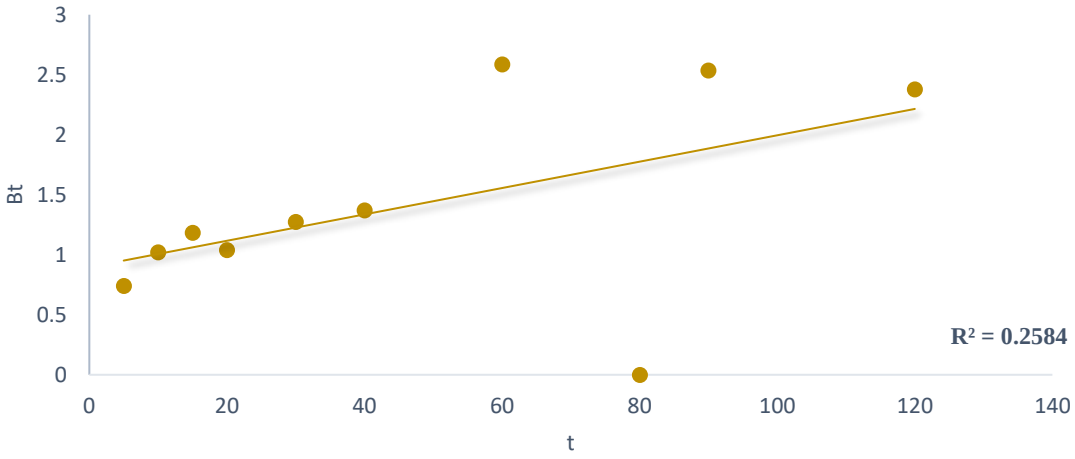

Figure 9.12: Adsorption of copper using banana peel by equation 2.12 of the Boyd and Reichenburg kinetic model at an initial concentration of 50mg/L.

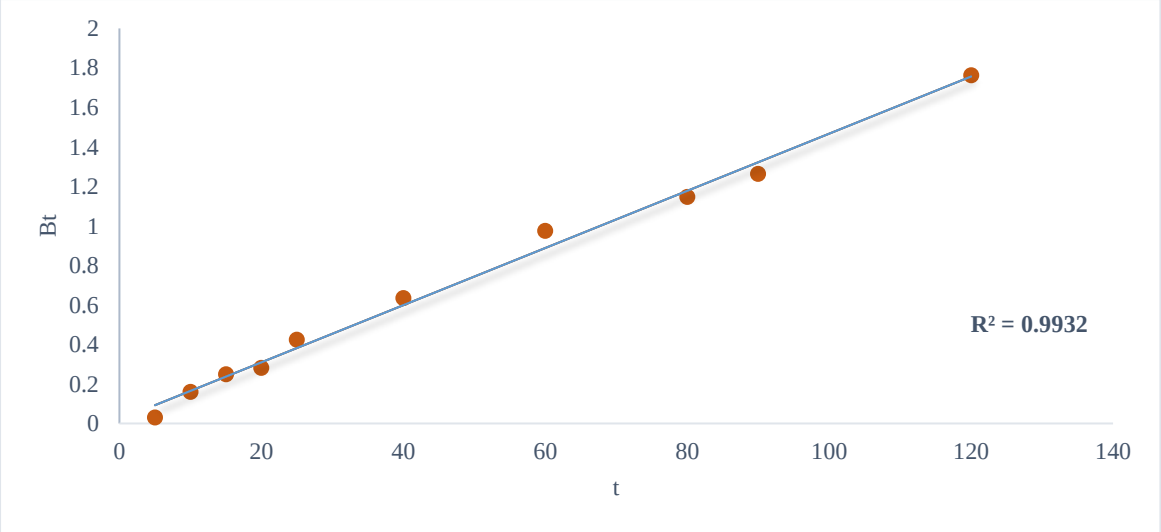

Figure 9.13: Adsorption of copper using orange peel by equation 2.13 of the Boyd and Reichenburg kinetic model at an initial concentration of 50mg/L.

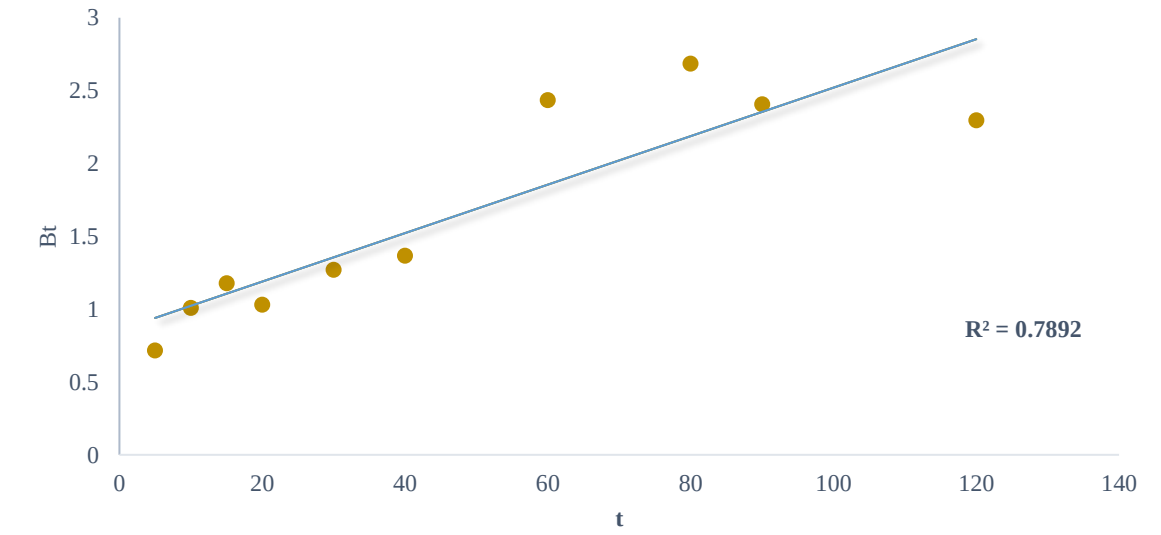

Figure 9.14: Adsorption of copper using banana peel by equation 2.13 of the Boyd and Reichenburg kinetic model at an initial concentration of 50mg/L.

The data was plotted using both the equations based on the specified equation conditions (see Table 9.5). As such, figures 9.11 and 9.12 show the plots according to equation 2.12 because they satisfies one condition of the equation: all the values of q_t/q_e orange peels except the last three points which are less than 0.85 while the first half of the banana peel q_t/q_e values fall below 0.85. It can be seen from the plots that the plot of the adsorption of Cu using orange peels is linear and almost crosses through the origin using both equations. Besides, the high correlation factors (see Figures 9.11 and 9.13) are a good indication of the model fitting the data evaluated. Therefore, the non-zero intercepts are a clear indication that intraparticle diffusion is not the sole rate-limiting process. Comparatively, looking at the plots of the banana peels (Figures 9.12 and 9.14) as an adsorbent, it

can be seen that the only relationship resembling a linear plot is observed at the initial stage of the process. However, as time increases from 40 minutes, there is no observable correlation. Also, the evaluated data presented with low correlation factors as seen in figures 9.12 and 9.14. This poor fit exhibited by the banana peels suggest that intraparticle diffusion may be hindered by other factors. There are also two possible explanations for this unexpected behaviour (Viegas et al., 2014; Wu et al., 2009b): (1) Diffusion within particles is complicated because not only do molecules diffuse through pores, but they also interact with the solid surface. Pore structure and interaction between fluid and solid phases affect the overall rate of diffusion. Therefore, intraparticle diffusion is usually system-dependent. (2) The choice of the diffusion model also affects intraparticle diffusion, as the models are based on various diffusion mechanisms. For this reason, it is possible that the model could not fully account for intraparticle diffusion in banana peels for the chosen data set or there were inherent limitations based on the method of linearity used to simplify the model.

Therefore, there is a need to explore the possibility of film diffusion being the rate-limiting step as the adsorption process may be controlled by film diffusion or by both film and intraparticle diffusions.

9.2.4 Film diffusion

A model based on Fick's law was used to quantitatively assess the diffusion mechanism. It is well known that metal ion adsorption processes can be explained by film or porous diffusion (Nibou et al., 2010). The film diffusion mechanism is expressed as equation 2.8 as presented in table 9.1. The values of the liquid film diffusion were determined from the slopes of the linear plots of the $\ln\left(1-\frac{q_t}{q_e}\right)$ vs t (see Figures 9.15 and 9.16). From the presented results, both the plots were linear. The orange peel plot was closer to the origin as opposed to the banana peel plot with correlation factors of 0.90 and 0.96 for the banana and orange peels as adsorbents for the adsorption of Cu, respectively.

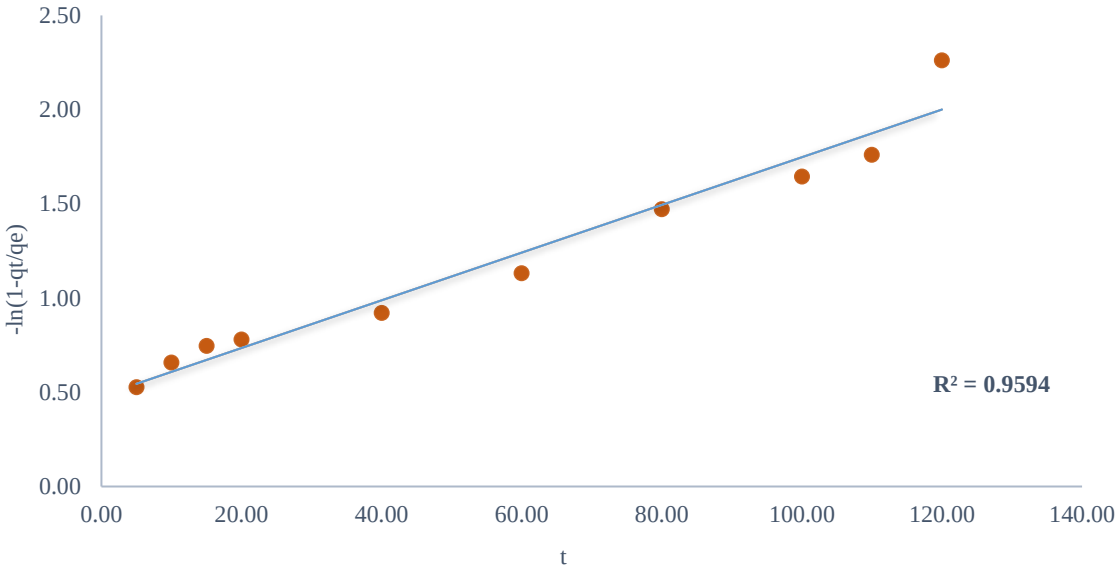

Figure 9.15: Liquid film diffusion model for the adsorption of Cu using orange peels at an initial solution concentration of 50mg/L.

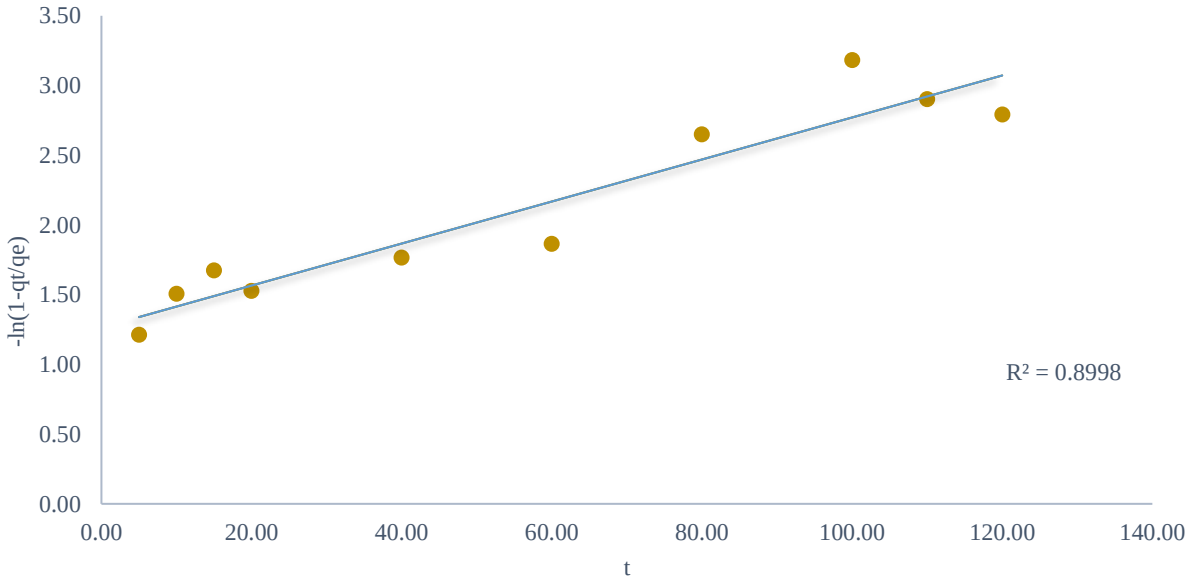

Figure 9.16: Liquid film diffusion model for the adsorption of Cu using banana peels at an initial solution concentration of 50mg/L.

The intercept values for orange peels for the adsorption of copper ions is 0.481 while that of banana peels is 1.26. Both values are higher than zero but the intercept of orange peels is close to the origin showing the significance of liquid film diffusion being the rate determination of the adsorption process as opposed to that of banana peels. Also, the R^2 values for orange (0.9594) and banana (0.8998) peels were relatively high, showing the possible significance of film diffusion as a rate-determining factor in the adsorption process of Cu onto banana and orange peels.

The calculated values of the diffusion coefficient for pore and film diffusion for the adsorption of Cu onto banana and orange peels at an initial concentration 50mg/L are presented below in table 9.5. From the results presented in the table below, pore diffusion seems to be faster than film diffusion based on the diffusivity coefficients of the banana peels, the same trend is observed for the orange peels.

Table 9.5: Diffusion coefficients for the adsorption of Cu ions by orange and banana peels.

Adsorbent type	Diffusion coefficients (cm/s)	
	Film diffusion	Pore Diffusion
Banana peel	9.35×10^{-23}	5.85×10^{-16}
Orange peel	6.6×10^{-16}	3.2×10^{-16}

The structures of the two materials can also be used to explain the diffusion rates relative to each other. From the results presented in table 9.5, pore diffusion is much slower when using banana peels as opposed to orange peels. The first reason to account for this is that diffusion is affected by the material structure as well as the interactions between the solid and liquid phases. Banana peels have a smaller diameter relative to the orange peels. This could mean that there is more pore diffusion resistance therefore, diffusion through pores is hindered because of the small size of the pathway and irregular pore structure (Koh et al., 1998). Furthermore, according to IUPAC definition (Vohlidal, 2004): a porous medium is a solid with pores that is, cavities, channels or interstices. However, based on the SEM results obtained in Chapter 4, banana peels have a fibrous structure with crater-like structures that are hollow and wide therefore, inhibiting the diffusion process. Lastly, banana peels have a crystalline structure as opposed to the orange peels that displayed an amorphous nature (explained in Chapter 4). Diffusion through grain boundaries is faster than bulk diffusion: grain boundaries are simply an area where structure is absent, or the arrangement is amorphous (Harsh, 2005). They behave as highways for diffusion. Therefore, in the case of a crystalline material, due to a limited availability of grain boundaries, the rate of diffusion is much slower than its counterpart i.e. amorphous material.

It is further known that the relative magnitude of film and intraparticle mass transfer resistance depends on adsorption conditions such as stirring, speed and adsorbent size. High stirring can reduce or even eliminate film mass transfer resistance while smaller particle size usually means lower intraparticle diffusion resistance (Yao and Chen, 2017). Banana peels have smaller radius (explained in Chapter 4) and according to the evaluated results obtained using the Weber-Morris kinetic model (Chapter 9), where the intercept is not zero, indicate the presence of a bigger

boundary layer compared to orange peels. Therefore, these observations can be considered as reasons for internal diffusion being faster than external diffusion. No research was found that explains this, as such, further investigation needs to be done to explain how adsorbents' characteristics are related to kinetic model parameters.

According to literature (Sağ and Aktay, 2000; Mohan and Singh, 2002), three distinct cases occur during the adsorption of species by porous adsorbents:

Case I: external transport > internal transport

Case II: external transport < internal transport

Case III: external transport ≈ internal transport

In cases I and II, respectively, the rate is governed by the diffusion of films and particles. In case III, it may not be possible to transport ions to the boundary at a significant rate, resulting in the formation of a liquid film with a concentration gradient surrounding the adsorbent particles (Sağ and Aktay, 2000; Mohan and Singh, 2002). From the presented results, one can see that both the orange and banana peels fall under case II. Also, external transport is commonly the rate-limiting step in systems that have (1) inadequate mixing, (2) dilute adsorbate concentration, (3) small particle size, and (4) high affinity for the adsorbent. The intraparticle pathway, on the other hand, limits overall transfer for systems with (1) high adsorbate concentration, (2) good mixing, (3) large adsorbent particle size, and (4) low affinity for the adsorbent (Lu et al., 2009). Drawing from this explanation, the following process conditions can be noted about the current study that explains the possible role of both external and internal mass transfer: dilute concentrations, small particles, good mixing, high affinity for adsorbent (orange peel), and low affinity (banana peel). Thus, confirming the possibility of both external and internal diffusion being controlling mechanisms for the adsorption of Cu ions.

Some articles can be found in literature. For instance, comparative research by Kursunge et al. (2014), on Cu adsorption on fresh orange peels and pectin extracted orange peels found that Cu adsorption for both adsorbents is regulated by film diffusion-based solely on the outcomes of intraparticle diffusion. Also, Deshmukh et al. (2017) used dried banana peels for the removal of cadmium from aqueous solutions. They suggested that intraparticle diffusion may not be a limiting factor but surface adsorption along with intraparticle diffusion may play a significant role in the adsorption of cadmium on dried banana peels.

9.3 Mechanisms of Copper adsorption

The mechanisms by which heavy metals are adsorbed on adsorbents can include physical adsorption, electrostatic interaction, and exchange of ions, surface complexation and precipitation. In general, intermolecular interactions between functional groups and heavy metals are complex; they depend on the adsorbent surface's heterogeneity and its chemistry, the aqueous solution's ionic environments, and the nature of the adsorbent (Aguayo-Villarreal et al., 2017). Chemisorption (exchange of ions, surface complexation, precipitation) generally plays a greater role in removing heavy metals from an aqueous solution than physisorption (electrostatic interaction and physical adsorption) (Mohan et al., 2008). Also, notice that in a particular aqueous solution, several mechanisms may be at play. For instance, ion exchange, electrostatic interaction, and surface complexation are strongly linked to surface functional groups by through electrostatic forces, binding sites formation, and covalent bonding (Yang et al., 2019).

Despite a large number of literature studies on adsorption of heavy metals using agricultural waste, few have performed a quantitative assessment of the role of adsorbent characteristics in heavy metal adsorption (Aguayo-Villarreal et al., 2017; Xie et al., 2017; Yang et al., 2019). Therefore, the following discussion tries to identify the links between each adsorption mechanism and different adsorbent characteristics along with supporting literature examples.

9.3.1 Physical adsorption

Physical adsorption is a weak process involving the diffusional movement of heavy metals into the adsorbent pores and then deposition on the surface without chemical bonds being formed. Physical adsorption is generally strongly influenced by the distribution of pores and the adsorbent surface area (Kruk et al., 1999). Increasing microspores can significantly improve the surface area to facilitate physical adsorption, while increasing mesoporous levels can enhance the diffusion of contaminants to speed up adsorption kinetics (Fomkin et al., 2017). From the results in Chapter 4, under pore classification, both peels were classified as having mesopores therefore, mass transfer operations are expected to play a role in the adsorption of copper using banana and orange peels. The extent of adsorption however, will be determined by the pore size and pore distributions. If attention is drawn to results of the intraparticle diffusion model, both peels exhibit good correlation and fitting to the diffusion models. However, orange peels seem to show better correlations which may be due to the bigger mesopores found on the peels and a higher pore volume (discussed in Chapter 4).

The heterogeneity and polarity of the adsorbent surface combined with functional groups can help in the physical adsorption of heavy metals, particularly through electrostatic attraction and ion-dipole forces (Sun et al., 2014). Both adsorbents exhibited highly heterogeneous surfaces based on the FTIR results (Chapter 4). Physical adsorption for heavy metals is prevalent but unlikely to serve as a predominant mechanism of adsorption. Nonetheless, some studies have highlighted the significance of physical adsorption of aqueous heavy metals for the adsorption on adsorbent materials. For instance, Nayak et al. (2017) studied the effect of activated conditions on activated carbon and concluded that physical and pore diffusion mechanisms were operative. Some researchers have found that Pb(II) adsorption on biochar is a physical endothermic process (Liu and Zhang, 2009).

9.3.2 Electrostatic interactions

Electrostatic interaction takes place between heavy metals that are strongly charged and carbon adsorbents that are negatively charged, particularly with the presence of functional groups. Additionally, the contribution of electrostatic interaction to heavy metal adsorption on adsorbents is a weak process and usually considered to only be secondary. (Cui et al., 2015; Yang et al., 2019). The physicochemical characterization of the bioadsorbent surface, specifically acid-base behaviour of functional groups, may play a crucial role in the ionic interactions that occur during the process (Palma et al., 2011a), thus, it is essential to postulate the mechanisms involved. Furthermore, the information about pH_{pzc} allows one to hypothesize on the ionization of functional groups and their interaction with ionic species in solution. Also, most adsorbent surfaces are variably charged and the occurrence of electrostatic interaction in heavy metal adsorption is depended on solution pH and an adsorbent's point of zero charges (Yang et al., 2019)

All adsorbents are characterized by having two main regions with a buffering capacity in the pH ranges between 3-4 and 8-10 where the first range could correspond to carboxylic groups and the second to hydroxyl groups (Pagnanelli et al., 2003). It has also been reported that the adsorption of metal ions depends on the carboxyl and hydroxyl groups present in cellulose (Thirumavalavan et al., 2010). From table 4.5 in Chapter 4, the surface pH of orange peels falls under the first range while bananas fall under the second. Furthermore, based on the results presented in chapter 4, the orange peels were found to be positively charged (acidic) while banana peels were found to be positively charged (basic). Thus, mechanisms of uptake and the extent of electrostatic interactions will be different. Some evidence from the literature (Goyne et al., 2002), corroborates this.

9.3.3 Ion exchange

One of the main mechanisms for the adsorption of heavy metals by agricultural adsorbents is the exchange of ions between heavy metals and protons on oxygen-containing functional groups such as carboxyl and hydroxyl group (Pagnanelli et al., 2003). In addition, the efficiency of ion exchange processes in the adsorption of heavy metals on carbon surfaces largely depends on the ion size of the adsorbent's metal contaminant and surface functional group (Aguayo-Villarreal et al., 2017; Xie et al., 2017; Yang et al., 2019).

The results of the FTIR were presented and discussed in Section 4.5. The results presented after the adsorption of Cu ions showed a significant shift in the peaks. This shift in wavelength represents a change in bond energy of the functional groups indicating a change in the bonding pattern after adsorption (Lasheen et al., 2012). Further, this study produced results that corroborate the findings of previous work in this field (Sha et al., 2009; Khaskheli et al., 2011; Lasheen et al., 2012). The shift of the peaks was attributed to chemical interaction of the sorbate with carboxylic and hydroxyl groups through ion exchange or complexation or even a combination of both (Feng et al., 2010, 2009; Liang et al., 2011). Other authors also reported similar findings. For example, the metal uptake of Cu ions using chemically modified orange peels by Lü et al. (2010) was achieved through ion exchange involving the acid carboxylic groups.

Furthermore, Aguayo-Villarreal et al. (2017), stated that carbon adsorbents with K, Na and Ca elements attached in single-metal solutions were the best activated carbons for heavy metal adsorption; these adsorbents also contain surface areas and a significant content of oxygenated functional groups suitable for binding metal ions. In addition, the dominant adsorption mechanism was ascribed to the exchange of ions in this research. Results of the EDS (chapter 4) showed that both adsorbents contained some, if not all, of the above-mentioned metals that disappeared after adsorption. This behaviour in conjunction with the above explanation draws attention to the possibility of ion exchange during adsorption (Liu and Zhang, 2009).

9.3.4 Surface Complexation

Surface complexation (internal and external sphere) forms multi-atomic (i.e. complex) structures with distinctive metal-functional interactions, playing a primary role in heavy metal adsorption on some adsorbents (Yang et al., 2019). Heavy metals can be efficiently linked to the functional groups of carboxyl, phenolic and lactonic (Liu and Zhang, 2009). The FTIR results (chapter 4) revealed the presence of carboxyl groups in both adsorbents which could be responsible for the binding of Cu ions through complexation. Other examples from literature corroborate this: the characterization study on banana and orange peels done by Kamsonlian et al. (2011b) revealed that changes in the bands are usually a result of complexation. Chao et al. (2014) further explained that agricultural

waste contains within it cellulose and functional groups that to some extent have the ability to donate electrons form complexes with metal ions in aqueous solutions. Marín et al. (2010) also indicated the involvement of carboxylic groups in the adsorption of Cu by modified orange peel adsorbents.

Carboxylic and hydroxyl groups have been reported as the main groups participating in the adsorption of metal ions in banana and orange peel studies. However, the existence of these functional groups does not guarantee that the ions will be attached to the surface of the adsorbent because the process may be influenced by a number of factors such as (1) the number of active sites, (2) the accessibility of the sites, chemical states, and the affinity between sites and targeted ions (Park et al., 2010; Nguyen et al., 2013). Thus, to try and account for some of these and increase the efficiency of ion adsorption, authors have modified the adsorbents (Liang et al., 2010; Lü et al., 2010; Marín et al., 2010). Contrary to the studies focused on targeting carboxylic and hydroxyl groups, other authors reported similar mechanisms using other functional groups and attaching elements like Mg and K to the bioadsorbents (Liang et al., 2010). Although polar substances contain high levels of –OH group that enhances their adsorption capacity toward metal ion, the lone pair electrons (O or N) present in carbonyl and amine groups, also play an important role in the adsorption process and are capable of forming metal complexes (Park et al., 2010). Both banana and orange peels contain carbonyl and amine groups. Thus, from the results presented above, it can be seen that adsorption mechanisms depend heavily on the characteristics of the adsorbent, the type of ion species and the process parameters such as pH, temperature, agitation speed, etc.

9.4 Final remarks and conclusions

Pseudo first and pseudo second-order kinetic models are the most popular empirical models in liquid adsorption and a number of theoretical interpretations have been suggested (Dursun, 2006). The mechanism of these two models is supposed to fit chemical reaction controlled kinetics. Theoretical interpretations, however, have indicated that satisfactory application of these pseudo models alone is no guarantee of control of chemisorption. Thus, the characterization of the adsorbents was done to postulate possible reasons the adsorption of Cu using banana and orange peels would follow a reaction mechanism. The FTIR results (presented in Chapter 4) indicate that the peels have heterogeneous surfaces that contain a number of functional groups which are capable of taking part in a number of reactions depending on the process conditions (see subsection 9.3). Furthermore, FTIR analysis indicated the presence of carboxylic, carbonyl, hydroxyl, amine and aromatic compounds with carboxylic acid, hydroxyl and carbonyl which are argued to be the main binding sites accounting for metal adsorption (subsection 9.3). From the presented results, banana peels seem to fit well with both pseudo-first order and pseudo-second order kinetic models as

opposed to the orange peels. Also, the calculated q_e values for the adsorption of Cu ions on banana peels showed a good agreement to the experimental q_e values calculated using the reaction kinetic models. These results indicate that the adsorption process may have a significant reaction process with the sharing or exchanging of electrons between the Cu ions and the banana peel adsorbent. A similar phenomenon has been observed in the adsorption of various metal ions onto lignocellulosic waste compost (Jia et al., 2002; Wu et al., 2009a).

Furthermore, to understand the adsorption mechanism, knowledge of the adsorbent's speciation diagram and surface chemistry is necessary. Although speciation tests are not accessible for this research, it has been established from literature (Paulson and Kester, 1980; Jia et al., 2002) that the hydrolysis of $Cu^{2+}(aq)$ leads to the formation of $Cu_2(OH)_2^{2+}$. Mononuclear species $Cu(OH)^+$, $Cu(OH)_2$, and $Cu(OH)_3^-$ are formed in dilute solution with increasing pH in the range 8−12, with $Cu(OH)_4^{2-}$ formed in the more alkaline solutions. Therefore, it is reasonable to say that $(OH)^+$ species at the initial metal concentration of 50mg / L (which is deemed a dilute solution) and pH range (5.5) used in this research are not essential in terms of equilibrium with the orange peel surface. However, this may apply to banana peels as they are basic in nature (pH: 7.79), and their addition to the solution may raise the pH leading to the formation of an environment that drives surface responses. In addition, Cu complexes in the pH range of 6.8–8.4 (Paulson and Kester, 1980). This can therefore, explain why the banana peels fit well with the reaction kinetics compared to the acidic orange peels.

The Weber-Morris model is the third most popular model in water treatment after the pseudo first- and second-order models for liquid adsorption kinetics. The line should run through the origin (I= 0) for kinetics governed by intraparticle diffusion alone. However, in most cases like the data presented in this chapter, the plot demonstrates multi-linearity over the whole adsorption period, and offers better fit if not forced through the origin (C >0) (Wu et al., 2009a). Multi-linearity in q_t vs. $t^{1/2}$ plots was considered (that is, two or three steps are usually involved to follow the whole process). In this form, the external surface adsorption or instantaneous adsorption occurs in the first step; the second step is the gradual adsorption step, where intraparticle diffusion is controlled; and the third step is the final equilibrium step, where the solute moves slowly from larger pores to micropores causing a slow adsorption rate (Wu et al., 2009a). From the results presented, only two distinct steps can be identified because both peels contain mesopores from the evaluated BET results presented in Chapter 4. Therefore, the last slow steps involving micropores is not present. In addition, according to McKay et al. (1980), a large C corresponds to a high resistance to film

diffusion. Therefore, relative to each other, banana peels are expected to have a lower resistance to film diffusion compared to orange peels.

Furthermore, based on of Langmuir fluid kinetics, Douven et al. (2015) established a theoretical context for the Weber–Morris model. They indicated that film diffusion dominates for very short periods over the whole process of adsorption and can be left out for model derivation. However, the validation spectrum is somewhat more restricted than that generally recognized in the literature. Nonetheless, they found that the model is valid if these conditions are fulfilled: intraparticle control, Henry regime adsorption, and infinite volume of bulk solution. However, Henry regime is governed by physical adsorption and based on the evidence presented by several authors (Chakraborty et al., 2009; Parkes et al., 2013; Canivet et al., 2014), bio-waste based adsorbents have a finite number of binding sites. Based on this, it makes sense that the plot does not cross the origin indicating an intraparticle diffusion-controlled system because (1) The adsorbents have heterogeneous surfaces which are capable of taking part in surface reactions under favourable conditions; Both banana and orange peels showed a good fit to the pseudo-second order reaction model with correlation coefficients as high as 0.99, and (2). They have a finite number of binding sites.

The Banghan's pore diffusion model has been used to check whether pore diffusion is a possible mechanism in the adsorption of copper ions by orange and banana peels. A linear plot was observed when $\log\log\left(\frac{C_i}{C_i - q_t m}\right)$ was plotted against logt confirming pore-diffusion. In addition, k_0 and α are constants whose roles have not been defined. Thus, no efforts to calculate them was made. This model was used solely to confirm the existence of pore diffusion in the study. Similar 'pore-diffusion' confirmatory evaluations using Banghan's model have been made by numerous authors (Aharoni et al., 1979; Foo and Hameed, 2010; Gupta et al., 2011), with no effort made to explain the implications of the calculated constants.

This section discussed the possible governing mechanisms of Cu ions onto banana and orange peels by evaluating six kinetic models. The fitting of the models revealed that there is more than one mechanism responsible for the uptake of Cu using orange and banana peels. Also, the adsorption of Cu ions on the fruit peels' surface may be considered to involve the ion-exchange mechanism as well as some other weaker types of interactions, like physical force and complexation. This study also provided an insight into some important characteristics of bioadsorbents that are responsible in binding Cu onto the peels, which is also a helpful selection for a particular design of wastewater treatment units.

10 Conclusion and Recommendations

10.1 Introduction

Adsorption has become a competitive wastewater treatment technique and the kinetics of adsorption is one of the primary factors that need to be known before any adsorbent is acceptable and/or considered for any application. Furthermore, knowledge about kinetics is a basic requirement for optimum design of operations of adsorption and separation. In addition, good kinetic models play a key role in transforming technology from laboratory scale to a full scale application. Furthermore, good models aid in analysing and interpreting experimental data, and also predicting the response of a system to different conditions. Therefore, the main aim of this research was to provide a pragmatic understanding of the mechanisms and kinetic aspects of the adsorption of Cu onto orange and banana peels in order to establish a sound basis and an understanding of adsorption for modeling purposes.

The specific objectives were as follows:

- To characterize adsorbents in order to understand their surface morphology and subsequently propose possible adsorption mechanisms.
- To identify and evaluate factors that affect the adsorption capacity of the biomaterials and to optimize the process.
- To critically evaluate suitable equilibrium isotherms and kinetic models so as to analyse the adsorbate-sorbent interaction.

10.1.1 Characterization

In order to acquire data on how the material is expected to perform during the adsorption of metal ions, the composition, physical and chemical characteristics of banana and orange peels were investigated. Due to the complex nature of bioadsorption processes and adsorbent materials, a combination of characterization techniques such as FTIR, SEM / EDX, XRD, BET and titration methods were used to determine the structural characteristics of the banana and orange peels.

This information was informative and based on the information collected, the following conclusions were possible:

- Functional groups of the peels play an important role in the removal of Cu from water. Adsorption processes such as electrostatic interactions, surface complexation, ion

exchange, and physical adsorption can be directly and indirectly affected by interactions between functional groups and copper ions.

- Amorphous and crystalline phases in the adsorbents affects the rate of adsorption. Amorphous orange peels have a higher rate of diffusion as opposed to the crystalline banana peels.
- Larger pore sizes and volume allows for better metal removal during adsorption.
- Surface charges and pH affect metal adsorption. This is also linked to process conditions such as the initial pH of the solution, temperature and type of metal ion.

10.1.2 Identification of influential factors and statistical optimization

The aim of this section was to investigate and identify factors that have a significant impact on adsorption of copper ions using banana and orange peels. The study used DOE as a research instrument to design an experimental plan to determine the significant factors that affect the process of copper adsorption.

Initial Cu concentration, temperature, type of adsorbent, adsorbent dosage and shaking speed were the factors investigated. Factors were studied at their maximum and minimum levels. The experimental results were statistically analysed and indicated the following:

- Initial Cu concentration, adsorbent dosage and shaking speed were statistically significant.
- The results also showed that Cu recovery was maximized at low concentration, low shaking speed, low temperatures, low initial concentration, high adsorbent dosages and that orange peels were the better adsorbent.
- The interaction between most of the variables was found to be statistically insignificant within the ranges studied, with the exception of one that included initial Cu concentration, adsorbent dosage and shaking speed, which showed a marked influence on the process of copper recovery.

Thereafter, a statistically-based optimization technique called response surface methodology was used for parametric optimization of, initial metal concentration, adsorbent dosage and agitation speed. CCRD was used to design the experiments. Experimental results were then analysed with appropriate statistical tools using Design Expert.

Cu recovery was found to depend on adsorbent dosage, initial metal concentration and agitation speed. This is because these elements affect the mechanisms of adsorption: (1) the amount of adsorbent available determines the amount of available binding sides for the copper ions, (2) the initial metal concentration has an effect on the concentration gradient for mass transfer, and (3) the

agitation speed has an influence on the external film of the particles by reducing the film layer surrounding the particles which then affects the rate of adsorption. These observations indicate that the choice of suitable working ranges for these parameters is paramount in the adsorption of Cu ions on banana and orange peels in this study.

10.1.3 Isotherms and statistical validity

Equilibrium studies were carried out to determine the best model to use to generate data for adsorption kinetic studies. Two isotherm correlations, namely Langmuir and Freundlich linear equations, were used to analyse the experimental data. Furthermore, the best-fitting model was evaluated using four different error functions. The analysis of the values showed that the Langmuir isotherm equation produced the best correlation factors (0.99 >) and thus, was statistically the best fit equilibrium model for the adsorption process using both the peels as adsorbents.

Even though, the choice of the isotherm model was chosen based on statistical validity, it is known that adsorption equilibrium and kinetics are considerably affected by the heterogeneity of the adsorbent surface. Banana and orange peels are heterogeneous adsorbents and contain more than one type of adsorption site capable of binding the adsorbent. Furthermore, they contain amorphous (orange peels) and crystalline (banana peels) phases. From literature, Langmuir isotherm can define a large amount of adsorption schemes, many of which have heterogeneous surface features.

10.1.4 Batch kinetic models

The adsorption kinetics of Cu onto banana and orange peels was investigated using two reaction models and four diffusion models. The pseudo first- and second-order kinetic models are most commonly used to evaluate processes that may be dominated by chemisorption for heavy metal adsorption. Hence, pseudo first- and second-order kinetic models were used to evaluate the possibility of kinetic reactions pathways in the adsorption of Cu. Results revealed a good fit for pseudo second-order kinetics with high rate constants and correction factors. However banana showed a stronger conformity to the model because it is basic in nature and more likely to form metal complexes at higher pH when placed in an aqueous solution of pH 5.5. Furthermore, it contains lone pairs of nitrogen and oxygen from its heterogeneous surface structure which behave as possible binging sites.

Even though the existence of reaction pathways was established, it is known that the reaction step is very rapid. Thus, it cannot be the rate-limiting step. Therefore, in order to investigate the rate-limiting steps, the diffusion models were used to assess the adsorption of Cu using banana and orange peels with four diffusion models. The models confirmed the existence of both pore and film diffusion. Also, no one model perfectly fitted the experimental data because the processes of

adsorption depends on various factors, including adsorbent and adsorptive types, their characteristics and conditions of operation. Thus, the rate-control phase may change during the adsorption process. The possible mechanisms were identified, but it was challenging to identify which of these were rate-limiting.

Furthermore, the interactions of metals and functional groups are often reported in the literature however, large uncertainties still remain on assessing the contribution of physical and chemical adsorption. Therefore, it was of high importance to identify the adsorption mechanisms, and assess the role of the physical properties and functional groups on adsorption. This is indispensable for identifying adsorption process parameters, and also provides useful information for adsorbent selection in the particular design of a wastewater treatment unit. The results demonstrated that the functional groups on the peels played an important role in the adsorption of Cu. Among various surface functional groups, the oxygen-containing group was found to play a critical role in the Cu uptake onto the peels. Ion-exchange was identified as the dominant mechanism in the Cu uptake by banana and orange peels. Some other types of interactions, like complexation and electrostatic interactions were also proven to be involved in the adsorption process, while physical force was found to play a small role in the copper uptake.

10.2 Industrial application.

This research contributes to a potential alternative solutions that can assist in addressing the shortage of knowledge of adsorption kinetics which are crucial for design and development purposes. Furthermore, the adsorption capacity of the adsorbents being examined is suitable for use in low concentration operations. Therefore, their successful use would be around small-scale operations such as communities or households. A breakthrough in this area (with other adsorbent modifications in mind) could result, for example, in the development and implementation of: (1) modular mobile wastewater treatment plant solutions that can be easily deployed in small communities that are negatively affected by ion metals in their portable water, and (2) design of filter using adsorbents for family applications in taps, drinking bottles or water drums.

10.3 Final remarks and recommendations

To advance and further promote the research on the kinetics of bioadsorbent, with the knowledge that has been gathered from this work, the following recommendations for further studies are proposed:

- Non-linear evaluation of batch kinetic models: analysis of linear regression is easy to establish and applies to a wide range of kinetic adsorption processes. The linear form of the kinetic model were fitted to a data set, the best fit model was determined based on the R^2 value and the model

parameters obtained were compared with the experimental values. However, one challenge is that different linearized versions of kinetic models provide varying equations and parameter values that make it difficult to make comparisons with literature and reach generalized findings about behaviour. Therefore, it is proposed that nonlinear regression be used to minimise this issue. This is because during nonlinear regression, the iterative technique allows the parametric values to evolve continually to the values that minimize a predefined error function. This progression is dependent on a chosen optimization algorithm (e.g., algorithm Levenberg–Marquardt), which determines how the projected set of values converges towards their optimized initial values. Therefore, making it a stronger choice to provide stronger outcomes and insight into understanding processes for adsorption using agricultural peels. This will be a step closer to making generalizations which will assist in comparative studies.

- The model selection of adsorption kinetics and isotherms: a step-by-step technique must be created from first adapting the easiest and most appropriate to selecting a more complicated one if necessary for further assessment. In addition, if a new parameter is added without physical justification into the model, its precision should be confirmed, for example, by testing its sensitivity to varying system condition.
- To create a database to aid in determining which model will best wok based on process parameters and adsorbent types: there is a lot of duplicate information and it has increased the likelihood of errors and inconsistencies. As such, creating a good database would: (1) provide access to information required which will be linked accordingly to give useful relationships, (2) it will aid support and ensure accuracy and integrity of information, and (3) it will help with data processing and reporting needs. This would be a good step to establishing a solid source that would help create a more correct and reliable information. For instance, one could start with a small prototype database that will keep a list of information (process parameters, adsorbent types and kinetic models) for the purpose of building a community based water treatment plant for the removal of metal ions in what should be “portable” water. Initiating this process should start with existing data. For example, listing all the relevant parameters in the model equations, the information required to calculate them, factors that influence them, etc. The goal is trying to breakdown everything to the smallest useful parts or details. This should then be followed by establishing relationships between all the different elements. However, with all the information that is already published, the database could get complex depending on who will use it. Therefore, careful attention should also be directed to: (1) how information will be collected and organised, (2) setting standard requirements for the information that can be used, and (3) appointing qualified persons to evaluate submitted results.

- To study and include metal speciation data: in most aqueous environmental systems, inorganic and organic metal complexes represent a significant contribution to the total soluble metal. The adsorption of metals is often a pH-dependent phenomenon. Such behaviour can usually be linked to changes in the speciation of metals with solution acidity and variability in the extent of surface protonation. Therefore, because the ability of adsorbents to adsorb species may vary drastically between different metal species, (e.g. Cu^{2+} (aq) compared to $CuOH^{+}$) a knowledge of metal species distribution is essential to understanding and interpreting metal adsorption behaviour.

- Developing new practical models that have an empirical form with physio-chemically sound parameters: integrating the mechanism into a model would significantly improve the model's predictive capacity and allow process simulation and optimization across a broad spectrum of operating conditions, thus saving experimental costs. However, it is computationally challenging and time consuming to solve mechanistic models of such complexity. Thus, for practical design considerations, a balance between lumped and mechanistic modeling approach is recommended.

Despite the research conducted - characterization of adsorbents, preliminary studies, identification of significant factors, process optimization , and isotherm fitting and validity, due to the uncertainty of kinetic systems, the obtained lumped rate constant have no clear kinetic significance. In addition, most of the studies in literature rarely attempt to further understand the underlying adsorbent-adsorbent fundamental interactions. Possible reasons responsible for this lack of information could be: first, rather than concentrating on the role of kinetics, the research found in literature focus on the novelty of adsorbent material. Secondly, it is hard to interpret current theoretical models as the scope of applicability of these models is not clearly described or experimentally demonstrated.

The data produced in this research is a good start to establishing new ways to tackle and better understand adsorption kinetics; information from this research proved that more work and time needs to be dedicated to individual parameters such as absorbent dosage, adsorbent type, type of metal being adsorbed, operating temperature, etc, to better understand the underlying mechanisms. The adsorption operation is complex from a theoretical perspective and the measured total uptake rate can be contributed by a single adsorption route or multiple parallel adsorption routes. Each route is controlled by different mechanisms at different adsorption times thus, tracking these changes in all adsorption systems is virtually impossible for the whole period by using a universal

model. Therefore, with the results of this research, future researchers have a chance to divide the adsorption process into several periods and model each period with a theoretically sound model to probe into such complex mechanism.

11 References

Abbas, Salman H., Ismail, I.M., Mostafa, T.M., Sulaymon, A.H., 2014. Biosorption of heavy metals: a review. Journal of Chemical Science and Technology 3, 74–102.

Abbas, Salman H, Ismail, I.M., Mostafa, T.M., Sulaymon, A.H., 2014. Biosorption of Heavy Metals: A Review. Journal of Chemical Science and Technology 3, 30.

Abdi, O., Kazemi, M., 2015. A review study of biosorption of heavy metals and comparison between different biosorbents. J. Mater. Environ. Sci 6, 1386–1399.

Acemioglu, B., Alma, M.H., 2001. Equilibrium Studies on Adsorption of Cu(II) from Aqueous Solution onto Cellulose. Journal of Colloid and Interface Science 243, 81–84.

Achife, E.C., Ibemesi, J.A., 1989. Applicability of the Freundlich and Langmuir adsorption isotherms in the bleaching of rubber and melon seed oils. J Am Oil Chem Soc 66, 247–252.

Aguayo-Villarreal, I.A., Bonilla-Petriciolet, A., Muñiz-Valencia, R., 2017. Preparation of activated carbons from pecan nutshell and their application in the antagonistic adsorption of heavy metal ions. Journal of Molecular Liquids 230, 686–695.

Aharoni, C., Sideman, S., Hoffer, E., 1979. Adsorption of phosphate ions by collodion-coated alumina. Journal of Chemical Technology and Biotechnology 29, 404–412.

Ali, A., Saeed, K., Mabood, F., 2016. Removal of chromium (VI) from aqueous medium using chemically modified banana peels as efficient low-cost adsorbent. Alexandria Engineering Journal 55, 2933–2942.

Allen, T., 1981. Other methods for determining surface area. In: Allen, T. (Ed.), Particle Size Measurement, Powder Technology Series. Springer US, Boston, MA, pp. 514–537.

Amarasinghe, B.M.W.P.K., Williams, R.A., 2007. Tea waste as a low cost adsorbent for the removal of Cu and Pb from wastewater. Chemical Engineering Journal 132, 299–309.

Annadurai, G., Juang, R.S., Lee, D.J., 2003. Adsorption of heavy metals from water using banana and orange peels. Water Science and Technology 47, 185–190.

Arunakumara, K., Walpola, B.C., Yoon, M.-H., 2013. Banana Peel: A Green Solution for Metal Removal from Contaminated Waters. Korean J. Environ. Agric 32, 108–116.

Azizian, S., 2004. Kinetic models of sorption: a theoretical analysis. Journal of Colloid and Interface Science 276, 47–52.

Batagarawa, S.M., Dayo, L.Y., 2017. Millet husk as efficient adsorbent for removal of lead, cadmium, and nickel ions from aqueous solution 3, 13.

Benderdouche, N., Bestani, B., Hamzaoui, M., 2018. The use of linear and nonlinear methods for adsorption isotherm optimization of basic green 4-dye onto sawdust-based activated carbon.

Bhatnagar, A., Sillanpää, M., Witek-Krowiak, A., 2015. Agricultural waste peels as versatile biomass for water purification – A review. Chemical Engineering Journal 270, 244–271.

Bhaumik, R., Mondal, N.K., 2016. Optimizing adsorption of fluoride from water by modified banana peel dust using response surface modelling approach. Appl Water Sci 6, 115–135.

Bonnamy, S., Oberlin, A., 2016. Chapter 4 - Transmission Electron Microscopy. In: Inagaki, M., Kang, F. (Eds.), Materials Science and Engineering of Carbon. Butterworth-Heinemann, pp. 45–70.

Borba, C.E., Guirardello, R., Silva, E.A., Veit, M.T., Tavares, C.R.G., 2006. Removal of nickel(II) ions from aqueous solution by biosorption in a fixed bed column: Experimental and theoretical breakthrough curves. Biochemical Engineering Journal 30, 184–191.

Box, G.E.P., Hunter, J.S., Hunter, W.G., 2005. Statistics for Experimenters: Design, Innovation, and Discovery, 2nd Edition, 2nd edition. Ed. Wiley-Interscience, Hoboken, N.J.

Boyd, G.E., Adamson, A.W., Myers, L.S., 1947. The Exchange Adsorption of Ions from Aqueous Solutions by Organic Zeolites. II. Kinetics [1]. J. Am. Chem. Soc. 69, 2836–2848.

Bradshaw, A.M., 1977. G. Wedler: Chemisorption: An Experimental Approach Butterworths, London. Boston 1976. 250 Seiten, Prets: £ 12. - (Übersetzt von D. F. Klemperer). Berichte der Bunsengesellschaft für physikalische Chemie 81, 705–705.

Canivet, J., Bonnefoy, J., Daniel, C., Legrand, A., Coasne, B., Farrusseng, D., 2014. Structure–property relationships of water adsorption in metal–organic frameworks. New J. Chem. 38, 3102–3111.

Chakraborty, A., Saha, B.B., Ng, K.C., Koyama, S., Srinivasan, K., 2009. Theoretical insight of physical adsorption for a single component adsorbent+adsorbate system: II. The Henry region. Langmuir 25, 7359–7367.

Chakrapani, C., Babu, C.S., Vani, K.N.K., Rao, K.S., 2010. Adsorption Kinetics for the Removal of Fluoride from Aqueous Solution by Activated Carbon Adsorbents Derived from the Peels of Selected Citrus Fruits [WWW Document]. Journal of Chemistry. URL https://www.hindawi.com/journals/jchem/2010/582150/abs/ (accessed 8.24.19).

Chao, H.-P., Chang, C.-C., Nieva, A., 2014. Biosorption of heavy metals on Citrus maxima peel, passion fruit shell, and sugarcane bagasse in a fixed-bed column. Journal of Industrial and Engineering Chemistry 20, 3408–3414.

Chatterjee, A., Schiewer, S., 2014. Multi-resistance kinetic models for biosorption of Cd by raw and immobilized citrus peels in batch and packed-bed columns. Chemical Engineering Journal 244, 105–116.

Chen, J., Feng, J., Yan, W., 2016. Influence of metal oxides on the adsorption characteristics of ppy/metal oxides for Methylene Blue. Journal of Colloid and Interface Science 475, 26–35.

Chen, J., Shapiro, V., Suresh, K., Tsukanov, I., 2007. Shape optimization with topological changes and parametric control. International Journal for Numerical Methods in Engineering 71, 313–346.

Chen, J., Shu, C., Wang, N., Feng, J., Ma, H., Yan, W., 2017. Adsorbent synthesis of polypyrrole/tio2 for effective fluoride removal from aqueous solution for drinking water purification: Adsorbent characterization and adsorption mechanism. Journal of Colloid and Interface Science 495, 44–52.

Crittenden, B., Thomas, W.J., 1998. Adsorption Technology and Design. Butterworth-Heinemann.

Cui, L., Wang, Y., Gao, L., Hu, L., Yan, L., Wei, Q., Du, B., 2015. EDTA functionalized magnetic graphene oxide for removal of Pb(II), Hg(II) and Cu(II) in water treatment: Adsorption mechanism and separation property. Chemical Engineering Journal 281, 1–10.

Dada, A.O., Adekola, F.A., Odebunmi, E.O., 2017. Kinetics, mechanism, isotherm and thermodynamic studies of liquid phase adsorption of Pb2+ onto wood activated carbon supported zerovalent iron (WAC-ZVI) nanocomposite. Cogent Chemistry 3, 1351653.

Das, N., Vimala, R., Karthika, P., 2008. Biosorption of heavy metals–An overview. IJBT Vol.7(2) [April 2008].

Demirbas, A., 2008. Heavy metal adsorption onto agro-based waste materials: A review. Journal of Hazardous Materials 157, 220–229.

Deshmukh, P.D., Khadse, G.K., Shinde, V.M., Labhasetwar, P., 2017. Cadmium Removal from Aqueous Solutions Using Dried Banana Peels as An Adsorbent: Kinetics and Equilibrium Modeling. J Bioremediat Biodegrad 08.

Dhal, B., Abhilash, Pandey, B.D., 2018. Mechanism elucidation and adsorbent characterization for removal of Cr(VI) by native fungal adsorbent. Sustainable Environment Research 28, 289–297.

Dias, A., Ciminelli, V.S.T., 2000. Analysis of nitrogen adsorption-desorption isotherms for the estimation of pore-network dimensions and structure of ferroelectric powders. Ferroelectrics 241, 9–16.

Douven, S., Paez, C.A., Gommes, C.J., 2015. The range of validity of sorption kinetic models. Journal of Colloid and Interface Science 448, 437–450.

Dursun, A.Y., 2006. A comparative study on determination of the equilibrium, kinetic and thermodynamic parameters of biosorption of copper(II) and lead(II) ions onto pretreated Aspergillus niger. Biochemical Engineering Journal 28, 187–195.

Dutta, S., Bhattacharyya, A., Ganguly, A., Gupta, S., Basu, S., 2011. Application of Response Surface Methodology for preparation of low-cost adsorbent from citrus fruit peel and for removal of Methylene Blue. Desalination 275, 26–36.

Ebnesajjad, S., 2014. Chapter 4 - Surface and Material Characterization Techniques. In: Ebnesajjad, S. (Ed.), Surface Treatment of Materials for Adhesive Bonding (Second Edition). William Andrew Publishing, Oxford, pp. 39–75.

El-Azazy, M., El-Shafie, A.S., Issa, A.A., Al-Sulaiti, M., Al-Yafie, J., Shomar, B., Al-Saad, K., 2019. Potato Peels as an Adsorbent for Heavy Metals from Aqueous Solutions: Eco-Structuring of a Green Adsorbent Operating Plackett–Burman Design [WWW Document]. Journal of Chemistry. URL https://www.hindawi.com/journals/jchem/2019/4926240/ (accessed 5.27.19).

Faria, P.C.C., Órfão, J.J.M., Pereira, M.F.R., 2004. Adsorption of anionic and cationic dyes on activated carbons with different surface chemistries. Water Research 38, 2043–2052.

Fathy, N.A., El-Shafey, O.I., Khalil, L.B., 2013. Effectiveness of Alkali-Acid Treatment in Enhancement the Adsorption Capacity for Rice Straw: The Removal of Methylene Blue Dye [WWW Document]. International Scholarly Research Notices. URL https://www.hindawi.com/journals/isrn/2013/208087/ (accessed 5.3.19).

Feng, N., Guo, X., 2012. Characterization of adsorptive capacity and mechanisms on adsorption of copper, lead and zinc by modified orange peel. Transactions of Nonferrous Metals Society of China 22, 1224–1231.

Feng, N., Guo, X., Liang, S., 2009. Kinetic and thermodynamic studies on biosorption of Cu(II) by chemically modified orange peel. Transactions of Nonferrous Metals Society of China 19, 1365–1370.

Feng, N., Guo, X., Liang, S., 2010. Enhanced Cu(II) adsorption by orange peel modified with sodium hydroxide. Transactions of Nonferrous Metals Society of China 20, s146–s152.

Fiol, N., Villaescusa, I., 2009. Determination of sorbent point zero charge: usefulness in sorption studies. Environ Chem Lett 7, 79–84.

Fomina, M., Gadd, G.M., 2014. Biosorption: current perspectives on concept, definition and application. Bioresource Technology, Special Issue on Biosorption 160, 3–14.

Fomkin, A.A., Men'shchikov, I.E., Pribylov, A.A., Gur'yanov, V.V., Shkolin, A.V., Zaitsev, D.S., Tvardovskii, A.V., 2017. Methane adsorption on microporous carbon adsorbent with wide pore size distribution. Colloid J 79, 144–151.

Foo, K.Y., Hameed, B.H., 2010. Insights into the modeling of adsorption isotherm systems. Chemical Engineering Journal 156, 2–10.

Gadd, G.M., 2009. Biosorption: critical review of scientific rationale, environmental importance and significance for pollution treatment. J. Chem. Technol. Biotechnol. 84, 13–28.

Garg, U.K., Kaur, M.P., Sud, D., Garg, V.K., 2009. Removal of hexavalent chromium from aqueous solution by adsorption on treated sugarcane bagasse using response surface methodological approach. Desalination 249, 475–479.

Ghosal, P.S., Gupta, A.K., 2017. Determination of thermodynamic parameters from Langmuir isotherm constant-revisited. Journal of Molecular Liquids 225, 137–146.

Grassi, M., Kaykioglu, G., Belgiorno, V., Lofrano, G., 2012. Removal of Emerging Contaminants from Water and Wastewater by Adsorption Process. In: Emerging Compounds Removal from Wastewater, springerbriefs in Molecular Science. Springer, Dordrecht, pp. 15–37.

Gupta, R., Ahuja, P., Khan, S., Saxena, R.K., Mohapatra, H., 2000. Microbial biosorbents: Meeting challenges of heavy metal pollution in aqueous solutions. Current Science 78, 967–973.

Gupta, V.K., Gupta, B., Rastogi, A., Agarwal, S., Nayak, A., 2011. Pesticides removal from waste water by activated carbon prepared from waste rubber tire. Water Research 45, 4047–4055.

Gutierrez, I.R., Tovar, A.K., Godínez, L.A., 2018. Sustainable Sorbent Materials Obtained from Orange Peel as an Alternative for Water Treatment. Wastewater and Water Quality.

Hafizovic, J., Bjørgen, M., Olsbye, U., Dietzel, P.D.C., Bordiga, S., Prestipino, C., Lamberti, C., Lillerud, K.P., 2007. The Inconsistency in Adsorption Properties and Powder XRD Data of MOF-5 Is Rationalized by Framework Interpenetration and the Presence of Organic and Inorganic Species in the Nanocavities. J. Am. Chem. Soc. 129, 3612–3620.

Hanumantharao, Y., Kishore, M., Ravindhranath, K., Author, C., 2012. Characterization And Adsorption Studies Of "Lagenaria siceraria" Shell Carbon For The Removal Of Fluoride 4, 16.

Harsh, J., 2005. Amorphous materials. In: Hillel, D. (Ed.), Encyclopedia of Soils in the Environment. Elsevier, Oxford, pp. 64–71.

Haul, R., 1982. S. J. Gregg, K. S. W. Sing: Adsorption, Surface Area and Porosity. 2. Auflage, Academic Press, London 1982. 303 Seiten, Preis: $ 49.50. Berichte der Bunsengesellschaft für physikalische Chemie 86, 957–957.

Ho, Y.-S., 2006. Review of second-order models for adsorption systems. J. Hazard. Mater. 136, 681–689.

Ho, Y.S., mckay, G., 1998. A Comparison of Chemisorption Kinetic Models Applied to Pollutant Removal on Various Sorbents. Process Safety and Environmental Protection 76, 332–340.

Ho, Y.-S., mckay, G., 1999. Pseudo-second order model for sorption processes. Process biochemistry 34, 451–465.

Ho, Y.S., Ng, J.C.Y., mckay, G., 2001. Removal of lead(II) from effluents by sorption on peat using second-order kinetics. Sep. Sci. Technol. 36, 241–261.

Hossain, M.A., Ngo, H.H., Guo, W.S., Nguyen, T.V., 2012. Biosorption of Cu(II) From Water by Banana Peel Based Biosorbent: Experiments and Models of Adsorption and Desorption 18.

Hubbe, M.A., Hasan, S.H., Ducoste, J.J., 2011. Cellulosic substrates for removal of pollutants from aqueous systems: a review. 1. Metals. Bioresources 6, 2161–2287.

Iftekhar, S., Ramasamy, D.L., Srivastava, V., Asif, M.B., Sillanpää, M., 2018. Understanding the factors affecting the adsorption of Lanthanum using different adsorbents: A critical review. Chemosphere 204, 413–430.

Ismaiel, A.M., Shopak, W., Mohamed, Z.H., Elmorsi, T.M., 2014. Kinetic and Equilibrium Isotherms Studies of Adsorption of Pb(II) from Water onto Natural Adsorbent. Journal of Environmental Protection 5, 720–726.

Jaishankar, M., Mathew, B.B., Shah, M.S., 2014. Biosorption of Few Heavy Metal Ions Using Agricultural Wastes. Journal of Environment Pollution and Human Health 2, 7.

Jaria, G., Silva, C.P., Ferreira, C.I.A., Otero, M., Calisto, V., 2017. Sludge from paper mill effluent treatment as raw material to produce carbon adsorbents: An alternative waste management strategy. Journal of Environmental Management 188, 203–211.

Jarrett, R., 2000. Introduction to the Design and Analysis of Experiments. G. M. Clarke and R. E. Kempson, Arnold, London, 1997. No. Of pages. Vii+334. Price: £19.99. ISBN 0-340-64555-5. Statistics in Medicine 19, 882–883.

Jia, Y.F., Xiao, B., Thomas, K.M., 2002. Adsorption of Metal Ions on Nitrogen Surface Functional Groups in Activated Carbons. Langmuir 18, 470–478.

Kamsonlian, S., Suresh, S., Chand, S., 2011a. Characterization of banana and orange peels:biosorption mechanism [WWW Document]. Researchgate. URL https://www.researchgate.net/publication/228325735_characterization_of_banana_and_orange_peelsbiosorption_mechanism (accessed 5.7.19).

Kamsonlian, S., Suresh, S., Majumder, C.B., S, S, Chand, 2011b. Characterization of banana and orange peels:biosorption mechanism [WWW Document]. Researchgate. URL https://www.researchgate.net/publication/228325735_CHARACTERIZATION_OF_BANANA_AND_ORANGE_PEELSBIOSORPTION_MECHANISM (accessed 3.7.19).

Kaushal, A., Singh, S.K., 2017. Critical analysis of adsorption data statistically. Appl Water Sci 7, 3191–3196.

Khaskheli, M.I., Memon, S.Q., Siyal, A.N., Khuhawar, M.Y., 2011. Use of Orange Peel Waste for Arsenic Remediation of Drinking Water. Waste Biomass Valor 2, 423.

Koh, J.-H., Wankat, P.C., Wang, N.-H.L., 1998. Pore and Surface Diffusion and Bulk-Phase Mass Transfer in Packed and Fluidized Beds. Ind. Eng. Chem. Res. 37, 228–239.

Kosmulski, M., 2002. The ph-Dependent Surface Charging and the Points of Zero Charge. Journal of Colloid and Interface Science 253, 77–87.

Kratochvil, D., Volesky, B., 1998. Advances in the biosorption of heavy metals. Trends in Biotechnology 16, 291–300.

Kruk, M., Jaroniec, M., Gadkaree, K.P., 1999. Determination of the Specific Surface Area and the Pore Size of Microporous Carbons from Adsorption Potential Distributions. Langmuir 15, 1442–1448.

Kursunge, H., Deshmukh, A.W., Ugwekar, D.R.P., Waghmare, M., 2014. Comparative study of adsorption of cu (ii) on fresh orange peel and pectin extracted orange peel 5.

Largitte, L., Pasquier, R., 2016. A review of the kinetics adsorption models and their application to the adsorption of lead by an activated carbon. Chemical Engineering Research and Design 109, 495–504.

Lasheen, M.R., Ammar, N.S., Ibrahim, H.S., 2012. Adsorption/desorption of Cd(II), Cu(II) and Pb(II) using chemically modified orange peel: Equilibrium and kinetic studies. Solid State Sciences 14, 202–210.

Lee, S.B., Kim, I.H., Ryu, D.D.Y., Taguchi, H., 1983. Structural properties of cellulose and cellulase reaction mechanism. Biotechnology and Bioengineering 25, 33–51.

Lemay, J.; B.E.B.C.J.M.T.L.B.H.E., 2015. Chemistry - The Central Science - AP Edition, 13th edition. Ed. Pearson.

Leofanti, G., Padovan, M., Tozzola, G., Venturelli, B., 1998. Surface area and pore texture of catalysts. Catalysis Today 41, 207–219.

Liang, S., Guo, X., Feng, N., Tian, Q., 2010. Isotherms, kinetics and thermodynamic studies of adsorption of Cu2+ from aqueous solutions by Mg2+/K+ type orange peel adsorbents. Journal of Hazardous Materials 174, 756–762.

Liang, S., Guo, X., Tian, Q., 2011. Adsorption of Pb2+ and Zn2+ from aqueous solutions by sulfured orange peel. Desalination 275, 212–216.

Liu, C., Ngo, H.H., Guo, W., Tung, K.-L., 2012. Optimal conditions for preparation of banana peels, sugarcane bagasse and watermelon rind in removing copper from water. Bioresource Technology 119, 349–354.

Liu, Y., Liu, Y.-J., 2008. Biosorption isotherms, kinetics and thermodynamics. Separation and Purification Technology 61, 229–242.

Liu, Y., Shen, L., 2008. A general rate law equation for biosorption. Biochemical Engineering Journal 38, 390–394.

Liu, Z., Zhang, F.-S., 2009. Removal of lead from water using biochars prepared from hydrothermal liquefaction of biomass. Journal of Hazardous Materials 167, 933–939.

Lodeiro, P., Herrero, R., Vicente, M.E.S. de, 2007. Thermodynamic and Kinetic Aspects on the Biosorption of Cadmium by Low Cost Materials: A Review. Environ. Chem. 3, 400–418.

Lowell, S., Shields, J.E., Thomas, M.A., Thommes, M., 2004. Characterization of Porous Solids and Powders: Surface Area, Pore Size and ... - S. Lowell, Joan E. Shields, Martin A. Thomas, Matthias Thommes - Google Books [WWW Document]. URL https://books.google.co.za/books?Id=iwvsbwaaqbaj&dq=physical+characterization+surface+area+and+porosity&lr=&source=gbs_navlinks_s (accessed 8.27.18).

Lu, D., Cao, Q., Li, X., Cao, X., Luo, F., Shao, W., 2009. Kinetics and equilibrium of Cu(II) adsorption onto chemically modified orange peel cellulose biosorbents. Hydrometallurgy 95, 145–152.

Lü, L., Chen, L., Shao, W., Luo, F., 2010. Equilibrium and Kinetic Modeling of Pb(II) Biosorption by a Chemically Modified Orange Peel Containing Cyanex 272. J. Chem. Eng. Data 55, 4147–4153.

Malkoc, E., Nuhoglu, Y., 2006. Potential of tea factory waste for chromium(VI) removal from aqueous solutions: Thermodynamic and kinetic studies. Separation and Purification Technology 54, 291–298.

Marín, A.B.P., Ortuño, J.F., Aguilar, M.I., Meseguer, V.F., Sáez, J., Lloréns, M., 2010. Use of chemical modification to determine the binding of Cd(II), Zn(II) and Cr(III) ions by orange waste. Biochemical Engineering Journal, Special Section: CHEMPOR2008 - Integration of Life Sciences and Engineering 53, 2–6.

Martín-Lara, M.A., Blázquez, G., Ronda, A., Pérez, A., Calero, M., 2013. Development and Characterization of Biosorbents To Remove Heavy Metals from Aqueous Solutions by Chemical Treatment of Olive Stone. Ind. Eng. Chem. Res. 52, 10809–10819.

Mckay, G., Blair, H.S., Gardner, J.R., 1982. Adsorption of dyes on chitin. I. Equilibrium studies. Journal of Applied Polymer Science 27, 3043–3057.

Mckay, G., Otterburn, M.S., Sweeney, A.G., 1980. The removal of colour from effluent using various adsorbents—III. Silica: Rate processes. Water Research 14, 15–20.

Memon, J.R., Memon, S.Q., Bhanger, M.I., Memon, G.Z., El-Turki, A., Allen, G.C., 2008. Characterization of banana peel by scanning electron microscopy and FT-IR spectroscopy and its use for cadmium removal. Colloids and Surfaces B: Biointerfaces 66, 260–265.

Michalak, I., Chojnacka, K., Witek-Krowiak, A., 2013. State of the Art for the Biosorption Process—a Review. Applied Biochemistry and Biotechnology 170, 1389–1416.

Mohamad, O.A., Hao, X., Xie, P., Hatab, S., Lin, Y., Wei, G., 2012. Biosorption of Copper (II) from Aqueous Solution Using Non-Living Mesorhizobium amorphae Strain CCNWGS0123. Microbes Environ 27, 234–241.

Mohan, D., Singh, K.P., 2002. Single- and multi-component adsorption of cadmium and zinc using activated carbon derived from bagassefan agricultural waste$. Water Research 15.

Mohan, D., Singh, K.P., Singh, V.K., 2008. Wastewater treatment using low cost activated carbons derived from agricultural byproducts—A case study. Journal of Hazardous Materials 152, 1045–1053.

Myers, R.H., Montgomery, D.C., Anderson-Cook, C.M., 2016. Response Surface Methodology: Process and Product Optimization Using Designed Experiments. John Wiley & Sons.

Nayak, A., Bhushan, B., Gupta, V., Sharma, P., 2017. Chemically activated carbon from lignocellulosic wastes for heavy metal wastewater remediation: Effect of activation conditions. Journal of Colloid and Interface Science 493, 228–240.

Nguyen, T.A.H., Ngo, H.H., Guo, W.S., Zhang, J., Liang, S., Yue, Q.Y., Li, Q., Nguyen, T.V., 2013. Applicability of agricultural waste and by-products for adsorptive removal of heavy metals from wastewater. Bioresource Technology 148, 574–585.

Nibou, D., Mekatel, H., Amokrane, S., Barkat, M., Trari, M., 2010. Adsorption of Zn2+ ions onto naa and nax zeolites: kinetic, equilibrium and thermodynamic studies. J Hazard Mater 173, 637–646.

Noeline, B.F., Manohar, D.M., Anirudhan, T.S., 2005. Kinetic and equilibrium modelling of lead(II) sorption from water and wastewater by polymerized banana stem in a batch reactor. Separation and Purification Technology 45, 131–140.

Nurchi, V.M., Villaescusa, I., 2008. Agricultural biomasses as sorbents of some trace metals. Coordination Chemistry Reviews, ISMEC2007: XVIII Italian - Spanish Congress on the Thermodynamics of Metal Complexes 252, 1178–1188.

Pagnanelli, F., Mainelli, S., Vegliò, F., Toro, L., 2003. Heavy metal removal by olive pomace: biosorbent characterisation and equilibrium modelling. Chemical Engineering Science 58, 4709–4717.

Palma, C., Contreras, E., Urra, J., Martínez, M.J., 2011a. Eco-friendly Technologies Based on Banana Peel Use for the Decolourization of the Dyeing Process Wastewater. Waste and Biomass Valorization 2, 77–86.

Palma, C., Contreras, E., Urra, J., Martínez, M.J., 2011b. Eco-friendly Technologies Based on Banana Peel Use for the Decolourization of the Dyeing Process Wastewater. Waste Biomass Valor 2, 77–86.

Park, D., Yun, Y.-S., Park, J.M., 2010. The past, present, and future trends of biosorption. Biotechnol Bioproc E 15, 86–102.

Parkes, M.V., Staiger, C.L., Perry, J.J., Allendorf, M.D., Greathouse, J.A., 2013. Screening metal-organic frameworks for selective noble gas adsorption in air: effect of pore size and framework topology. Phys Chem Chem Phys 15, 9093–9106.

Pashai Gatabi, M., Milani Moghaddam, H., Ghorbani, M., 2016. Point of zero charge of maghemite decorated multiwalled carbon nanotubes fabricated by chemical precipitation method. Journal of Molecular Liquids 216, 117–125.

Pathak, P.D., Mandavgane, S.A., Kulkarni, B.D., 2016a. Characterizing fruit and vegetable peels as bioadsorbents. Current Science (00113891) 110.

Pathak, P.D., Mandavgane, S.A., Kulkarni, B.D., 2016b. Characterizing fruit and vegetable peels as bioadsorbents. Current Science (00113891) 110.

Pathak, P.D., Mandavgane, S.A., Kulkarni, B.D., 2017. Fruit Peel Waste:Characterization and its Potential Uses. Current Science 113, 444.

Paulson, A.J., Kester, D.R., 1980. Copper(II) ion hydrolysis in aqueous solution. J Solution Chem 9, 269–277.

Plazinski, W., 2010. Applicability of the film-diffusion model for description of the adsorption kinetics at the solid/solution interfaces. Applied Surface Science, Seventh International Symposium Effects of Surface Heterogeneity in Adsorption and Catalysis on Solids - ISSHAC-7 256, 5157–5163.

Plazinski, W., Rudzinski, W., Plazinska, A., 2009a. Theoretical models of sorption kinetics including a surface reaction mechanism: A review. Advances in Colloid and Interface Science 152, 2–13.

Plazinski, W., Rudzinski, W., Plazinska, A., 2009b. Theoretical models of sorption kinetics including a surface reaction mechanism: A review. Advances in Colloid and Interface Science 152, 2–13.

Qiu, H., Lv, L., Pan, B., Zhang, Qing-jian, Zhang, W., Zhang, Quan-xing, 2009. Critical review in adsorption kinetic models. J. Zhejiang Univ. Sci. A 10, 716–724.

Rangabhashiyam, S., Anu, N., Giri Nandagopal, M.S., Selvaraju, N., 2014a. Relevance of isotherm models in biosorption of pollutants by agricultural byproducts. Journal of Environmental Chemical Engineering 2, 398–414.

Rangabhashiyam, S., Anu, N., Giri, N.M.S., Selvaraju, N., 2014b. A Novel approach of the modified BET Isotherm towards continuous column study. JSIR Vol.73(07) [July 2014].

Rangabhashiyam, S., Anu, N., Giri, N.M.S., Selvaraju, N., 2014c. A Novel approach of the modified BET Isotherm towards continuous column study. JSIR Vol.73(07) [July 2014].

Rao, K.S., Anand, S., Venkateswarlu, P., 2010. Adsorption of cadmium(ii) ions from aqueous solution by tectona grandis l.f. (teak leaves powder) 20.

Reichenberg, D., 1953. Properties of Ion-Exchange Resins in Relation to their Structure. III. Kinetics of Exchange. J. Am. Chem. Soc. 75, 589–597.

Rengaraj, S., Moon, S.-H., Sivabalan, R., Arabindoo, B., Murugesan, V., 2002. Removal of phenol from aqueous solution and resin manufacturing industry wastewater using an agricultural waste: rubber seed coat. Journal of Hazardous Materials 89, 185–196.

Rey, C., Collins, B., Goehl, T., Dickson, I.R., Glimcher, M.J., 1989. The carbonate environment in bone mineral: A resolution-enhanced fourier transform infrared spectroscopy study. Calcif Tissue Int 45, 157–164.

Robalds, A., Naja, G.M., Klavins, M., 2016. Highlighting inconsistencies regarding metal biosorption. Journal of Hazardous Materials 304, 553–556.

Rudzinski, W., Plazinski, W., 2007. Studies of the Kinetics of Solute Adsorption at Solid/Solution Interfaces: On the Possibility of Distinguishing between the Diffusional and the Surface Reaction Kinetic Models by Studying the Pseudo-First-order Kinetics. J. Phys. Chem. C 111, 15100–15110.

Sağ, Y., Aktay, Y., 2000. Mass transfer and equilibrium studies for the sorption of chromium ions onto chitin. Process Biochemistry 36, 157–173.

Schiewer, S., Volesky, B., 1995. Modeling of the proton-metal ion exchange in biosorption. Environmental science & technology 29, 3049–3058.

Sen Gupta, S., Bhattacharyya, K.G., 2011. Kinetics of adsorption of metal ions on inorganic materials: A review. Advances in Colloid and Interface Science 162, 39–58.

Sha, L., Xueyi, G., Ningchuan, F., Qinghua, T., 2009. Adsorption of Cu2+ and Cd2+ from aqueous solution by mercapto-acetic acid modified orange peel. Colloids and Surfaces B: Biointerfaces 73, 10–14.

Shrestha, S.L., 2016. Chemical , Structural and Elemental Characterization of Biosorbents Using FE-SEM , SEM-EDX , XRD / XRPD and ATR-FTIR Techniques.

Simate, G.S., Ndlovu, S., Gericke, M., 2009. Bacterial leaching of nickel laterites using chemolithotrophic microorganisms: Process optimisation using response surface methodology and central composite rotatable design. Hydrometallurgy 98, 241–246.

Sing, K., 2001. The use of nitrogen adsorption for the characterisation of porous materials. Colloids and Surfaces A: Physicochemical and Engineering Aspects 187–188, 3–9.

Speakman, S.A., 2016. Introduction to X-Ray Powder Diffraction Data Analysis.

Srivastava, S., Goyal, P., 2010. Biosorption: Application Strategies. In: Novel Biomaterials, Environmental Science and Engineering. Springer, Berlin, Heidelberg, pp. 53–55.

S.Shanavas, Kunju, A.S., Varghese, H.T., Panicker, C.Y., 2011. Comparison of Langmuir and Harkins-Jura Adsorption Isotherms for the Determination of Surface Area of Solids. Oriental Journal of Chemistry 27, 245–252.

Stojilovic, N., 2012. Why Can't We See Hydrogen in X-ray Photoelectron Spectroscopy? [WWW Document]. URL https://pubs.acs.org/doi/abs/10.1021/ed300057j (accessed 5.9.19).

Sud, D., Mahajan, G., Kaur, M.P., 2008. Agricultural waste material as potential adsorbent for sequestering heavy metal ions from aqueous solutions - a review. Bioresour. Technol. 99, 6017–6027.

Sun, Y., Gao, B., Yao, Y., Fang, J., Zhang, M., Zhou, Y., Chen, H., Yang, L., 2014. Effects of feedstock type, production method, and pyrolysis temperature on biochar and hydrochar properties. Chemical Engineering Journal 240, 574–578.

Thirumavalavan, M., Lai, Y.-L., Lee, J.-F., 2011. Fourier Transform Infrared Spectroscopic Analysis of Fruit Peels before and after the Adsorption of Heavy Metal Ions from Aqueous Solution. J. Chem. Eng. Data 56, 2249–2255.

Thirumavalavan, M., Lai, Y.-L., Lin, L.-C., Lee, J.-F., 2010. Cellulose-Based Native and Surface Modified Fruit Peels for the Adsorption of Heavy Metal Ions from Aqueous Solution: Langmuir Adsorption Isotherms. Journal of Chemical & Engineering Data 55, 1186–1192.

Tien, C., 2008. Remarks on adsorption manuscripts revised and declined: An editorial. Journal of Hazardous Materials 150, 2–3.

Tien-Jui Liang, Joseph Yue-Cheung Tsai, 1995a. Sorption kinetics of cesium on natural mordenite. Applied Radiation and Isotopes 46, 7–12.

Tien-Jui Liang, Joseph Yue-Cheung Tsai, 1995b. Sorption kinetics of cesium on natural mordenite. Applied Radiation and Isotopes 46, 7–12.

Tofan, L., Paduraru, C., Bilba, D., Rotariu, M., 2008. Thermal power plants ash as sorbent for the removal of Cu(II) and Zn(II) ions from wastewaters. Journal of Hazardous Materials 156, 1–8.

Tofighy, M.A., Mohammadi, T., 2011. Adsorption of divalent heavy metal ions from water using carbon nanotube sheets. Journal of Hazardous Materials 185, 140–147.

Tran, H.N., You, S.-J., Hosseini-Bandegharaei, A., Chao, H.-P., 2017. Mistakes and inconsistencies regarding adsorption of contaminants from aqueous solutions: A critical review. Water Research 120, 88–116.

Tripathi, A., Ranjan, M.R., 2015. Heavy Metal Removal from Wastewater Using Low Cost Adsorbents. Journal of Bioremediation & Biodegradation.

Tsukamoto, M., Ohe, T., 1991. Intraparticle diffusion of cesium and strontium cations into rock materials. Chemical Geology 90, 31–44.

Viegas, R.M.C., Campinas, M., Costa, H., Rosa, M.J., 2014. How do the HSDM and Boyd's model compare for estimating intraparticle diffusion coefficients in adsorption processes. Adsorption 20, 737–746.

Vijayaraghavan, K., Balasubramanian, R., 2015. Is biosorption suitable for decontamination of metal-bearing wastewaters? A critical review on the state-of-the-art of biosorption processes and future directions. Journal of Environmental Management 160, 283–296.

Vijayaraghavan, K., Yun, Y.-S., 2008. Bacterial biosorbents and biosorption. Biotechnology Advances 26, 266–291.

Vohlidal, J., 2004. Definitions of terms relating to reactions of polymers and to functional polymeric materials (IUPAC Recommendations 2003). Pure and Applied Chemistry 76, 889–906.

Volesky, B., 1990. Biosorption of Heavy Metals. CRC Press.

Volesky, B., 2001. Detoxification of metal-bearing effluents: biosorption for the next century. Hydrometallurgy 59, 203–216.

Volesky, B., 2003a. Biosorption process simulation tools. Hydrometallurgy, Biohydrometallurgy: Fundamentals, Technology and Sustainable Development 71, 179–190.

Volesky, B., 2003b. Biosorption process simulation tools. Hydrometallurgy, Biohydrometallurgy: Fundamentals, Technology and Sustainable Development 71, 179–190.

Volesky, B., 2003c. Sorption and biosorption. BV Sorbex, St. Lambert, Québec.

Volesky, B., 2007. Biosorption and me. Water Research 41, 4017–4029.

Walton, H.F., 1962. Ion Exchange. F. G. Helfferich. Mcgraw-Hill, New York, 1962. Ix + 624 pp. Illus. $16. Science 138, 133–133.

Witek-Krowiak, A., Chojnacka, K., Podstawczyk, D., Dawiec, A., Pokomeda, K., 2014. Application of response surface methodology and artificial neural network methods in modelling and optimization of biosorption process. Bioresource Technology, Special Issue on Biosorption 160, 150–160.

Worch, E., 2012. Adsorption Technology in Water Treatment: Fundamentals, Processes, and Modeling. Walter de Gruyter.

Wu, F.-C., Tseng, R.-L., Juang, R.-S., 2009a. Initial behavior of intraparticle diffusion model used in the description of adsorption kinetics. Chemical Engineering Journal 153, 1–8.

Wu, F.-C., Tseng, R.-L., Juang, R.-S., 2009b. Initial behavior of intraparticle diffusion model used in the description of adsorption kinetics. Chemical Engineering Journal 153, 1–8.

Xie, R., Jin, Y., Chen, Y., Jiang, W., 2017. The importance of surface functional groups in the adsorption of copper onto walnut shell derived activated carbon. Water Sci Technol 76, 3022–3034.

Xie, Z., Guan, W., Ji, F., Song, Z., Zhao, Y., 2014. Production of Biologically Activated Carbon from Orange Peel and Landfill Leachate Subsequent Treatment Technology [WWW Document]. Journal of Chemistry. URL https://www.hindawi.com/journals/jchem/2014/491912/ (accessed 3.8.19).

Xu, Z., Cai, J., Pan, B., 2013. Mathematically modeling fixed-bed adsorption in aqueous systems. J. Zhejiang Univ. Sci. A 14, 155–176.

Yang, M.-Z., Lui, G.-X., Sun, L.-O., 2015. Bioadsorption of Cadmium(II) from aqeous solution by fruiting body of Agaricus Blazei Murill 27, 2567–2574.

Yang, R.T., 2003. Adsorbents: Fundamentals and Applications. John Wiley & Sons.

Yang, X., Wan, Y., Zheng, Y., He, F., Yu, Z., Huang, J., Wang, H., Ok, Y.S., Jiang, Y., Gao, B., 2019. Surface functional groups of carbon-based adsorbents and their roles in the removal of heavy metals from aqueous solutions: A critical review. Chemical Engineering Journal 366, 608–621.

Yao, C., Chen, T., 2017. A film-diffusion-based adsorption kinetic equation and its application. Chemical Engineering Research and Design 119, 87–92.

Young, R.A., Rowell, R.M., 1986. Cellulose: Structure, Modification, and Hydrolysis. Wiley.

Yuan, M., Joseph, V.R., Lin, Y., 2007. An Efficient Variable Selection Approach for Analyzing Designed Experiments. Technometrics 49, 430–439.

12 Appendices

Appendix A

Preparation of 1000ppm solution of metal ions.

These calculations were carried out for all the metal ions that were used. Futher, this was used to prepare 1M solution of NaOH(LeMay, 2015):

Sample calculation using copper

Molecular weight (M_R) (Cu) = 63.55g/mol

Molecular weight (M_R) ($CuSO_4 \cdot 5H_2O$) = 246.68g/mol

1000ppm ≡ 1000mg/L

1. The number of moles was calculated:

   $$M = \frac{n}{V}$$

   But

   $$n = \frac{m}{M_R} \therefore$$

   $$M = \frac{m}{V \times M_R}$$

   Substituting in the values yields

   $$\left(\frac{1000\text{mg}}{\text{L}}\right) \times \left(\frac{1\text{g}}{1000\text{mg}}\right) \times \left(\frac{1\text{mol}}{63.55\text{g}}\right) = 0.01574\text{mol/L}$$

2. The mass required can now be calculated

   $$g = M_R \times M \times V$$

   $$\frac{249.68\text{g}}{\text{mol}} \times \frac{0.01574\text{mol}}{\text{L}} \times 1\text{L} = 3.93\text{g}$$

Dilution Calculations

A sample calculation is shown below for the preparation of 100ppm of a volume of 100mL from a 100ppm solution (LeMay, 2015):

$$M_1V_1 = M_2V_2$$

$$1000\text{ppm} \times V_1 = 100\text{ppm} \times 100\text{mL}$$

$\therefore V_1 = 10\text{mL}$

Preparation of acid and base solutions

A 0.1M solution of NaOH was prepared in the same way as the metal synthetic solutions

Preparation of 0.1M from a 32% HCl acid solution

1. The mass was calculated

   $mass = volume \times density$

   $= 1000mL \times \frac{1.19g}{mL}$

   $= 1190g$

2. The mass percentage

   $32\% = 0.32$

3. The molecular weight of HCl

   $36.46g/mol$

4. The number of moles were then calculated

   $\frac{\frac{1190g}{mol} \times 0.32}{\frac{36.46g}{mol}}$

   $10.44mol/L$

5. The volume was calculated like the dilution calculation above

   $\therefore V_1 = \frac{\frac{0.1mol}{L} \times 0.5L}{10.44\frac{mol}{L}}$

   $= 4.79mL$

Titration calculations

The solutions for the titrants (HCl and NaOH) were calculated as shown above

Calculating the number of acids and base sites available in the adsorbents surfaces available

Sample calculation using banana peels:

Initial base volume = 50mL

Mass of adsorbent used = 0.5g

Titrant= 0.1M HCl

Average volume of titrant added = 5.45mL

1. The number of acidic sites

   $= \frac{0.1\text{mol}}{\text{L}} \times 5.45 \times 10^{-3}\text{L} = 5.45 \times 10^{-4}\text{moles}$

2. $\text{c} = \frac{\text{n}}{\text{V}}$

   $= \frac{5.45 \times 10^{-4}\text{mol}}{0.5\text{L}} = 1.09 \times 10^{-3}\text{mol/L}$

3. amount of acid sites per gram of adsorbent given in g/L

   So 0.5g ≡ 1g/L

   $\therefore \frac{1.09 \times \frac{10^{-3}\text{mol}}{\text{L}}}{\frac{1\text{g}}{\text{L}}} = 1.09 \times \frac{10^{-3}\text{mol}}{\text{g}} = \frac{1.09\text{mmol}}{\text{g}}$

Appendix B: Identification of influential factors

- The probability plots were used to plot the actual value of the effect estimates against their cumulative normal probabilities.
- The effects were rearranged in ascending order
- Cumulative normal probability of numbered effect, ***i***, was calculated using equation 6.2
- Significant factors were identified by looking for non-zero means and points that do not do not lie on the straight line, i.e. they will not be normalized.

Table B1: Probability plot for the adsorption of orange peels

order number ì	Effect	Identity of effect	P= 100(i-1/2)/31
1	-24	B	1.6
2	-9.6	ABCD	4.8
3	-7.6	BDE	8.1
4	-6.4	ABE	11.3
5	-6.2	ACD	14.5
6	-5.7	A	17.7
7	-4.9	BE	21.0
8	-4	ABCDE	24.2
9	-2.5	D	27.4
10	-1.1	ACDE	30.6
11	-0.6	ABD	33.9
12	-0.3	ADE	37.1
13	-0.2	DE	40.3
14	-0.2	CE	43.5
15	0.2	AB	46.8
16	0.7	BD	50.0
17	1.5	BCE	53.2
18	1.6	AE	56.5
19	1.6	CDE	59.7
20	2.6	AD	62.9
21	2.7	BC	66.1
22	2.9	ACE	69.4
23	3	BCDE	72.6
24	3.7	ABCE	75.8
25	7.1	C	79.0
26	7.3	ABDE	82.3
27	7.8	CD	85.5
28	8.6	AC	88.7
29	9.5	E	91.9
30	9.9	ABC	95.2
31	10.2	BCD	98.4

Appendix C: Optimization of significant factors

Table C1: Experimental factors and levels for controlled factors

k	3
q	0
a	1.682
N_c	6

Temperature (°C)		Initial Cu Concentration(mg/L)		Adsorbent dosage (g/L)	
ξ (–1)	25	ξ (–1)	5	ξ (–1)	1
ξ (+1)	40	ξ (+1)	110	ξ (+1)	6
Code	Actual	Code	Actual	Code	Actual
-α	25.00	-α	5.00	-α	1.00
-1	28.04	-1	26.28	-1	2.01
0	32.50	0	57.50	0	3.50
+1	36.96	+1	88.72	+1	4.99
+α	40.00	+α	110.00	+α	6.00

Table C2: Confirmitory test results

Initial concentration	Final concentration	% Removed Cu
51.60	9.27	82.04
51.60	8.98	82.59
51.60	9.42	81.74
Average		82.13

Appendix D: Equilibrium isotherms and model validity

Equations 2.4 (Langmuir) and 2.7 (Freundlich) were used to model the experimental data and an excel spreadsheet was used for calculations. The tables containing the calculated data for plots and parameters is presented below.

Table D1: Experimental data used to model the isotherms for parametric calculations of the individual models

flask#	C_i mg/L)	Ce(mg/L)	V (L)	M (g)	q_e (mg/g)	C_e/qe	lnqe	lnCe
1	5	0.67	0.1	0.35	1.24	0.54	0.21	-0.40
2	10	1.48	0.1	0.35	2.43	0.61	0.89	0.39
3	15	1.84	0.1	0.35	3.76	0.49	1.32	0.61
4	20	2.29	0.1	0.35	5.06	0.45	1.62	0.83
5	25	3.50	0.1	0.35	6.14	0.57	1.82	1.25
6	30	4.73	0.1	0.35	7.22	0.66	1.98	1.55
7	35	6.31	0.1	0.35	8.20	0.77	2.10	1.84
8	40	7.88	0.1	0.35	9.18	0.86	2.22	2.06
9	45	8.66	0.1	0.35	10.38	0.83	2.34	2.16
10	50	11.39	0.1	0.35	11.03	1.03	2.40	2.43

Table D2: Model parameters for both equilibrium models using orange peels as an adsorbent.

Langmuir isotherm	
Slope	0.05
intercept	0.43
Parameters for the model	
q_{max}	20.00
K_L	0.12
R_L	0.15
Freundlich Isotherm	
Slope	0.74
Intercept	0.64
Parameters for the model	
n	1.35
Kf	1.90

Table D3: Experimental data used to model new q_e values with calculated parametric calculations of the Langmuir isotherm model using orange peels as an adsorbent.

no of points	A = $1/k_L$ x q_{max}	B = Ce/q_{max}	X= A+B	q_e =Ce/X
1	0.43	0.03	0.46	1.45
2		0.07	0.50	2.94
3		0.09	0.52	3.52
4		0.11	0.54	4.21
5		0.18	0.61	5.79
6		0.24	0.67	7.10
7		0.32	0.75	8.46
8		0.39	0.82	9.56

9		0.43	0.86	10.04
10		0.57	1.00	11.40

Table D4: Experimental data used to model new q_e values with calculated parametric calculations of the Freundlich isotherm model using orange peels as an adsorbent.

	A	B	C	D		
no of points	lnK_f	1/n	LnC_e	AxB	D+A	$q_{e,\ calc}$
1	0.64	0.74	-0.40	-0.29	0.35	1.41
2			0.39	0.29	0.93	2.54
3			0.61	0.45	1.09	2.97
4			0.83	0.61	1.25	3.50
5			1.25	0.93	1.57	4.79
6			1.55	1.15	1.79	5.99
7			1.84	1.36	2.00	7.41
8			2.06	1.53	2.17	8.74
9			2.16	1.60	2.24	9.37
10			2.43	1.80	2.44	11.47

Table D5: Experimental data used to model the isotherms for parametric calculations of the individual models

flask#	C_i mg/L)	Ce(mg/L)	V (L)	M (g)	q_e (mg/g)	C_e/qe	lnqe	lnCe
1	5	1.34	0.1	0.35	1.05	1.28	0.29	0.04
2	10	2.24	0.1	0.35	2.22	1.01	0.81	0.80
3	15	3.42	0.1	0.35	3.31	1.03	1.23	1.20
4	20	3.48	0.1	0.35	4.72	0.74	1.25	1.55
5	25	6.11	0.1	0.35	5.40	1.13	1.81	1.69
6	30	7.88	0.1	0.35	6.32	1.25	2.06	1.84
7	35	9.67	0.1	0.35	7.24	1.34	2.27	1.98
8	40	10.39	0.1	0.35	8.46	1.23	2.34	2.14
9	45	12.97	0.1	0.35	9.15	1.42	2.56	2.21
10	50	14.81	0.1	0.35	10.06	1.47	2.70	2.31

Table D6: Model parameters for both equilibrium models using orange peels as an adsorbent.

Langmuir isotherm	
Slope	0.03
intercept	0.94
Parameters for the model	
q_{max}	33.33
K_L	0.03
R_L	0.39
Freundlich Isotherm	
Slope	0.86
Intercept	0.09
Parameters for the model	

n	1.16
K_f	1.09

Table D7: Experimental data used to model new qe values with calculated parametric calculations of the Langmuir isotherm model using banana peels as an adsorbent.

no of points	A = $1/k_L$ x q_{max}	B = Ce/q_{max}	X= A+B	q_e =Ce/X
1	0.94	0.04	0.98	1.37
2		0.07	1.01	2.22
3		0.10	1.04	3.28
4		0.10	1.04	3.33
5		0.18	1.12	5.44
6		0.24	1.18	6.70
7		0.29	1.23	7.86
8		0.31	1.25	8.30
9		0.39	1.33	9.76
10		0.44	1.38	10.70

Table D8: Experimental data used to model new q_e values with calculated parametric calculations of the Freundlich isotherm model using banana peels as an adsorbent

	A	B	C	D		
no of points	lnK_f	1/n	LnC_e	AxB	D+A	$q_{e,\ calc}$
1	0.09	0.86	0.29	0.25	0.34	1.41
2			0.81	0.69	0.78	2.19
3			1.23	1.06	1.15	3.15
4			1.25	1.07	1.16	3.20
5			1.81	1.56	1.65	5.19
6			2.06	1.78	1.87	6.46
7			2.27	1.95	2.04	7.70
8			2.34	2.01	2.10	8.19
9			2.56	2.20	2.29	9.91
10			2.70	2.32	2.41	11.11

Appendix E: Adsorption kinetics

Pseudo first order kinetic model

Equations presented in Chapter 9 table 9.1 were used to calculate the parameters on an excel spreadsheet. The tables with the model values are presented below. Please note that the qt values were modelled using the Langmuir isotherm.

Table E1: Pseudo first-order kinetic model for orange peels

q_e(mg/g)	q_t	t	$\ln(q_e-q_t)$
14.09	5.78	5	0.92
13.86	6.68	10	0.86
13.76	7.24	15	0.81
13.63	7.38	20	0.80
13.48	8.12	40	0.73
12.65	8.57	60	0.61
12.48	9.62	80	0.46
12.03	9.71	100	0.37
11.81	9.78	110	0.31
11.03	9.88	120	0.06

Table E2: Pseudo first-order kinetic model for banana peels

q_e(mg/g)	q_t	t	$\ln(q_e-q_t)$
7.94	5.58	5.00	0.37
7.04	5.48	10.00	0.19
7.78	6.32	15.00	0.16
7.81	6.11	20.00	0.23
8.52	7.07	40.00	0.16
8.76	7.41	60.00	0.13
8.93	8.45	80.00	-0.32
8.98	8.60	100.00	-0.43
9.11	8.61	110.00	-0.30
9.18	8.62	120.00	-0.25

Pseudo second-order kinetic model

Table E3: Pseudo second-order kinetic model data for orange peels

q_t	t	t/q_t	m
5.78	5	0.86	0.6848
6.68	10	1.50	C
7.24	15	2.07	0.693
7.38	20	2.71	q_e
8.12	40	4.93	1.46028
8.57	60	7.00	k
9.62	80	8.32	0.676697
9.71	100	10.30	h
9.78	110	11.25	1.443001
9.88	120	12.14	

Table E4: Pseudo second-order kinetic model data for banana peels

q_t	t	t/q_t	m
5.58	5	0.90	0.1096
5.48	10	1.82	C
6.32	15	2.37	0.8553
6.11	20	3.27	q_e
7.07	40	5.66	9.124088
7.41	60	8.10	k
8.45	80	9.47	0.014044
8.60	100	11.62	h
8.61	110	12.77	1.16918
8.62	120	13.92	

Diffusion Models

Weber-Morris model

Table E5: Weber-Morris model data for orange peels

q_e(mg/g)	t	$t^{1/2}$	q_t	q_t/q_e		
14.09	5	2.24	5.78	0.41	q_e	2.273244
13.86	10	3.16	6.68	0.48	m	0.4399
13.76	15	3.87	7.24	0.53	q_e^2	5.167638
13.63	20	4.47	7.38	0.54	intercept	5.4507
13.48	25	5.00	8.12	0.60	K'	0.035502
12.65	40	6.32	8.57	0.68		
12.48	60	7.75	9.62	0.77		
12.03	100	10.00	9.71	0.81		
11.81	110	10.49	9.78	0.83		
11.03	120	10.95	9.88	0.90		

Table E6: Weber-Morris model data for banana peels

q_e(mg/g)	t	$t^{1/2}$	q_t	q_t/q_e		
7.94	5	2.24	5.58	0.70	q_e	2.547771
7.04	10	3.16	5.48	0.78	q_e^2	6.491136
7.78	15	3.87	6.32	0.81	intercept	4.684
7.81	20	4.47	6.11	0.78	K'	0.03289
8.52	30	5.48	7.07	0.83		
8.76	40	6.32	7.41	0.84		
8.93	60	7.75	8.45	0.95		
8.98	100	10.00	8.60	0.96		
9.11	110	10.49	8.61	0.95		
9.18	120	10.95	8.62	0.94		

Banghan's model

Table E7: Banghan's model data for orange peels at an initial concentration of 50mg/L and adsorbent mass of 3.5g/L in a 100mL solution.

q_t	t	M x q_t = A	C_i - A = B	C = C_i/B	log t	log(logB)
5.78	5.00	20.23	29.77	1.68	0.70	-0.65
6.68	10.00	23.39	26.61	1.88	1.00	-0.56
7.24	15.00	25.34	24.66	2.03	1.18	-0.51
7.38	20.00	25.84	24.16	2.07	1.30	-0.50
8.12	40.00	28.42	21.58	2.32	1.60	-0.44
8.57	60.00	30.00	20.00	2.50	1.78	-0.40
9.62	80.00	33.67	16.33	3.06	1.90	-0.31
9.71	100.00	33.99	16.02	3.12	2.00	-0.31
9.78	110.00	34.23	15.77	3.17	2.04	-0.30
9.88	120.00	34.59	15.41	3.24	2.08	-0.29

Where m, is the adsorbent mass. The product of M and q_t is A, the difference of C_i and A is B and the division of C_i by B is C

Table E8: Banghan's model data for orange peels at an initial concentration of 50mg/L and adsorbent mass of 3.5g/L in a 100mL solution.

q_t	t	M x q_t = A	ci - A = B	C = C_i/B	log t	log(logB)
5.6	5.0	19.5	30.5	1.6	0.7	-0.7
5.5	10.0	19.2	30.8	1.6	1.0	-0.7
6.3	15.0	22.1	27.9	1.8	1.2	-0.6
6.1	20.0	21.4	28.6	1.7	1.3	-0.6
7.1	40.0	24.7	25.3	2.0	1.6	-0.5
7.4	60.0	25.9	24.1	2.1	1.8	-0.5
8.5	80.0	29.6	20.4	2.4	1.9	-0.4
8.6	100.0	30.1	19.9	2.5	2.0	-0.4
8.6	110.0	30.1	19.9	2.5	2.0	-0.4
8.6	120.0	30.2	19.8	2.5	2.1	-0.4

Where m, is the adsorbent mass. The product of M and q_t is A, the difference of C_i and A is B and the division of C_i by B is C

Boyd-Reichenberg model

Table E9: Boyd-Reichenberg model model for orange peels at an initial concentration of 50mg/L using equation 2.12

q_e(mg/g)	t	$t^{1/2}$	q_t	q_t/q_e	pi/3	Pi/3 x q_t/q_e = K	1-K	J= sqrt(1-K)	(1-J)^2 =L	Pi * L = Bt
14.09	5.00	2.24	5.78	0.41	3.14	0.43	0.57	0.76	0.06	0.19
13.86	10.00	3.16	6.68	0.48	1.05	0.50	0.50	0.70	0.09	0.28
13.76	15.00	3.87	7.24	0.53		0.55	0.45	0.67	0.11	0.34
13.63	20.00	4.47	7.38	0.54		0.57	0.43	0.66	0.12	0.37
13.48	25.00	5.00	8.12	0.60		0.63	0.37	0.61	0.15	0.48
12.65	40.00	6.32	8.57	0.68		0.71	0.29	0.54	0.21	0.67
12.48	60.00	7.75	9.62	0.77		0.81	0.19	0.44	0.31	0.99
12.03	100.00	10.00	9.71	0.81		0.84	0.16	0.39	0.37	1.15
11.81	110.00	10.49	9.78	0.83		0.87	0.13	0.36	0.40	1.27
11.03	120.00	10.95	9.88	0.90		0.94	0.06	0.25	0.56	1.77

Where the product of Pi/3 and q_t/q_e is K, J the square root of (1-K) and $(1-K)^2$ is L

Table E10: Boyd-Reichenberg model model for orange peels at an initial concentration of 50mg/L using equation 2.13

q_e(mg/g)	t	$t^{1/2}$	q_t	q_t/q_e	pi/3	pi^2 =A	A/6	ln(1- qt/qe)	Bt
14.09	5.00	2.24	5.78	0.41	3.14	9.87	1.64	-0.53	0.03
13.86	10.00	3.16	6.68	0.48	1.05		-ln A/6	-0.66	0.16
13.76	15.00	3.87	7.24	0.53			-0.50	-0.75	0.25
13.63	20.00	4.47	7.38	0.54				-0.78	0.28
13.48	25.00	5.00	8.12	0.60				-0.92	0.42
12.65	40.00	6.32	8.57	0.68				-1.13	0.63
12.48	60.00	7.75	9.62	0.77				-1.47	0.97
12.03	100.00	10.00	9.71	0.81				-1.64	1.15
11.81	110.00	10.49	9.78	0.83				-1.76	1.26
11.03	120.00	10.95	9.88	0.90				-2.26	1.76

Table E11: Boyd-Reichenberg model model for banana peels at an initial concentration of 50mg/L using equation 2.12

q_e(mg/g)	t	$t^{1/2}$	q_t	q_t/q_e	pi/3	Pi/3 x q_t/q_e = K	1-K	J= sqrt(1-K)	(1-J)^2 =L	Pi * L = Bt
7.94	5.00	2.24	5.58	0.70	3.14	0.74	0.26	0.51	0.24	0.74
7.04	10.00	3.16	5.48	0.78	1.05	0.81	0.19	0.43	0.32	1.02
7.78	15.00	3.87	6.32	0.81	pi/3	0.85	0.15	0.39	0.38	1.18
7.81	20.00	4.47	6.11	0.78		0.82	0.18	0.42	0.33	1.04
8.52	30.00	5.48	7.07	0.83		0.87	0.13	0.36	0.41	1.27
8.76	40.00	6.32	7.41	0.84		0.88	0.12	0.34	0.44	1.37
8.93	60.00	7.75	8.45	0.95		0.99	0.01	0.09	0.82	2.59
9.11	110.00	10.49	8.61	0.95		0.99	0.01	0.10	0.81	2.54
9.18	120.00	10.95	8.62	0.94		0.98	0.02	0.13	0.76	2.38

Where the product of Pi/3 and q_t/q_e is K, J the square root of (1-K) and $(1-K)^2$ is L

Table E12: Boyd-Reichenberg model model for banana peels at an initial concentration of 50mg/L using equation 2.3

q_e(mg/g)	t	$t^{1/2}$	q_t	q_t/q_e	pi/3	pi^2 =A	A/6	ln(1- qt/qe)	Bt
7.94	5.00	2.24	5.58	0.70	3.14	9.87	1.64	-1.21	0.71
7.04	10.00	3.16	5.48	0.78	1.05		-ln A/6	-1.51	1.01
7.78	15.00	3.87	6.32	0.81			-0.50	-1.67	1.18
7.81	20.00	4.47	6.11	0.78				-1.53	1.03
8.52	30.00	5.48	7.07	0.83				-1.77	1.27
8.76	40.00	6.32	7.41	0.84				-1.86	1.37
8.93	60.00	7.75	8.45	0.95				-2.93	2.43
8.98	100.00	10.00	8.60	0.96				-3.18	2.68
9.11	110.00	10.49	8.61	0.95				-2.90	2.40
9.18	120.00	10.95	8.62	0.94				-2.79	2.29

Film diffusion

Table E13: Film diffusion data for orange peels.

q_e(mg/g)	q_t	q_t/q_e	t	$-\ln(q_t/q_e)$
14.09	5.78	0.41	5.00	0.53
13.86	6.68	0.48	10.00	0.66
13.76	7.24	0.53	15.00	0.75
13.63	7.38	0.54	20.00	0.78
13.48	8.12	0.60	40.00	0.92
12.65	8.57	0.68	60.00	1.13
12.48	9.62	0.77	80.00	1.47
12.03	9.71	0.81	100.00	1.64
11.81	9.78	0.83	110.00	1.76
11.03	9.88	0.90	120.00	2.26

Table E14: Film diffusion data for banana peels

q_e(mg/g)	q_t	q_t/q_e	t	$-\ln(q_t/q_e)$
7.94	5.58	0.70	5.00	1.21
7.04	5.48	0.78	10.00	1.51
7.78	6.32	0.81	15.00	1.67
7.81	6.11	0.78	20.00	1.53
8.52	7.07	0.83	40.00	1.77
8.76	7.41	0.84	60.00	1.86
8.93	8.30	0.93	80.00	2.65
8.98	8.60	0.96	100.00	3.18
9.11	8.61	0.95	110.00	2.90
9.18	8.62	0.94	120.00	2.79